

Научном већу Института за физику Београд

Београд, ____ . септембар 2016.

Предмет:

Покретање поступка за стицање звања истраживач сарадник

Молим Научно веће Института за физику да покрене поступак за мој избор у звање истраживач сарадник.

У прилогу достављам:

1. Кратку стручну биографију
2. Мишљење руководиоца пројекта на коме је подносилац захтева запослен и предлог чланова комисије за избор у звање
3. Уверење о упису докторских академских студија
4. Списак објављених научних радова и њихову копију
5. Уверења о завршеним основним и мастер академским студијама

С поштовањем,
Илија Симоновић
истраживач приправник

Научном већу Института за физику

Београд, ____. септембар 2016.

Мишљење руководиоца пројекта за избор Илије Симоновића у звање истраживач сарадник

Основна област истраживања Илије Симоновића је кинетичка теорија транспорта наелектрисаних честица и њена примена у различитим областима примењене физике и технологије. У првом делу своје докторске дисертације, Илија Симоновић је посветио највећу пажњу проучавању транспортних коефицијента вишег реда за електроне и позитроне у гасовима. Он је проширио постојећа мулти терм решења Болцманове једначине у домен транспортних коефицијената вишег реда. Ова решења су верификована у Монте Карло симулацијама. Посебан акценат у овом делу истраживања је стављен на проучавање симетрија које постоје између индивидуалних елемената тензорских транспортних коефицијената вишег реда примењујући теорију групних пројектора. Значајну пажњу у овом делу истраживања је посветио проучавању дуалне природе транспортних коефицијената вишег реда која је индикована експлицтним утицајем неконзервативних судара.

У другом делу своје докторске дисертације, Илија Симоновић се посветио проучавању транспорта електрона у течностима. Он је проширио постојећу инфраструктуру базирану на Монте Карло методи и теорији за пренос импулса из домена гасова у домен неполарних течности. Резултати ових проучавања су искоришћени за истраживања транзиције електронских лавина у стримере и њихову пропагацију у течностима. Илија Симоновић проучава на који начин комплексност флуидних модела за пропагацију стримера, природа транспортних коефицијената који се користе у моделовању и елементарни процеси попут рекомбинације електрона и позитивних јона утичу на динамику стримера у течностима.

Резултати досадашњег рада су послати у два рада (M21a и M21) која су прихваћена за публикавање. Илија Симоновић је био коаутор на неколико уводних предавања и аутор већег броја радова на домаћим и међународним конференцијама.

За састав Комисије за избор Илије Симоновића у звање истраживач сарадник предлажу се:

1. др Саша Дујко, научни саветник, Институт за физику, Београд
2. проф. др Срђан Буквић, редовни професор, Физички факултет, Београд
3. академик др Зоран Љ. Петровић, научни саветник, Институт за физику, Београд

Руководилац пројекта ОИ171037

академик др Зоран Љ. Петровић

СТРУЧНА БИОГРАФИЈА

Образовање:

Илија Симоновић рођен је 31. јула 1989. године у Крагујевцу где је завршило основну и средњу школу. Школске 2008/2009 године је уписао основне студије на Физичком факултету Универзитета у Београду, смер Теоријска и експериментална физика. Завршио је основне студије школске 2011/2012 године са просечном оценом 9.85. Студентски пројекат под називом "Градијентне теорије на некомутативном простору" урадио је на Физичком факултету под менторством Проф. др Марије Димитријевић. Мастер студије је уписао школске 2012/2013, и завршио их је са просечном оценом 10.0. Мастер рад под насловом "Некомутативна гравитација на Мојаловом простору" је одбранио 1. октобра 2013. године, под менторством Проф. др Воје Радовановића. Докторске студије на Физичком факултету Универзитета у Београду уписао је школске 2013/2014. године на смеру Физика јонизованог гаса, плазме и технологија плазме.

Радно искуство:

Школске 2012/2013 године је држао рачунске вежбе, као сарадник у настави, из предмета Електродинамика 1 и Електродинамика 2 код Проф. др Воје Радовановића на Физичком факултету, Универзитета у Београду.

Од 1. октобра 2013. године запослен је као истраживач приправник у Лабораторији за гасну електронику Института за физику у Београду. Ангажован је на пројекту Министарства науке, просвете и технолошког развоја ОИ171037 „Фундаментални процеси и примене транспорта честица у неравнотежним плазмама, траповима и наноструктурама ” под менторством др Саше Дујка. Руководилац пројекта је академик др Зоран Љ. Петровић.

Списак објављених радова и других публикација разврстан по важећим категоријама прописаним од Министарства

РАД У МЕЂУНАРОДНОМ ЧАСОПИСУ ИЗУЗЕТНИХ ВРЕДНОСТИ (M21a)

1. J. Mirić, D. Bošnjaković, **I. Simonović**, Z.Lj. Petrović and S. Dujko, “*Electron swarm properties under the influence of a very strong attachment in SF₆ and CF₃I obtained by Monte Carlo rescaling procedures*”, Plasma Sources Science and Technology **25** (2016) 065010. (IF2014= 3.591) doi: 10.1088/0963-0252/25/6/065010

ПРЕДАВАЊЕ ПО ПОЗИВУ СА МЕЂУНАРОДНОГ СКУПА ШТАМПАНО У ЦЕЛИНИ (M31)

1. S. Dujko, D. Bošnjaković, J. Mirić, **I. Simonović**, Z.M. Raspopović, R.D. White, A.H. Markosyan, U. Ebert and Z.Lj. Petrović, “*Recent results from studies of non-equilibrium electron transport in modeling of low-temperature plasmas and particle detectors*”, in Proceedings of the 9th EU-Japan Joint Symposium on Plasma Processing (JSPP2014) and EU COST MP1101 Workshop on Atmospheric Plasma Processes and Sources, 19-23 January 2014, Bohinjska Bistrica, Slovenia

ПРЕДАВАЊЕ ПО ПОЗИВУ СА МЕЂУНАРОДНОГ СКУПА ШТАМПАНО У ИЗВОДУ (M32)

1. S. Dujko, Z.Lj. Petrović, R.D. White, G. Boyle, A. Banković, **I. Simonović**, D. Bošnjaković, J. Mirić, A.H. Markosyan and S. Marjanović “*Transport processes for electrons and positrons in gases and soft-condensed matter: Basic phenomenology and applications*”, XXIX International Conference on Photonic, Electronic and Atomic Collisions, 22-28 July 2015, Toledo, Spain
2. Z.Lj. Petrović, S. Dujko, D. Marić, D. Bošnjaković, S. Marjanović, J. Mirić, O. Šašić, S. Dupljanin, **I. Simonović** and R.D. White “*Swarms as an exact representation of weakly ionized gases*”, XIX International Symposium on Electron-Molecule Collisions and Swarms & XVIII International Workshop on Low-Energy Positron and Positronium Physics, POSMOL 2015, 17-20 July 2015, Lisboa, Portugal, Book of Abstracts, p. 4

САОПШТЕЊЕ СА МЕЂУНАРОДНОГ СКУПА ШТАМПАНО У ЦЕЛИНИ (M33)

1. **I. Simonović**, Zoran Lj. Petrović, Saša Dujko, “*Third-order transport coefficients for electrons I. Structure of skewness tensor*”, Proc. 27th Symposium on Physics of Ionized Gases - SPIG 2014,

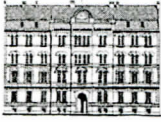
- Belgrade, Serbia, (26 - 29 August 2014), Contributed Papers and Abstracts of Invited Lectures, Topical Invited Lectures and Progress Reports (Eds. D. Marić, A.R. Milosavljević and Z. Mijatović), pp. 130-133. ISBN: 978-86-7762-600-6
2. **I. Simonović**, Zoran Lj. Petrović, Saša Dujko, “*Third-order transport coefficients for electrons II. Molecular gases*”, Proc. 27th Symposium on Physics of Ionized Gases - SPIG 2014, Belgrade, Serbia, (26 - 29 August 2014), Contributed Papers and Abstracts of Invited Lectures, Topical Invited Lectures and Progress Reports (Eds. D. Marić, A.R. Milosavljević and Z. Mijatović), pp. 134-137. ISBN: 978-86-7762-600-6
 3. J. Mirić, D. Bošnjaković, **I. Simonović**, Z.Lj. Petrović and S. Dujko, “*Monte Carlo Simulations of Electron Transport in CF₃I and SF₆ Gases*”, Proc. 28th Summer School and International Symposium on the Physics of Ionized Gases - SPIG 2016, Belgrade, Serbia, (Aug. 29 – Sep. 2), Contributed Papers and Abstracts of Invited Lectures, Topical Invited Lectures, Progress Reports and Workshop Lectures (Eds. D. Marić, A. Milosavljević, B. Obradović and G. Poparić), pp. 104-107. ISBN: 978-86-84539-14-6
 4. J. Mirić, **I. Simonović**, D. Bošnjaković, Z.Lj. Petrović and S. Dujko, “*Electron Transport in Mercury Vapor: Dimer Induced NDC and Analysis of Transport Phenomena in Electric and Magnetic Fields*”, Proc. 28th Summer School and International Symposium on the Physics of Ionized Gases - SPIG 2016, Belgrade, Serbia, (Aug. 29 – Sep. 2), Contributed Papers and Abstracts of Invited Lectures, Topical Invited Lectures, Progress Reports and Workshop Lectures (Eds. D. Marić, A. Milosavljević, B. Obradović and G. Poparić), pp. 108-111. ISBN: 978-86-84539-14-6
 5. **I. Simonović**, Z. Lj. Petrović, R.D. White and S. Dujko, “*Transport coefficients for electron swarms in liquid argon and liquid xenon*”, Proc. 28th Summer School and International Symposium on the Physics of Ionized Gases - SPIG 2016, Belgrade, Serbia, (Aug. 29 – Sep. 2), Contributed Papers and Abstracts of Invited Lectures, Topical Invited Lectures, Progress Reports and Workshop Lectures (Eds. D. Marić, A. Milosavljević, B. Obradović and G. Poparić), pp. 120-123. ISBN: 978-86-84539-14-6
 6. **I. Simonović**, Z. Lj. Petrović, R.D. White and S. Dujko, “*Transition of an electron avalanche into a streamer in liquid argon and liquid xenon*”, Proc. 28th Summer School and International Symposium on the Physics of Ionized Gases - SPIG 2016, Belgrade, Serbia, (Aug. 29 – Sep. 2), Contributed Papers and Abstracts of Invited Lectures, Topical Invited Lectures, Progress Reports and Workshop Lectures (Eds. D. Marić, A. Milosavljević, B. Obradović and G. Poparić), pp. 124-127. ISBN: 978-86-84539-14-6

САОПШТЕЊЕ СА МЕЂУНАРОДНОГ СКУПА ШТАМПАНО У ИЗВОДУ (M34)

1. **I. Simonović**, Z.Lj. Petrović, and S. Dujko, “*Third order transport coefficients for electrons and positrons in gases*”, XXIX International Conference on Photonic, Electronic and Atomic Collisions, 22-28 July 2015, Toledo, Spain
2. **I. Simonović**, Z.Lj. Petrović, R.D. White and S. Dujko, “*Higher order transport coefficients for electrons and positrons in gases*”, XIX International Symposium on Electron-Molecule Collisions and Swarms & XVIII International Workshop on Low-Energy Positron and Positronium Physics, POSMOL 2015, 17-20 July 2015, Lisbon, Portugal, Book of Abstracts, p.70
3. **I. Simonović**, Z.Lj. Petrović, S. Dujko, “*Third-order transport properties of electrons and positrons in electric and magnetic fields*”, Gaseous Electronics Meeting GEM2016 Geelong, Australia, February 14-17, 2016 14 -17 February 2016, Deakin University, Geelong, Victoria, Australia, p. 76

ПРИХВАЋЕНО ЗА ОБЈАВЉИВАЊЕ: РАД У ВРХУНСКОМ МЕЂУНАРОДНОМ ЧАСОПИСУ (M21)

Z. Lj. Petrović, **I. Simonović**, S. Marjanović, D. Bošnjaković, D. Marić, G. Malović and S. Dujko “*Non-equilibrium of charged particles in swarms and plasmas—from binary collisions to plasma effects*”, Plasma Physics and Controlled Fusion (2016)



Република Србија
Универзитет у Београду
Физички факултет
Д.Бр.2013/8008
Датум: 12.11.2015. године

На основу члана 161 Закона о општем управном поступку и службене евиденције издаје се

УВЕРЕЊЕ

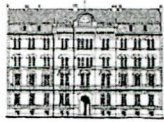
Симоновић (Бранислав) Илија, бр. индекса 2013/8008, рођен 31.07.1989. године, Крагујевац, Крагујевац-град, Република Србија, уписан школске 2015/2016. године, у статусу: финансирање из буџета; тип студија: докторске академске студије; студијски програм: Физика.

Према Статуту факултета студије трају (број година): три.
Рок за завршетак студија: у двоструком трајању студија.

Ово се уверење може употребити за регулисање војне обавезе, издавање визе, права на дечији додатак, породичне пензије, инвалидског додатка, добијања здравствене књижице, легитимације за повлашћену возњу и стипендије.



Овлашћено лице факултета



Република Србија
Универзитет у Београду
Физички факултет
Д.Бр.2013/8008
Датум: 12.11.2015. године

На основу члана 161 Закона о општем управном поступку и службене евиденције издаје се

УВЕРЕЊЕ

Симоновић (Бранислав) Илија, бр. индекса 2013/8008, рођен 31.07.1989. године, Крагујевац, Крагујевац-град, Република Србија, уписан школске 2015/2016. године, у статусу: финансирање из буџета; тип студија: докторске академске студије; студијски програм: Физика.

Према Статуту факултета студије трају (број година): три.
Рок за завршетак студија: у двоструком трајању студија.

Ово се уверење може употребити за регулисање војне обавезе, издавање визе, права на дечији додатак, породичне пензије, инвалидског додатка, добијања здравствене књижице, легитимације за повлашћену возњу и стипендије.



Овлашћено лице факултета



Република Србија

УБ

Универзитет у Београду
Физички факултет, Београд



Оснивач: Република Србија

Дозволу за рад број 612-00-02666/2010-04 од 10. децембра 2010.
године је издало Министарство просвете и науке Републике Србије

Илија

Илија, Бранислав, Симоновић

рођен 31. јула 1989. године у Крагујевцу, Република Србија, уписан школске 2008/2009.

године, а дана 19. септембра 2012. године завршио је основне академске студије,
првог степена, на студијском програму Теоријска и експериментална физика, обима
240 (двеста четрдесет) бодова ЕСПБ са просечном оценом 9,85 (девет и 85/100).

На основу тога издаје му се ова диплома о стицању високог образовања и стручном називу
дипломирани физичар

Број: 1942500

У Београду, 25. децембра 2013. године

Декан

Проф. др Јаблан Дојчиловић

Ректор

Проф. др Владимир Бумбаширевић

Потврђује се да је овај препис истоветан са његовим
изворником-овереним преписом-простим преписом који
је написан мастилом-писаћом машином-олазком који се
састоји од 2 полутабака. Изворна исправа-оверен
препис налази се код _____
(назив органа, име лица и место становања)

Такса за оверу од динара _____ је наплаћена.
По члану 19 тачка 11 Закона о републичким
административним таксама ослобођено од таксе.

Управа Градске општине Стари град
Београд

Број _____

Датум 23-09-2016



УНИВЕРЗИТЕТ У БЕОГРАДУ
ФИЗИЧКИ ФАКУЛТЕТ

Број 2422013

Београд, 07. 10. 2013. године

На основу члана 99. Закона о високом образовању ("Сл. гласник Републике Србије» број 76/05), и члана 9. и 184. Статута Физичког факултета (број 442/1 од 10.10.2006 и дате сагласности Универзитета у Београду број 02 612-1852 од 29.01.2007), у складу са Правилником о садржају и облику образаца јавних исправа које издају високошколске установе ("Сл. гласник Републике Србије» број 21/06, 66/06 и 8/07) издаје се следеће

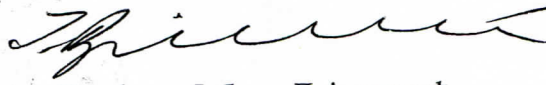
У В Е Р Е Њ Е

Симоновић (Бранислав) Илија рођен-а 31. 07. 1989. године у Крагујевцу, Крагујевац, Србија, уписан-а школске 2012/2013. године, завршио-ла је дипломске академске студије – студије другог степена (мастер) на студијском програму Физичког факултет Универзитета у Београду, смер: Теоријска и експериментална физика, дана 01. октобра 2013. године, са просечном оценом 10,00 (десет и 00/100) у току студија и постигнутим укупним бројем 60 ЕСПБ (шездесет ЕСП бодова) и тиме стекао-ла високо образовање и академски назив:

МАСТЕР ФИЗИЧАР - ТЕОРИЈСКА И ЕКСПЕРИМЕНТАЛНА ФИЗИКА- master

Уверење се издаје на лични захтев, а служи као доказ о завршеној стручној спреми до издавања дипломе.

Д Е К А Н



Проф. др Јаблан Дојчиловић

Потврђује се да је овај препис истоветан са његовим
изворником-овереним преписом-простим преписом који
је написан мастилом-писаћом машином-олазком који се
састоји од 1 полутабака. Изворна исправа-оверен
препис налази се код _____

(назив органа, име лица и место становања)

Такса за оверу од динара _____ је наплаћена.
По члану 17 тачка 11 Закона о републичким
административним таксама ослобођено од таксе.

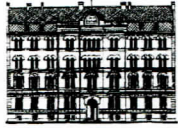
Управа Градске општине Срем
Београд

Број 2075 М.П.

Датум _____

23 -09- 2016





ДОКТОРСКЕ СТУДИЈЕ

**ПРЕДЛОГ ТЕМЕ ДОКТОРСКЕ ДИСЕРТАЦИЈЕ
КОЛЕГИЈУМУ ДОКТОРСКИХ СТУДИЈА**

Школска година
2015/2016

Подаци о студенту

Име
Презиме
Број индекса

Научна област дисертације

Подаци о ментору докторске дисертације

Име
Презиме

Научна област

Звање

Институција

Предлог теме докторске дисертације

Наслов

Уз пријаву теме докторске дисертације Колегијуму докторских студија, потребно је приложити следећа документа:

1. Семинарски рад (дужине до 10 страница)
2. Кратку стручну биографију писану у трећем лицу јединине
3. Фотокопију индекса са докторских студија

Датум	30.09.2016.	Потпис ментора	Sejo Dujko
		Потпис студента	Milica Simonovic

Мишљење Колегијума докторских студија

Након образложења теме докторске дисертације Колегијум докторских студија је тему

прихватио



није прихватио



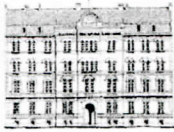
Датум

06.10.2016

Продекан за науку Физичког факултета

M. Simonovic





Република Србија
Универзитет у Београду
Физички факултет
Број индекса: 2013/8008
Датум: 22.09.2016.

На основу члана 161 Закона о општем управном поступку и службене евиденције издаје се

УВЕРЕЊЕ О ПОЛОЖЕНИМ ИСПИТИМА

Илија Симоновић, име једног родитеља Бранислав, рођен 31.07.1989.године, Крагујевац, Крагујевац-град, Република Србија, уписан школске 2013/2014. године на докторске академске студије, школске 2015/2016. године уписан на статус финансирање из буџета, студијски програм Физика, током студија положио је испите из следећих предмета:

Р.бр.	Шифра	Назив предмета	Оцена	ЕСПБ	Фонд часова**	Датум
1	ДС09ПФ8	Монте Карло симулације у физици	10 (десет)	15	I:(5+0+0)	01.07.2014.
2	ДС09КМ15	Статистичка физика неравнотежних система	10 (десет)	15	II:(5+0+0)	15.09.2014.
3	ДС09ФРНД1	Рад на докторату 1. део	П.	30	I:(0+0+15) II:(0+0+15)	
4	ДС09ЈП8	Одабрана поглавља физике јонизованих гасова	10 (десет)	15	III:(5+0+0)	13.11.2014.
5	ДС09ФРНД2	Рад на докторату 2. део	П.	30	III:(0+0+15) IV:(0+0+15)	
6	ДС09ЈП5	Физика електричних гасних пражњења	10 (десет)	15	IV:(5+0+0)	10.11.2015.

* - еквивалентиран/признат испит.

** - Фонд часова је у формату (предавања+вежбе+остало).

Општи успех: 10,00 (десет и 00/100) , по годинама студија (10,00, 10,00, /).

Овлашћено лице факултета



Кратак преглед научне активности кандидата

Кандидат, Илија Симоновић је ангажован на пројекту Министарства науке, просвете и технолошког развоја ОИ171037 „Фундаментални процеси и примене транспорта честица у неравнотежним плазмама, траповима и наноструктурама” под менторством др Саше Дујка. Основна област истраживања кандидата је кинетичка теорија транспорта наелектрисаних честица и њена примена у различитим областима примењене физике и технологије.

У првом делу својих истраживања, Илија Симоновић је посветио највећу пажњу проучавању транспортних коефицијента вишег реда за електроне и позитроне у гасовима. Применом методе групних пројектора кандидат је одредио структуру тензора, којим су репрезентовани транспортни коефицијенти трећег реда, у свим конфигурацијама електричног и магнетског поља. Примењени метод се може директно генерализовати на остале транспортне коефицијенте вишег реда. Поред тога, кандидат је проширио постојећа мулти терм решења Болцманове једначине у домен транспортних коефицијената вишег реда. Ова решења су верификована у Монте Карло симулацијама. Значајну пажњу у овом делу истраживања је посветио проучавању дуалне природе транспортних коефицијената вишег реда која је индукована експлицитним утицајем неконзервативних судара. При томе је примењено да су транспортни коефицијенти вишег реда осетљивији на експлицитне и имплицитне ефекте неконзервативних судара од брзине дрифта и дифузионог тензора.

У другом делу својих истраживања, Илија Симоновић се посветио проучавању транспорта електрона у течностима. Он је проширио постојећу инфраструктуру засновану на Монте Карло симулацијама и теорији за пренос импулса из домена гасова у домен неполарних течности. При томе је анализирао утицај различитог третмана нееластичних судара на профиле зависности транспортних коефицијента од редукованог електричног поља. Резултати ових проучавања су искоришћени за истраживања транзиције електронских лавина у стримере и њихову пропагацију у течностима. Кандидат проучава на који начин различит третман елементарних процеса попут рекомбинације електрона и позитивних јона, дуалност транспортних коефицијената и комплексност коришћених флуидних модела утичу на динамику стримера у течностима

Резултати досадашњег рада су приказани у два рада (M21a и M21). При томе је први рад објављен, а други је прихваћен за објављивање. Кандидат је коаутор на неколико уводних предавања и аутор већег броја радова на домаћим и међународним конференцијама.

Electron swarm properties under the influence of a very strong attachment in SF₆ and CF₃I obtained by Monte Carlo rescaling procedures

This content has been downloaded from IOPscience. Please scroll down to see the full text.

2016 Plasma Sources Sci. Technol. 25 065010

(<http://iopscience.iop.org/0963-0252/25/6/065010>)

View [the table of contents for this issue](#), or go to the [journal homepage](#) for more

Download details:

IP Address: 147.91.1.45

This content was downloaded on 20/10/2016 at 08:26

Please note that [terms and conditions apply](#).

You may also be interested in:

[Boltzmann equation and Monte Carlo studies of electron transport in resistive plate chambers](#)

D Bošnjakovi, Z Lj Petrovi, R D White et al.

[Non-conservative electron transport in CF₄](#)

S Dujko, R D White, K F Ness et al.

[Positron transport in water vapour](#)

A Bankovi, S Dujko, R D White et al.

[High-order fluid model for streamer discharges: I. Derivation of model and transport data](#)

S Dujko, A H Markosyan, R D White et al.

[A multi-term solution of the nonconservative Boltzmann equation](#)

S Dujko, R D White, Z Lj Petrovi et al.

[Monte Carlo studies of electron transport in CF₄](#)

S Dujko, Z M Raspopovi and Z Lj Petrovi

[Fluid modeling of resistive plate chambers: impact of transport data on development of streamers and induced signals](#)

D Bošnjakovi, Z Lj Petrovi and S Dujko

Electron swarm properties under the influence of a very strong attachment in SF₆ and CF₃I obtained by Monte Carlo rescaling procedures

J Mirić¹, D Bošnjaković¹, I Simonović¹, Z Lj Petrović^{1,2} and S Dujko¹

¹ Institute of Physics, University of Belgrade, PO Box 68, 11080 Belgrade, Serbia

² Serbian Academy of Sciences and Arts, Knez Mihailova 35, 11001 Belgrade, Serbia

E-mail: sasa.dujko@ipb.ac.rs

Received 13 May 2016, revised 28 July 2016

Accepted for publication 19 September 2016

Published 14 October 2016



Abstract

Electron attachment often imposes practical difficulties in Monte Carlo simulations, particularly under conditions of extensive losses of seed electrons. In this paper, we discuss two rescaling procedures for Monte Carlo simulations of electron transport in strongly attaching gases: (1) discrete rescaling, and (2) continuous rescaling. The two procedures are implemented in our Monte Carlo code with an aim of analyzing electron transport processes and attachment induced phenomena in sulfur-hexafluoride (SF₆) and trifluoroiodomethane (CF₃I). Though calculations have been performed over the entire range of reduced electric fields E/n_0 (where n_0 is the gas number density) where experimental data are available, the emphasis is placed on the analysis below critical (electric gas breakdown) fields and under conditions when transport properties are greatly affected by electron attachment. The present calculations of electron transport data for SF₆ and CF₃I at low E/n_0 take into account the full extent of the influence of electron attachment and spatially selective electron losses along the profile of electron swarm and attempts to produce data that may be used to model this range of conditions. The results of Monte Carlo simulations are compared to those predicted by the publicly available two term Boltzmann solver BOLSIG+. A multitude of kinetic phenomena in electron transport has been observed and discussed using physical arguments. In particular, we discuss two important phenomena: (1) the reduction of the mean energy with increasing E/n_0 for electrons in SF₆ and (2) the occurrence of negative differential conductivity (NDC) in the bulk drift velocity only for electrons in both SF₆ and CF₃I. The electron energy distribution function, spatial variations of the rate coefficient for electron attachment and average energy as well as spatial profile of the swarm are calculated and used to understand these phenomena.

Keywords: Monte Carlo, electron transport, electron attachment, SF₆, CF₃I

(Some figures may appear in colour only in the online journal)

1. Introduction

Electron transport in strongly attaching gases has long been of interest, with applications in many areas of fundamental physics and technology. Electron attaching gases support key processes for plasma etching and cleaning in semiconductor

fabrication [1, 2], high-voltage gas insulation [3] and particle detectors in high energy physics [4–6]. The importance of studies of electron attachment has also been recognized in other fields, including planetary atmospheres, excimer lasers, plasma medicine and lighting applications, as well as in life science for understanding radiation damage in biological matter.

The fundamental importance of electron attachment processes has led to many experimental and theoretical swarm studies. For some gases the cross sections for attachment may be very large resulting in a rapid disappearance of free electrons that greatly complicates the measurements of transport coefficients [1, 7–9]. The pioneering studies date back to the 1970s, and the well-known swarm method of deriving cross section for electron attachment developed by Christophorou and his co-workers [10]. According to this method, trace amounts of an electron attaching gas are mixed into the buffer gases, typically nitrogen to scan the lower mean energies and argon to scan the higher mean energies. This technique results in the removal of electrons without disturbing the electron energy distribution function. In such mixtures the losses depend only on the very small amount of the added gas and we may measure the density reduced electron attachment rate coefficient. Electron attachment cross sections can be determined by deconvoluting the mixture data, since the electron energy distribution function is a known function of E/n_0 as calculated for the pure buffer gas. Examples of this procedure are cross sections for electron attachment in SF₆ and SF₆-related molecules [11–15] as well as cross sections and rate coefficients for a range of fluorocarbons [1, 12, 16–18] and other relevant gases for applications [1, 19–22]. In addition to non-equilibrium data, there is a separate category of experiments, including flowing afterglow, the Cavalleri diffusion experiment [9, 23, 24], and others that provide attachment rates for thermal equilibrium (i.e. without an applied electric field). These may be taken at different temperatures, but the range of energies covered by this technique is very narrow. These two techniques have been used to evaluate the cross sections for SF₆ and CF₃I, always under the assumption that the effect of attachment is merely on the number of particles and not on any other swarm properties.

A thorough understanding of the influence of attachment on the drift and diffusion of the electrons provides information which could be used in analysis of kinetic phenomena in complex electronegative gases and related plasmas. The attachment cooling and heating [25, 26], negative absolute electron flux mobility [27, 60] and anomalous phase shifts of drift velocity in AC electric fields [28] are some examples of these phenomena in strongly attaching gases, which may not be trivially predicted on the basis of individual collision events and external fields. Negative differential conductivity (NDC) induced by 3-body attachment for lower E/n_0 and higher pressures in molecular oxygen and its mixture with other gases is another example of phenomena induced by strong electron attachment [29]. The duality in transport coefficients, e.g. the existence of two fundamentally different families of transport coefficients, the bulk and flux, is caused by the explicit effects of electron impact ionization and electron attachment [7, 30–32]. The differences between two sets of data vary from a few percents to a few orders of magnitude and hence a special care is needed in the implementation of data in fluid models of plasma discharges [7, 31, 33–35]. On one hand, most plasma modeling is based on flux quantities while experiments aimed at yielding cross section data provide mostly but not uniquely the bulk transport data. This differentiation between flux and

bulk transport properties is not merely a whimsey of theorists, but it is essential in obtaining and applying the basic swarm data. In addition, the production of negative ions has a large effect on the transport and spatial distribution of other charged particle species as well as on the structure of the sheath and occurrence of relaxation oscillations in charged particle densities [36–41].

There are three main approaches to the theoretical description of electron transport in gases: the kinetic Boltzmann equation, the stochastic particle simulation by the Monte Carlo method and semi-quantitative momentum transfer theory. Restrictions on the accuracy of momentum transfer theory for studies of electron transport in attaching gases, particularly under non-hydrodynamic conditions, have already been discussed and illustrated [31, 42, 43]. Boltzmann equation analyses for SF₆ and its mixtures with other gases (see for example [11, 44–50]) have been performed several times in the past. Two important studies devoted to the calculation of electron swarm parameters based on a Boltzmann equation have also been performed for CF₃I [51, 52]. Theories for solving the Boltzmann equation were usually restricted to low-order truncations in the Legendre expansions of the velocity dependence assuming quasi-isotropy in velocity space. The explicit effects of electron attachment were also neglected and electron transport was studied usually in terms of the flux data only. These theories had also restricted domains of validity on the applied E/n_0 in spite of their coverage of a considerably broader range. One thing that strikes the reader surveying the literature on electron transport in SF₆ is the systematic lack of reliable data for electron transport coefficients for E/n_0 less than 50 Td. Contemporary moment methods for solving Boltzmann's equation [31, 53] are also faced with a lot of systematic difficulties, particularly under conditions of the predominant removal of the lower energy electrons which results in an increase in the mean energy, i.e. attachment heating. Under these conditions the bulk of the distribution function is shifted towards a higher energy which in turn results in the high energy tail falling off much slower than a Maxwellian. This is exactly what may happen in the analysis of electron transport in strongly attaching gases such as SF₆ or CF₃I for lower E/n_0 . The moment method for solving Boltzmann's equation under these circumstances usually requires the prohibitive number of basis functions for resolving the speed/energy dependency of the distribution function and/or unrealistically large computation time. As a consequence, the standard numerical schemes employed within the framework of moment methods usually fail.

The present investigation is thus mainly concerned with the Monte Carlo simulations of electron transport in strongly attaching gases. Monte Carlo simulations have also been employed for the analysis of electron transport in the mixtures of SF₆ [46, 54–57] and CF₃I [58] with other gases usually with an aim of evaluating the insulation strength and critical electric fields. However, electron attachment in strongly electronegative gases often imposes practical difficulties in Monte Carlo simulations. This is especially noticeable at lower E/n_0 , where electron attachment is one of the dominant processes which may lead to the extensive vanishing of the seed electrons and

consequently to the decrease of the statistical accuracy of the output results. In extreme cases, the entire electron swarm might be consumed by attachment way before the equilibrated (steady-state regime) is achieved. An obvious solution would be to use a very large number of initial electrons, but this often leads to a dramatic increase of computation time and/or required memory/computing resources which are beyond practical limits. Given the computation restrictions of the time, the workers were forced to develop methods to combat the computational difficulties induced by the extensive vanishing of the seed electrons. Two general methods were developed: (1) addition of new electrons by uniform scaling of the electron swarm at certain time instants under hydrodynamic conditions [26, 59] or at certain positions under steady-state Townsend conditions [60], when number of electrons reaches a pre-defined threshold, and (2) implementation of an additional fictitious ionization channel/process with a constant collision frequency (providing that the corresponding ionization rate is chosen to be approximately equal to the attachment rate) [54]. On the other hand, similar rescaling may be applied for the increasing number of electrons as has been tested at the larger E/n_0 by Li *et al* [61]. Further distinction and specification between methods developed by Nolan *et al* [26] and Dyatko *et al* [60] on one hand and Raspopović *et al* [59] on the other, will be discussed in later sections. These methods have not been compared to each other in a comprehensive and rigorous manner. This raises a number of questions. How accurate, these methods are? Which is the more efficient? Which is easier for implementation? What is their relationship to each other? Which one is more flexible? In this paper, we will try to address some of these issues. In particular, the present paper serves to summarize the salient features of these methods in a way which we hope will be of benefit to all present and future developers of Monte Carlo codes. Finally, it is also important to note that in the present paper we extend the method initially developed by Yousfi *et al* [54], by introducing time-dependent collision frequency for the fictitious ionization process.

This paper is organized as follows: in section 2, we briefly review the basic elements of our Monte Carlo code, before detailing the rescaling procedures employed to combat the computational difficulties initiated by the rapid disappearance of electrons. In the same section, we illustrate the issue of electron losses by considering the evolution of the number of electrons for a range of E/n_0 in SF₆ and CF₃I. In section 3, we evaluate the performance of rescaling procedures by simulating electron transport in SF₆ and CF₃I over a wide range of E/n_0 . We will also highlight the substantial difference between the bulk and flux transport coefficients in SF₆ and CF₃I. Special attention will be paid to the occurrence of negative differential conductivity (NDC) in the profile of the bulk drift velocity. For electrons in SF₆ another phenomenon arises: for certain reduced electric fields we find regions where the swarm mean energy decreases with increasing E/n_0 . In the last segment of the section 3, we discuss two important issues: (1) how to use the rescaling procedures in Monte Carlo codes, and (2) rescaling procedures as a tool in the modeling of non-hydrodynamic effects in swarm experiments. In section 4, we present our conclusions and recommendations.

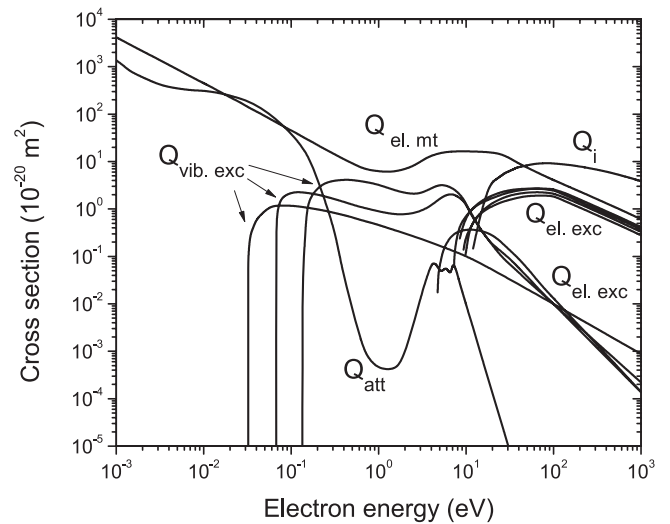


Figure 1. Electron impact cross-sections for CF₃I used in this study [62]: $Q_{el, mt}$ momentum transfer in elastic collisions, $Q_{vib, exc}$ vibrational excitation, $Q_{el, exc}$ electronic excitation, Q_{att} dissociative attachment and Q_i electron-impact ionization.

2. Input data and computational methods

2.1. Cross sections for electron scattering and simulation conditions

We begin this section with a brief description of cross sections for electron scattering in SF₆ and CF₃I. For the SF₆ cross sections we use the set developed by Itoh *et al* [47]. This set was initially based on published measurements of cross sections for individual collision processes. Using the standard swarm procedure, the initial set was modified to improve agreement between the calculated swarm parameters and the experimental values. The set includes one vibrational channel, one electronic excitation channel, as well as elastic, ionization and five different attachment channels.

This study considers electron transport in CF₃I using the cross section set developed in our laboratory [62]. This set of cross sections is shown in figure 1. It should be noted that this set is similar but not identical to that developed by Kimura and Nakamura [63]. We have used the measured data under pulsed Townsend conditions for pure CF₃I and its mixtures with Ar and CO₂ in a standard swarm procedure with the aim of improving the accuracy and completeness of a set of cross sections. It consists of the elastic momentum transfer cross section, three cross sections for vibrational and five cross sections for electronic excitations as well as one cross section for electron-impact ionization with a threshold of 10.4 eV and one cross section for dissociative attachment. For more details the reader is referred to our future paper [64].

For both SF₆ and CF₃I all electron scattering are assumed isotropic and hence the elastic cross section is the same as the elastic momentum transfer cross section. Simulations have been performed for E/n_0 ranging from 1 to 1000 Td. The pressure and temperature of the background gas are 1 Torr and 300 K, respectively. It should be mentioned that special care in our Monte Carlo code has been paid to proper treatment of the thermal motion of the host gas molecules and their influence

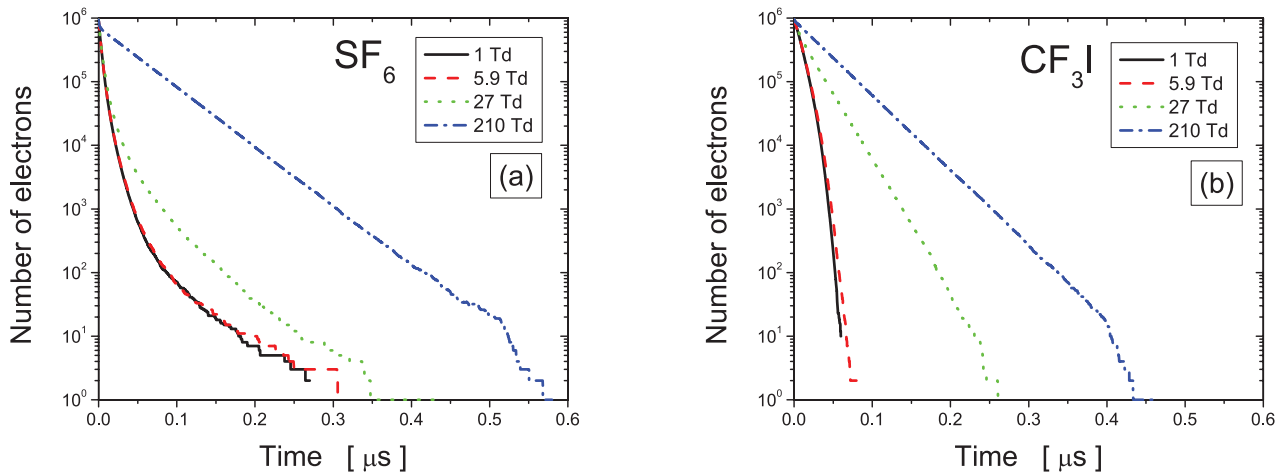


Figure 2. Electron number density decay for four different reduced electric fields as indicated on the graph. Calculations are performed for SF₆ (a) and CF₃I (b).

on electrons, which is very important at low electric fields, when the mean electron energy is comparable to the thermal energy of the host gas [65]. After ionization, the available energy is partitioned between two electrons in such a way that all fractions of the distribution are equally probable.

2.2. Monte Carlo method

The Monte Carlo simulation technique used in the present work is described at length in our previous publications [32, 53, 59, 66, 67]. In brief, we follow the spatiotemporal evolution of each electron through time steps which are fractions of the mean collision time. In association with random numbers, these finite time steps are used to solve the integral equation for the collision probability in order to determine the time of the next collision. The number of time steps is determined in such a way as to optimize the performance of the Monte Carlo code without reducing the accuracy of the final results. When the moment of the next collision is established, the additional sequences of random numbers are used, first to determine the nature of a collision, taking into account the relative probabilities of the various collision types, and second to determine the change in the direction of the electron velocity. All dynamic properties of each electron such as position, velocity, and energy are updated between and after the collisions. Sampling of electron dynamic properties is not correlated to the time of the next collision and is performed in a way that ensemble averages can be taken in both the velocity and configuration space. Explicit formulas for the bulk and flux transport properties have been given in our previous publications [59, 66]. To evaluate the accuracy of the Monte Carlo code, Boltzmann analyses were performed in parallel with the Monte Carlo calculations using the multi term method described in detail by Dujko *et al* [53]. In addition, we use the BOLSIG+, a publicly available Boltzmann solver based on a two term theory [68]. The most recent version of this code might be used to study the electron transport in terms of both the flux and bulk data which is very useful for some aspects of plasma modeling [7]. At the same time, the comparison between our results and those computed by BOLSIG+ which is presented in this paper, should

be viewed as the first benchmark for the bulk BOLSIG+ data. Our Monte Carlo code and multi term codes for solving the Boltzmann equation have been subject of a detailed testing for a wide range of model and real gases [31, 53, 59, 67].

In figure 2 we illustrate the losses of electrons during the evolution of the swarm towards the steady-state. The initial number of electrons is set to 1×10^6 and calculations are performed for a range of reduced electric fields E/n_0 as indicated on the graphs. For both SF₆ and CF₃I, we observe that at small E/n_0 , i.e. at low mean energies, the number of electrons decreases much faster. This is a clear sign that collision frequency for electron attachment increases with decreasing E/n_0 . Electrons in CF₃I are lost continuously and consequently the number of electrons in the swarm decreases exponentially with time. The same trend may be observed for electrons in SF₆ at 210 Td. For the remaining E/n_0 the number of electrons is reduced with time even faster. Comparing SF₆ and CF₃I, it is evident that the electrons are more efficiently consumed by electron attachment in SF₆ in the early stage of the simulation. Conversely, in the last stage of simulation the electrons are more consumed by electron attachment in CF₃I than in SF₆. In any case, the electron swarms in both cases are entirely consumed by attachment way before the steady-state regime and hence the simulations are stopped. In other words, the number density drops down by six orders of magnitude over the course of several hundred nanoseconds in both gases. To facilitate the numerical simulation, it is clear that some kind of rescaling of the number density is necessary to compensate for the electrons consumed by electron attachment. This procedure should not in any way disrupt the spatial gradients in the distribution function. On the other hand, releasing electrons with some fixed arbitrary initial condition would require that they equilibrate with the electric field during which time again majority of such additional electrons would be lost.

2.3. Rescaling procedures

To counteract the effect of attachment in an optimal fashion while keeping the statistical accuracy, the following rescaling procedures were proposed and applied so far:

- (1) Uniform generation of new electrons with initial properties taken from the remaining electrons thus taking advantage of the equilibration that has been achieved so far [59]. To make this procedure effective i.e. to avoid losing population in some smaller pockets of the ensemble the population should be allowed to oscillate between N_1 and N_0 , where $N_1 > N_0$ but their difference is relatively small. Here N_0 is minimum allowed number of electrons while N_1 is maximum number of electrons in the simulation after rescaling.
- (2) Uniform scaling of an electron swarm by a factor of 2 or 3 at certain instants of time [26] or distance [60] depending on the simulation conditions where the probability of scaling for each electron is set to unity.
- (3) Introduction of an additional fictitious ionization process with a constant ionization frequency (that is close to the rate for attachment), which artificially increases the number of simulated electrons [54, 61]. Uniform rescaling of the swarm is done by randomly choosing the electrons which are to be ‘duplicated’. The newborn electron has the same initial dynamic properties, coordinates, velocity, and energy as the original. Following the creation of a new electron their further histories diverge according to the independently selected random numbers.

Comparing the procedures (1) and (2), it is clear that there are no essential differences between them. The only difference lies in the fact that in the procedure (2) duplicating is performed for all the electrons in the simulation while according the procedure (1), the probability of duplication is determined by the current ratio of the number of electrons to the desired number of electrons in the simulation, which is specified in advance. On the other hand, fictitious ionization collision generates a new electron which is given the same position, velocity and energy as the primary electron that is not necessarily the electron lost in attachment. In this paper, we shall refer to the procedure (1) as *discrete rescaling*, since the procedure is applied at discrete time instants. The procedure (2) shall be termed as *swarm duplication* and finally we shall refer to the procedure (3) as the *continuous rescaling* since the rescaling is done during the entire simulation. An important requirement is that the rescaling must not perturb/change/disturb the normalized electron distribution function and its evolution. Li *et al* [61] showed that the continuous rescaling procedure meets this requirement. In case of discrete rescaling as applied to the symmetrical yet different problem of excessive ionization, it was argued that one cannot be absolutely confident that the rescaled distribution is a good representation of the original [69], except when steady state is achieved [70].

In what follows, we discuss the continuous rescaling. Following the previous works [54, 61], the Boltzmann equation for the distribution function $f(\mathbf{r}, \mathbf{c}, t)$ without rescaling and $f^*(\mathbf{r}, \mathbf{c}, t)$ with rescaling are given by:

$$(\partial_t + \mathbf{c} \cdot \nabla_{\mathbf{r}} + \mathbf{a} \cdot \nabla_{\mathbf{c}})f(\mathbf{r}, \mathbf{c}, t) = -J(f), \quad (1)$$

and

$$(\partial_t + \mathbf{c} \cdot \nabla_{\mathbf{r}} + \mathbf{a} \cdot \nabla_{\mathbf{c}})f^*(\mathbf{r}, \mathbf{c}, t) = -J(f^*) + \nu_{\text{fi}}(t)f^*, \quad (2)$$

where \mathbf{a} is the acceleration due to the external fields, $J(f)$ is the collision operator for electron-neutral collisions and ν_{fi} is time-dependent fictitious ionization rate. If the collision operator is linear (i.e. if electron–electron collisions are negligible) and if the initial distributions (at time $t = 0$) are the same, it can be easily shown that the following relationship holds

$$f^*(\mathbf{r}, \mathbf{c}, t) = f(\mathbf{r}, \mathbf{c}, t) \exp\left(\int_0^t \nu_{\text{fi}}(\tau) d\tau\right). \quad (3)$$

Substituting equation (3) into equation (2) and using the linearity of the collision operator yields the following equation

$$J(f^*) = \exp\left(\int_0^t \nu_{\text{fi}}(\tau) d\tau\right) J(f). \quad (4)$$

Note that in contrast to Li *et al* [61] the collision frequency for the fictitious ionization is now a time-dependent function. In terms of numerical implementation, the only difference between our continuous rescaling procedure and the one described in [54, 61] is that we do not need to provide the fictitious ionization rate which is estimated by trial and error, in advance (*a priori*). Instead, our fictitious ionization rate is initially chosen to be equal to the calculated attachment rate at the beginning of the simulation. Afterwards, it is recalculated at fixed time instants in order to match the newly developed attachment rates. As a result, the number of electrons during the simulation usually does not differ from the initial one by more than 10%. It should be noted that the fictitious ionization process must not in any way be linked to the process of real ionization. It was introduced only as a way to scale the distribution function, or in other words, as a way of duplicating the electrons.

3. Results and discussion

In this section the rescaling procedures and associated Monte Carlo code outlined in the previous section are applied to investigate transport properties and attachment induced phenomena for electrons in SF₆ and CF₃I. Electron transport in these two strongly attaching gases provides a good test of different rescaling procedures, particularly for lower E/n_0 where electron attachment is the dominant non-conservative process. In addition to comparisons between different rescaling procedures, the emphasis of this section is the observation and physical interpretation of the attachment induced phenomena in the E/n_0 -profiles of mean energy, drift velocity and diffusion coefficients. In particular, we investigate the differences between the bulk and flux transport coefficients. We do not compare our results with experimentally measured data as it would distract the reader’s attention to the problems associated with the quality of the sets of the cross sections for electron scattering. There are no new experimental measurements of transport coefficients for electrons in SF₆, particularly for E/n_0 less than 50 Td and thus we have deliberately chosen not to display the comparison. On the other hand, one cannot expect the multi term results to be useful here as the conditions with excessive attachment would make convergence difficult in the low E/n_0 region, where comparison would be of

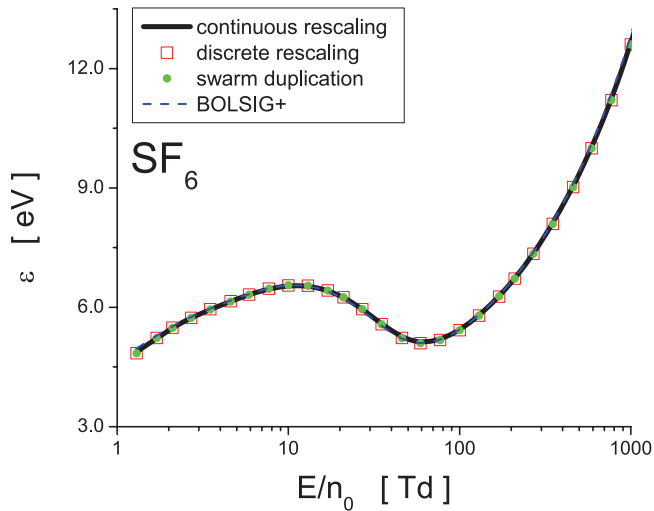


Figure 3. Variation of the mean energy with E/n_0 for electrons in SF_6 . Monte Carlo results using three different techniques for electron number density compensation (rescaling) are compared with the BOLSIG+ results.

interest. Thus, for clarity the multi term results are omitted. Both experimental and theoretical work on electron swarms in SF_6 prior to 1990 is summarized in the papers of Phelps and van Brunt [11], Gallagher *et al* [71] and Morrow [72]. Recent results can be found in the book by Raju [22] and the review article of Christophorou and Olthoff [12]. The swarm analysis and further improvements of the cross sections for electron scattering in CF_3I is a subject of our future work [64].

3.1. Transport properties for electrons in SF_6 and CF_3I

3.1.1. Mean energy. In figure 3 we show the variation of the mean energy with E/n_0 for electrons in SF_6 . The agreement between different rescaling procedures is excellent. This suggests that all rescaling procedures are equally valid for calculation of the mean energy (provided that rescaling is performed carefully). In addition, the BOLSIG+ results agree very well with those calculated by a Monte Carlo simulation technique. For lower E/n_0 , the mean energy initially increases with E/n_0 , reaching a peak at about 10 Td, and then surprisingly it starts to decrease with E/n_0 . The minimum of mean energy occurs at approximately 60 Td. For higher E/n_0 the mean energy monotonically increases with E/n_0 . The reduction in the mean energy with increasing E/n_0 has been reported for electrons in Ar [73] and O_2 [74] but in the presence of very strong magnetic fields. In the present work, however, the mean energy is reduced in absence of magnetic field which certainly represents one of the most striking and anomalous effects observed in this study. Moreover, this behavior is contrary to previous experiences in swarm physics as one would expect the mean swarm energy to increase with increasing E/n_0 . This is discussed in detail below.

In order to understand the anomalous behavior of the mean energy of electrons in SF_6 , in figure 4 we display the electron energy distribution functions for E/n_0 at 10, 27, 59 and 210 Td. Cross sections for some of the more relevant collision processes are also included, as indicated in the graph.

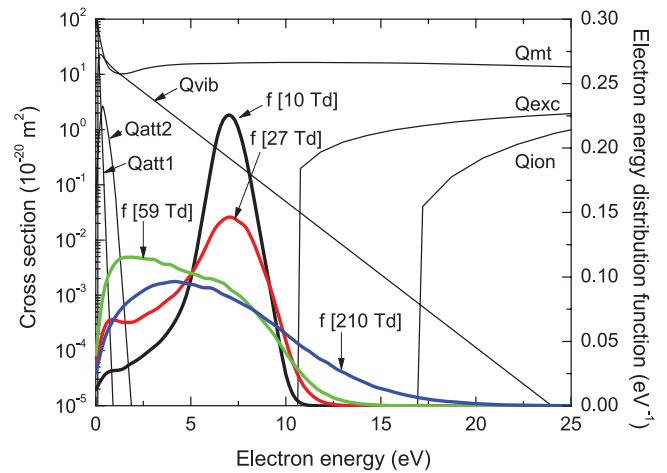


Figure 4. Electron energy distribution functions for E/n_0 of 10, 27, 59 and 210 Td. Cross sections for elastic momentum transfer (Qmt), electronic excitation (Qexc) and ionization (Qion) as well as for attachments that lead to the formation of SF_6^- (Qatt1) and SF_5^- (Qatt2) ions, are also included.

For clarity, the attachment cross sections for the formation of SF_4^- , F_2^- and F^- are omitted in the figure. For E/n_0 of 10 and 27 Td we observe the clear signs of ‘hole burning’ in the electron energy distribution function (EEDF). This phenomenon has been extensively discussed for electrons in O_2 [75, 76], O_2 mixtures [29, 77] and under conditions leading to the phenomenon of absolute negative electron mobility [27, 60] as well as for electrons in the gas mixtures of $\text{C}_2\text{H}_2\text{F}_4$, iso- C_4H_{10} and SF_6 used in resistive plate chambers in various high energy physics experiments at CERN [6]. For electrons in SF_6 , the collision frequency for electron attachment decreases with energy and hence the slower electrons at the trailing edge of the swarm are preferentially attached. As a consequence, the electrons are ‘bunched’ in the high-energy part of the distribution function which in turn moves the bulk of the distribution function to higher energies. This is the well-known phenomenon of attachment heating which has already been discussed in the literature for model [25, 26] and real gases [6, 29]. In the limit of the lowest E/n_0 we see that due to attachment heating the mean energy attains the unusually high value of almost 5 eV. For a majority of molecular gases, however, the mean energy is significantly reduced for lower E/n_0 due to presence of rotational, vibrational and electronic excitations which have threshold energies over a wide range. As E/n_0 further increases the mean energy is also increased as electrons are accelerated through a larger potential. However, in case of SF_6 , for E/n_0 increasing beyond 10 Td the mean energy is reduced. This atypical situation follows from the combined effects of attachment heating and inelastic cooling. From figure 4 we see that for E/n_0 of 27 and 59 Td the electrons from the tail of the corresponding distribution functions have enough energy to undergo the electronic excitation. Whenever an electron undergoes electronic excitations (or ionization) it loses the threshold energy of 9.8 eV (or 15.8 eV in case of ionization) and emerges from the collision with a reduced energy. This in turn diminishes the phenomenon of ‘hole burning’ in the distribution function by repopulating

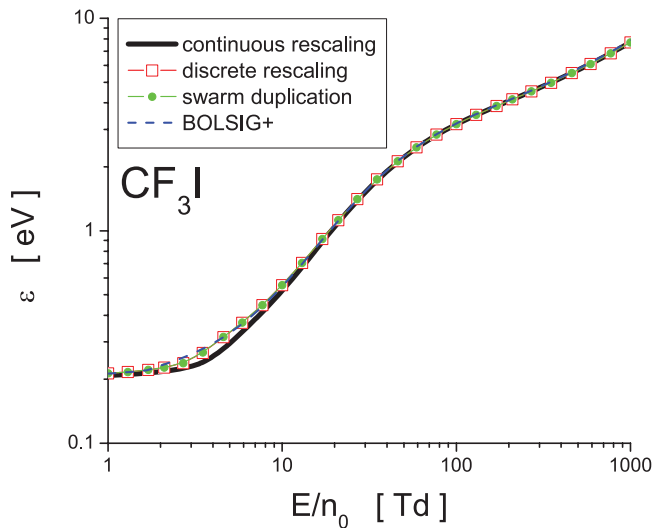


Figure 5. Variation of the mean energy with E/n_0 for electrons in CF_3I . Monte Carlo results using three different techniques for electron compensation are compared with the BOLSIG+ results.

the distribution function at the lower energy. The combined effects of attachment heating and inelastic cooling and subsequent redistribution of low-energy electrons are more significant for the energy balance than the energy gain from electric field and losses in other collisions. The vibrational excitation with the threshold of 0.098 eV is of less importance having in mind the actual values of the mean energy. For E/n_0 higher than 60 Td, the dominant part in the energy balance is the energy gain from the electric field while attachment heating and induced phenomena are significantly suppressed. Thus, for E/n_0 higher than 60 Td the mean energy monotonically increases with increasing E/n_0 .

The variation of the mean energy with E/n_0 for electrons in CF_3I is shown in figure 5. The agreement between different rescaling procedures is very good. Small deviations between discrete rescaling and swarm duplication from one side and continuous rescaling from the other side are present between approximately 3 and 20 Td. BOLSIG+ slightly overestimates the mean energy only in the limit of the lowest E/n_0 . In contrast to mean energy of the electrons in SF_6 , the mean energy of the electrons in CF_3I monotonically increases with E/n_0 without signs of anomalous behavior. If we take a careful look, then we can isolate three distinct regions of electron transport in CF_3I as E/n_0 increases. First, there is an initial region where the mean energy raises relatively slowly due to large energy loss of the electrons in low-threshold vibrational excitations. In this region the mean energy of the electrons is well above the thermal energy due to extensive attachment heating. The mean energy is raised much sharper between approximately 5 and 50 Td, indicating that electrons become able to overcome low-threshold vibrational excitations. The following region of slower rise follows from the explicit cooling of other inelastic processes, including electronic excitations and ionization, as these processes are now turned on. In conclusion, the nature of cross sections for electron scattering in CF_3I and their energy dependence as well as their mutual relations do not favor the development of the anomalous behavior of the swarm mean energy.

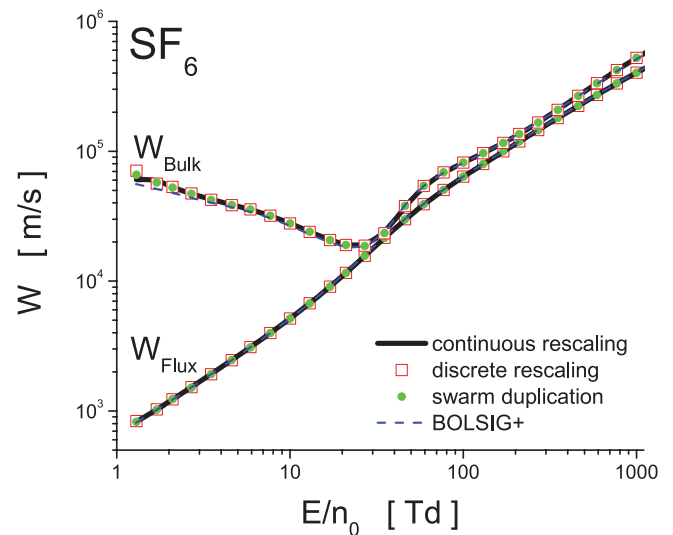


Figure 6. Variation of the drift velocity with E/n_0 for electrons in SF_6 . Monte Carlo results using three different techniques for electron number density compensation are compared with the BOLSIG+ results.

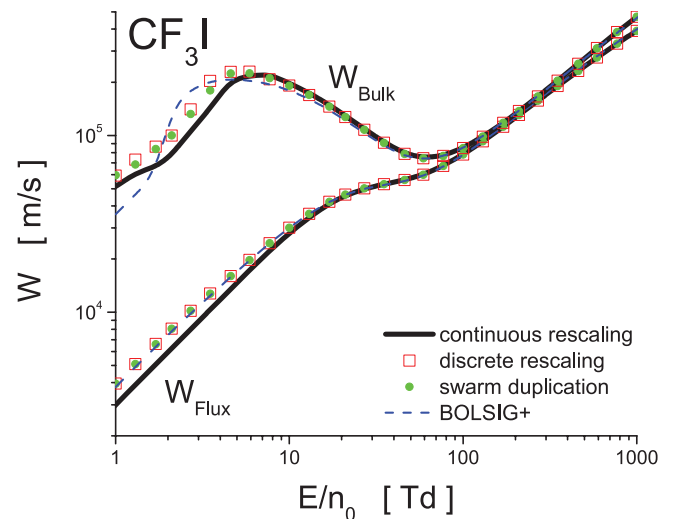


Figure 7. Variation of the drift velocity with E/n_0 for electrons in CF_3I . Monte Carlo results using three different techniques for electron number density compensation are compared with the BOLSIG+ results.

3.1.2. Drift velocity. In figures 6 and 7 we show variation of the bulk and flux drift velocity with E/n_0 for electrons in SF_6 and CF_3I , respectively. For electrons in SF_6 the agreement between different rescaling procedures for electron compensation is excellent for both the bulk and flux drift velocity over the entire E/n_0 range considered in this work. The BOLSIG+ bulk results slightly underestimate the corresponding bulk Monte Carlo results in the limit of the lowest E/n_0 . For electrons in CF_3I , the agreement among different rescaling procedures for electron compensation is also good except for lower E/n_0 where the continuous rescaling gives somewhat lower results than other techniques.

For both SF_6 and CF_3I , we see that the bulk dominates the flux drift velocity over the entire E/n_0 range considered in this work. For lower E/n_0 this is a consequence of a very intense

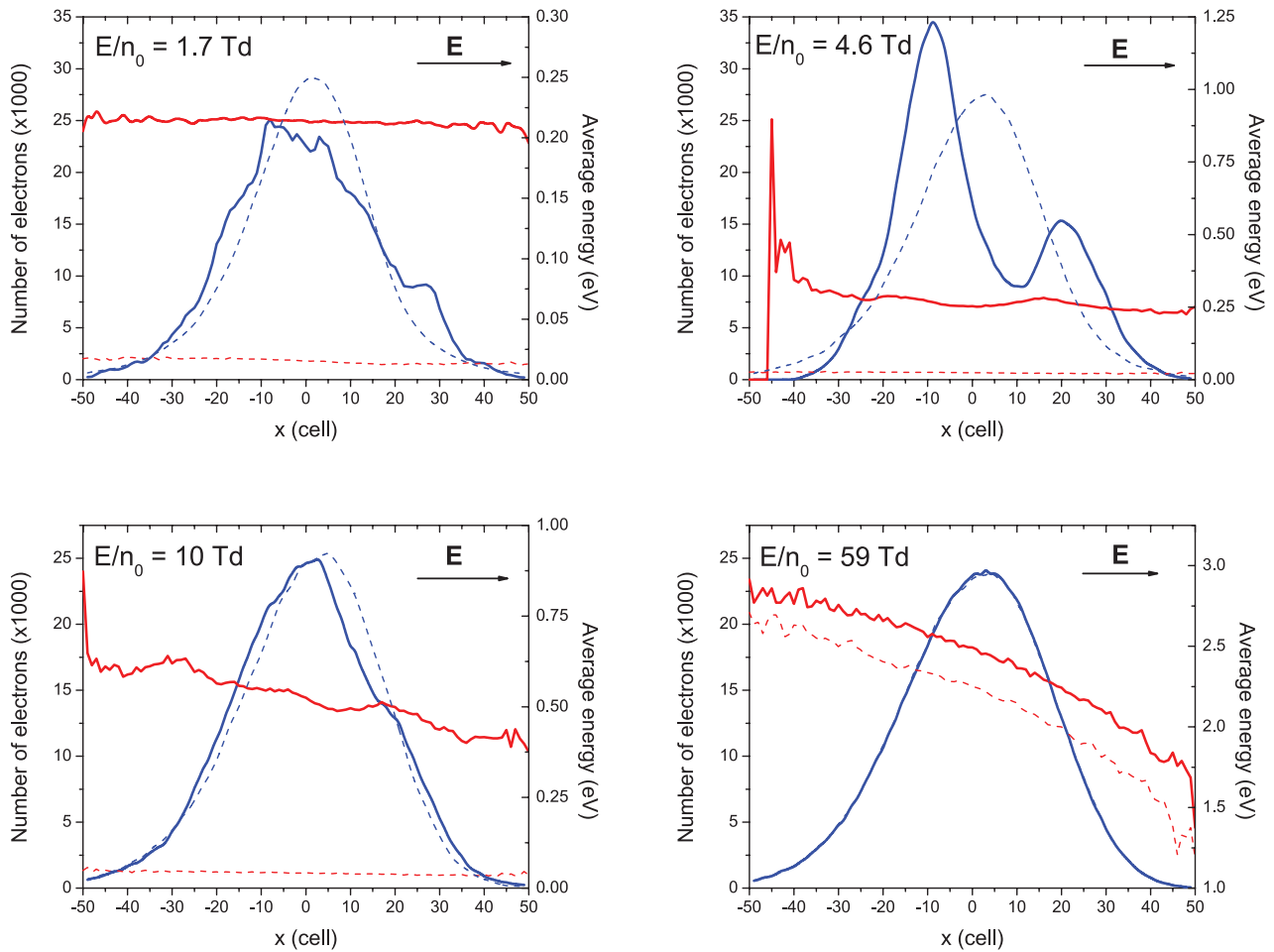


Figure 8. Spatial profile of electrons (blue curves) and spatially resolved averaged energy (red curves) at four different E/n_0 in CF_3I . Full lines denote the results when electron attachment is treated as a non-conservative process, while the dashed lines represent our results when electron attachment is treated as a conservative inelastic process with zero energy loss.

attachment heating while for higher E/n_0 this follows from the explicit effects of ionization. As mentioned above, when transport processes are greatly affected by attachment heating the slower electrons at the back of the swarm are consumed at a faster rate than those at the front of the swarm. Thus, in the case of drift, the electron attachment acts to push the centre of mass forward, increasing the bulk drift velocity above its flux component. For higher E/n_0 when ionization takes place, the ionization rate is higher for faster electrons at the front of the swarm than for slower electrons at the back of the swarm. As a result, electrons are preferentially created at the front of the swarm which results in a shift in the centre of mass. Of course, this physical picture is valid if collision frequency for ionization is an increasing function of electron energy. This is true for electrons in both SF_6 and CF_3I . The explicit effects of electron attachment are much stronger than those induced by ionization. When ionization is dominant non-conservative process, the differences between two sets of data are within 30% for both gases. When attachment dominates ionization, however, then the discrepancy between two sets of data might be almost two orders of magnitude, as for electrons in SF_6 in the limit of the lowest E/n_0 .

The flux drift velocity is a monotonically increasing function of E/n_0 while the bulk component behaves in a qualitatively

different fashion. A prominent feature of electron drift in SF_6 and CF_3I is the presence of a very strong NDC in the profile of the bulk drift velocity. On the other hand, a decrease in the flux drift velocity with increasing E/n_0 has not been observed. Such behavior is similar of the recently observed NDC effect for positrons in molecular gases [78, 79] where Positronium (Ps) formation plays the role of electron attachment.

In order to provide physical arguments for an explanation of NDC in the bulk drift velocity, in figure 8 we show the spatial profile and spatially resolved average energy of electrons in CF_3I . Calculations are performed for four different values of E/n_0 as indicated in the graph. The direction of the applied electric field is also shown. Two fundamentally different scenarios are discussed: (1) the electron attachment is treated as a conservative inelastic process with zero energy loss, and (2) the electron attachment is treated regularly, as a true non-conservative process. The first scenario is made with the aim of illustrating that NDC is not primarily caused by the shape of cross section for attachment but rather by the synergism of explicit and the implicit effects of the number changing nature of the process on electron transport. Sampling of spatially resolved data in our Monte Carlo simulations is performed using the continuous rescaling. The continuous rescaling produces smoother curves and in most cases it is more reliable

as compared to the discrete rescaling and swarm duplication. The results of the first scenario are presented by dashed lines while the second scenario where electron attachment is treated as a true non-conservative process, is represented by full lines.

When electron attachment is treated as a conservative inelastic process, the spatial profile of electrons has a well defined Gaussian profile with a small bias induced by the effect of electric field. The non-symmetrical feature of spatial profile is further enhanced with increasing E/n_0 . While for lower E/n_0 the spatial variation of the average energy is relatively low, for higher E/n_0 , e.g. for E/n_0 of 59 Td the slope of the average energy is quite high, indicating that the electron swarm energy distribution is normally spatially anisotropic. It is important to note that there are no imprinted oscillations in the spatial profile of the electrons or in the profile of the average energy which is a clear sign that the collisional energy loss is governed essentially by 'continuous' energy loss processes [32].

When electron attachment is treated as a true non-conservative process, the spatial profile and the average energy of electrons are drastically changed. For all considered reduced electric fields spatially resolved average energy is greater as compared to the case when electron attachment is treated as a conservative inelastic process. For E/n_0 of 1.7 and 4.6 Td the spatial profiles of electrons depart from a typical Gaussian shape. For 1.7 Td there is very little spatial variation in the average energy along the swarm. When $E/n_0 = 4.6$ Td, however, the spatial profile is skewed, asymmetric and shifted to the left. This shift corresponds approximately to the difference between bulk drift velocities in the two scenarios. We observe that the trailing edge of the swarm is dramatically cut off while the average energy remains essentially unaltered. At the leading edge of the swarm, however, we observe a sharp jump in the average energy which is followed by a sharp drop-off. In addition, the height of spatial profile is significantly increased in comparison to the Gaussian profile of the swarm when electron attachment is treated as a conservative inelastic process. For higher E/n_0 the signs of explicit effects of electron attachment are still present but are significantly reduced. For $E/n_0 = 10$ Td the spatial dependence of the average energy is almost linear with a small jump at the leading edge of the swarm. Comparing trailing edges of the swarms at 4.6 and 10 Td we see that for higher electric field the spatial profile of electrons is by far less cut off. This suggests that for increasing E/n_0 there are fewer and fewer electrons that are consumed by electron attachment. Finally, for $E/n_0 = 59$ Td the spatial profile of electrons is exactly the same as the profile obtained under conditions when electron attachment is treated as a conservative inelastic process.

The spatially resolved attachment rates are displayed in figure 9 and are calculated under the same conditions as for the spatial profile of the electrons and spatially averaged energy. We see that the attachment rate peaks at the trailing edge of the swarm where the average energy of the electrons is lower. Attachment loss of these lower energy electrons causes a forward shift to the swarm centre of mass, with a corresponding increase in the bulk drift velocity. For increasing E/n_0 , the spatially resolved attachment rate coefficients are reduced and linearly decrease from the trailing edge towards the leading

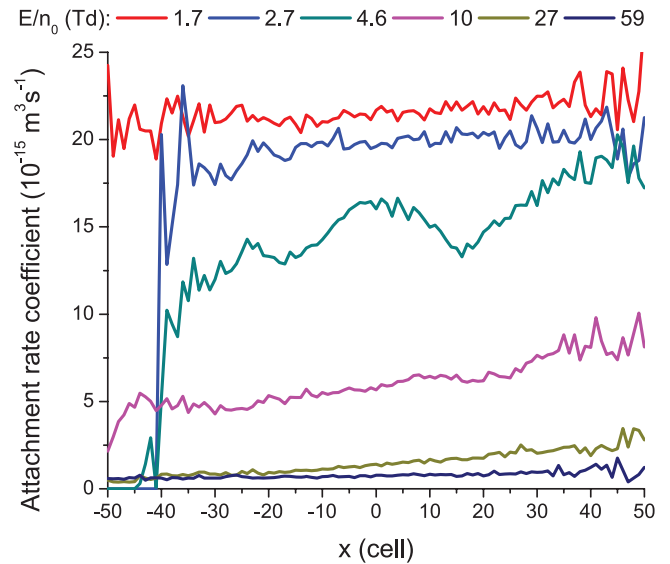


Figure 9. Spatially resolved attachment rate coefficient for a range of E/n_0 as indicated on the graph. Calculations are performed for electrons in CF_3I .

part of the swarm. At the same time the electrons at the leading edge of the swarm have enough energy to undergo ionization. This suggests much less explicit influence of electron attachment on the electron swarm behavior. As a consequence, NDC is removed from the profile of the bulk drift velocity.

In addition to the explicit effects of electron attachment there are implicit effects due to energy specific loss of electrons, which changes the swarm energy distribution as a whole, and thus indirectly changes the swarm flux. Generally speaking, it is not possible to separate the explicit from implicit effects, except by analysis with and without the electron attachment. Using these facts as motivational factors, in figure 10 we show the electron energy distribution functions for the same four values of E/n_0 considered above. The electron energy distribution functions are calculated when electron attachment is treated as a true non-conservative process (full line) and under conditions when electron attachment is assumed to be a conservative inelastic process (dashed line). As for electrons in SF_6 , we observe a 'hole burning' effect in the energy distribution function which is certainly one of the most illustrative examples of the implicit effects. Likewise, we see that the high energy tail of the distribution function falls off very slowly even slower than for Maxwellian. Under these circumstances, when the actual distribution function significantly deviates from a Maxwellian, the numerical schemes for solving the Boltzmann equation in the framework of moment methods usually fail. Indeed, for E/n_0 less than approximately 20 Td we have found a sudden deterioration in the convergence of the transport coefficients which was most pronounced for the bulk properties. Furthermore, we see that the 'hole burning' effect is not present when electron attachment is treated as a conservative inelastic process. The lower energy part of the distribution function is well populated while high energy part falls off rapidly. For increasing E/n_0 and when electron attachment is treated as a true non-conservative process, the effect of hole burning is reduced markedly while

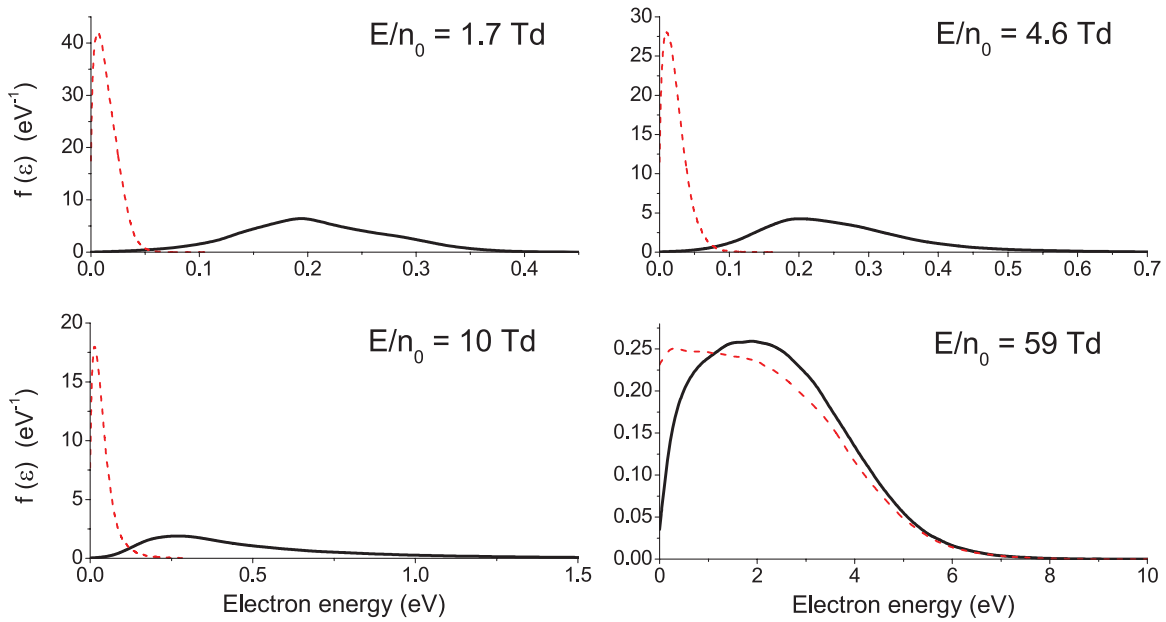


Figure 10. Energy distribution functions for four different E/n_0 for electrons in CF_3I . Black lines denote the results when electron attachment is treated as non-conservative process while dashed red lines represent our results when electron attachment is treated as a conservative inelastic process.

the high energy part of the distribution function coincides with the corresponding one when electron attachment is treated as a conservative inelastic process.

Before embarking on a discussion of our results for diffusion coefficients, one particular point deserves more mention. NDC phenomenon in the bulk drift velocity has not been experimentally verified, neither for SF_6 nor for CF_3I . On the other hand, as we have already seen, the two entirely different theoretical techniques for calculating the drift velocity predict the existence of the phenomenon. Thus, it would be very useful to extend the recent measurements of the drift velocity in both SF_6 and CF_3I to lower E/n_0 with the aim of confirming the existence of NDC. On the other hand, such measurements are most likely very difficult, even impossible due to rapid losses of electron density in experiment.

3.1.3. Diffusion coefficients. Variations of the longitudinal and transverse diffusion coefficients with E/n_0 for electrons in SF_6 are displayed in figures 11 and 12, respectively. From the E/n_0 -profiles of the longitudinal and transverse flux diffusion coefficients, we observe that different rescaling procedures for Monte Carlo simulations agree very well. For the bulk components, the agreement is also very good for intermediate and higher E/n_0 and only in the limit of the lowest E/n_0 the agreement is deteriorated. Over the range of E/n_0 considered we see that there is an excellent agreement between continuous and discrete rescaling.

Comparing Monte Carlo and BOLSIG+ results, the deviations are clearly evident. They might be attributed to the inaccuracy of the two term approximation of the Boltzmann equation which is always considerably higher for diffusion than for the drift velocity. For higher E/n_0 , inelastic collisions are significant and the distribution function deviates substantially from isotropy in velocity space. In these circumstances,

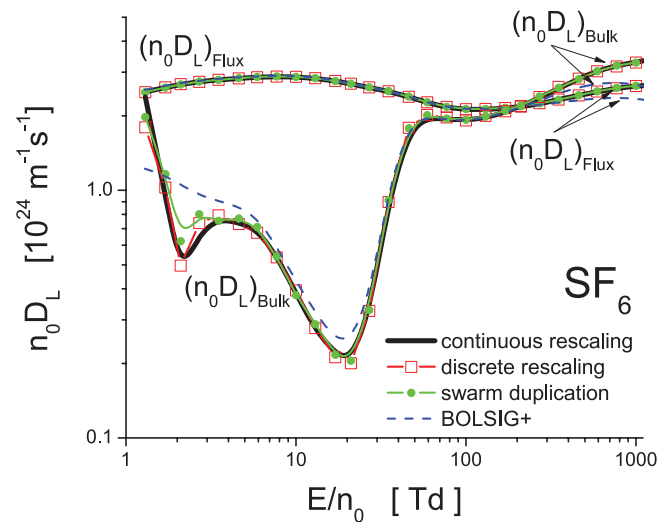


Figure 11. Variation of the longitudinal diffusion coefficient with E/n_0 for electrons in SF_6 . Monte Carlo results using three different techniques for electron number density compensation are compared with the BOLSIG+ results.

the two term approximation of the Boltzmann equation fails and multi-term Boltzmann equation analysis is required. For lower E/n_0 , however, the role of inelastic collisions is of less significance, but still discrepancies between the BOLSIG+ and Monte Carlo results are clearly evident, particularly for the longitudinal diffusion coefficient. This suggests that further analyses of the impact of electron attachment on the distribution function in velocity space of electrons in SF_6 would be very useful.

From the profiles of the longitudinal diffusion coefficient at lower and intermediate values of E/n_0 we observe the following interesting points. In contrast to drift velocity (and transverse diffusion coefficient shown in figure 12) we see

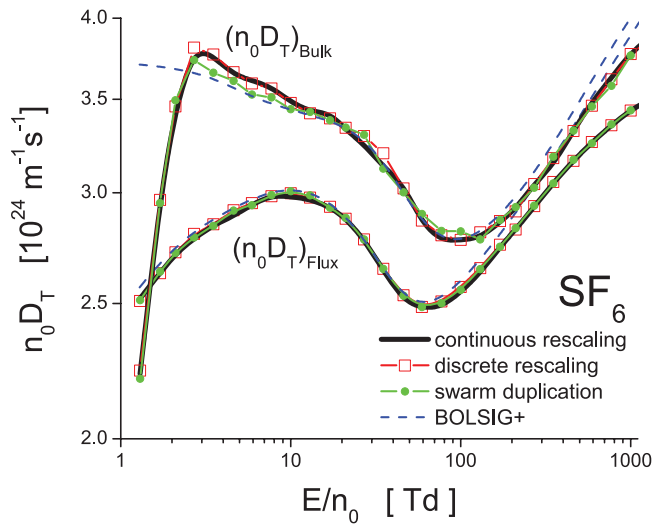


Figure 12. Variation of the transverse diffusion coefficient with E/n_0 for electrons in SF_6 . Monte Carlo results using three different techniques for electron number density compensation are compared with the BOLSIG+ results.

that the bulk diffusion coefficient is smaller than the corresponding flux component. This indicates that the decrease in electron numbers due to attachment weakens diffusion along the field direction. As already discussed, attachment loss of electrons from the trailing edge of the swarm causes a forward shift to the swarm centre of mass, with the corresponding increases in the bulk drift velocity and mean energy. The same effects result in an enhancement of the flux longitudinal diffusion. It should be noted that when attachment heating takes place, the opposite situation (bulk is higher than flux) has also been reported [25]. This is a clear sign that the energy dependence of the cross sections for electron attachment is of primary importance for the analysis of these phenomena. For higher E/n_0 , however, where the contribution of ionization becomes important, we observe that the diffusion is enhanced along the field direction, e.g. the bulk dominates the flux. This is always the case if the collision frequency for ionization is an increasing function of the electron energy, independently of the gaseous medium considered.

From the profiles of the transverse diffusion coefficient the bulk values are greater than the corresponding flux values over the range of E/n_0 considered in this work. Only in the limit of the lowest E/n_0 the opposite situation holds: the flux is greater than the bulk. In contrast to the longitudinal diffusion, spreading along the transverse directions is entirely determined by the thermal motion of the electrons. The flux of the Brownian motion through a transverse plane is proportional to the speed of the electrons passing through the same plane. Therefore, the higher energy electrons contribute the most to the transversal expansion, so attachment heating enhances transverse bulk diffusion coefficient.

Figures 13 and 14 show the variations of the longitudinal and transverse diffusion coefficients with E/n_0 for electrons in CF_3I , respectively. From the E/n_0 -profiles of the bulk diffusion coefficients we observe an excellent agreement between different rescaling procedures for $E/n_0 > 10$ Td. The same applies for the flux component of the longitudinal diffusion.

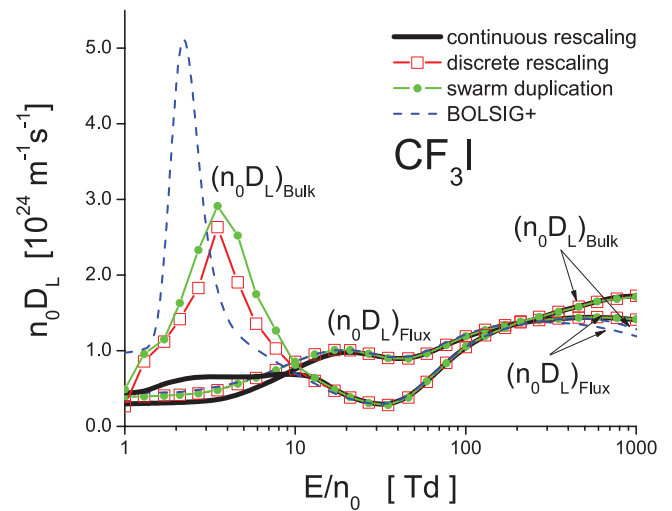


Figure 13. Variation of the longitudinal diffusion coefficient with E/n_0 for electrons in CF_3I . Monte Carlo results using three different techniques for electron number density compensation are compared with the BOLSIG+ results.

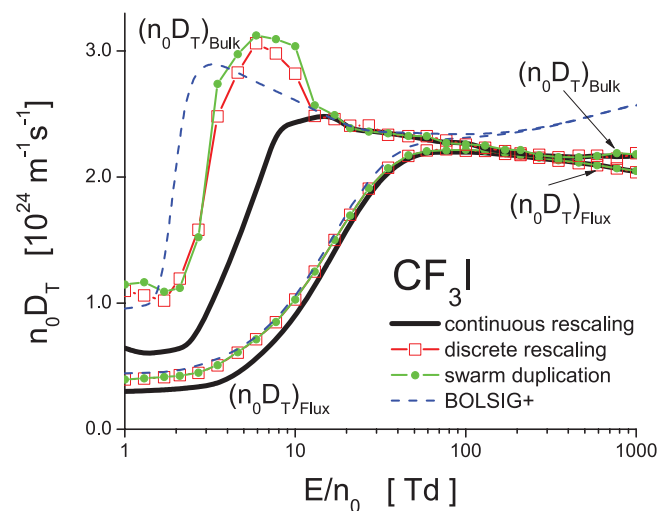


Figure 14. Variation of the transverse diffusion coefficient with E/n_0 for electrons in CF_3I . Monte Carlo results using three different techniques for electron number density compensation are compared with the BOLSIG+ results.

For $E/n_0 < 10$ Td the agreement is poor for bulk components, particularly between the continuous rescaling from one side and discrete rescaling and/or swarm duplication from the other side. The agreement is better for the flux components.

Comparing Monte Carlo and BOLSIG+ results, we see that the maximum error in the two term approximation, for both diffusion coefficients occurs at lower and higher E/n_0 . In contrast to SF_6 , CF_3I has rapidly increasing cross sections for vibrational excitations in the same energy region where the cross section of momentum transfer in elastic collisions decreases with the electron energy. Under these conditions, the energy transfer is increased and collisions no longer have the effect of randomizing the direction of electron motion. As a consequence, the distribution function deviates significantly from isotropy in velocity space and two term approximation of the Boltzmann equation fails.

When considering the differences between the bulk and flux values of diffusion coefficients the situation is much more complex comparing to SF₆. From the E/n_0 -profiles of the longitudinal diffusion coefficient one can immediately see that for lower and higher E/n_0 , the bulk is greater than the corresponding flux values while at intermediate E/n_0 the opposite situation holds: the flux is greater than the bulk. The behavior of the transverse diffusion coefficient is less complex, as over the entire of E/n_0 the bulk is greater than the corresponding flux values.

As we have demonstrated, in contrast to drift velocity the behavior and differences between the bulk and flux diffusion coefficients is somewhat harder to interpret. This follows from the complexity of factors which contribute to or influence the diffusion coefficients. The two most important factors are the following: (a) the thermal anisotropy effect resulting from different random electron motion in different directions; and (b) the anisotropy induced by the electric field resulting from the spatial variation of the average energy and local average velocities throughout the swarm which act so as to either inhibit or enhance diffusion. Additional factors include the effects of collisions, energy-dependent total collision frequency, and presence of non-conservative collisions. Couplings of these individual factors are always present and hence sometimes it is hard to elucidate even the basic trends in the behavior of diffusion coefficients. In particular, to understand the effects of electron attachment on diffusion coefficients and associated differences between bulk and flux components, the variation in the diffusive energy tensor associated with the second-order spatial variation in the average energy with E/n_0 should be studied. This remains the program of our future work.

3.1.4. Rate coefficients. In figure 15 we show the variation of steady-state Townsend ionization and attachment coefficients with E/n_0 for electrons in SF₆. The agreement between different rescaling procedures and BOLSIG+ code is very good. It is important to note that the agreement is very good, even in the limit of the lowest E/n_0 considered in this work where the electron energy distribution function is greatly affected by electron attachment. The curves show expected increase in α/n_0 and expected decrease in η/n_0 , with increasing E/n_0 . The value obtained for critical electric field is 361 Td which is in excellent agreement with experimental measurements of Aschwanden [80].

In figure 16 we show variation of the steady-state Townsend ionization and attachment coefficients with E/n_0 for electrons in CF₃I. The agreement between different rescaling procedure and BOLSIG+ code is excellent for ionization coefficient. From the E/n_0 -profile of attachment coefficient, we see that the continuous rescaling slightly overestimates the remaining scenarios of computation. The critical electric field for CF₃I is higher than for SF₆. This fact has been recently used as a motivational factor for a new wave of studies related to the insulation characteristics of pure CF₃I and its mixture with other gases, in the light of the present search for suitable alternatives to SF₆. The value obtained for critical electric field in our calculations is 440 Td which is in close agreement with experimental measurements under steady-state [63, 81]

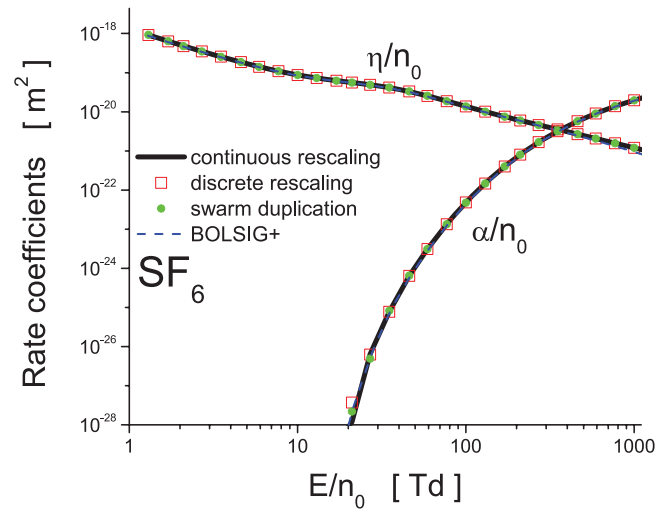


Figure 15. Variation of the rate coefficients with E/n_0 for electrons in SF₆. Monte Carlo results using three different techniques for electron number density compensation are compared with the BOLSIG+ results.

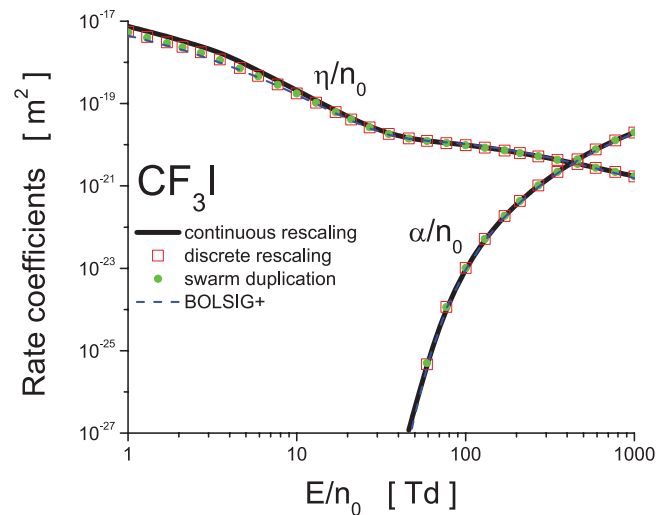


Figure 16. Variation of the rate coefficients with E/n_0 for electrons in CF₃I. Monte Carlo results using three different techniques for electron number density compensation are compared with the BOLSIG+ results.

and pulsed-Townsend [82] conditions, as well as with recent calculations performed by Kawaguchi *et al* [58] and Deng and Xiao [52].

3.2. Recommendations for implementation

In this section, we discuss the main features of the rescaling procedures and we give recommendations on how to use them in future Monte Carlo codes. Based on our experience achieved by simulating the electron transport in SF₆, CF₃I and other attaching gases, we have observed that if correctly implemented the procedures generally agree very well. The agreement between different rescaling procedures is always better for the flux than for the bulk properties. We found a poor agreement for the bulk diffusion coefficients, particularly for the lower E/n_0 while for mean energy, drift velocity and

rate coefficients the agreement is reasonably good. For lower E/n_0 when the distribution function is extremely affected by electron attachment, the agreement between swarm duplication and discrete rescaling is also good. This is not surprising as these two techniques are essentially the same.

In terms of implementation, the Monte Carlo codes can be relatively easily upgraded with the procedures for swarm duplication and/or discrete rescaling. Special attention during the implementation of these procedures should be given to the choice of the length of time steps after which the cloning of the electrons is done. If the length of this time step appears to be too long as compared to the time constant which corresponds to the attachment collision frequency, then the distribution function could be disturbed due to a low statistical accuracy. In other words, depleting certain pockets of the EEDF means that those cannot be recovered at all. On the other hand, if the length of the time steps is too small, the speed of simulation could be significantly reduced. The implementation of the continuous rescaling procedure is somewhat more complicated.

Which procedure is, the most flexible? It is difficult to answer this question because the answer depends on the criteria of flexibility. If the criterion for flexibility is associated with the need for *a priori* estimates which are necessary for setting the simulation, then the technique of continuous rescaling is certainly the most flexible. Once implemented, and thoroughly tested this procedure allows the analysis of electron transport in strongly attaching gases regardless of the energy dependence of the cross section for electron attachment. On the other hand, for the analysis of electron transport in weakly attaching gases, the discrete rescaling is very convenient because it is easier for implementation into the codes and less demanding in terms of the CPU time.

In terms of reliability and accuracy, the comparison of the results obtained for various transport properties using the rescaling procedures for Monte Carlo simulations and the Boltzmann equation codes shows that the rescaling procedures described herein are highly reliable. It should be noted that only the multi term codes for solving the Boltzmann equation may offer the final answer. Restrictions of the TTA for solving the Boltzmann equation were demonstrated many times in the past [7, 31], especially when it comes to the calculations of diffusion coefficients. Testing and benchmarking against other Boltzmann solvers are currently ongoing.

3.3. Experiments in strongly attaching gases: difficulties induced by non-hydrodynamic effects

It must be noted at this point that most processes scale with pressure, so the independence on pressure would be maintained and so would be the equilibration of EEDFs affected by excessive attachment. Most of the processes fall into that category. These processes are best visualized in an infinite uniform environment. Standard swarm experiments are built in such a way that boundaries are not felt over appreciable volume and thus, they mimic hydrodynamic conditions very well. However, going to high E/n_0 requires operating at lower pressures and there the boundaries may be felt over a larger

portion of the volume. In general, whenever boundaries of any kind are introduced selective losses resulting in very different mean free paths of different groups of particles may lead to selective losses. The resulting holes in the distribution may be filled in by collisions, so when considerable selective losses are introduced results may become the pressure dependent (even when the cross section is not dependent on the pressure). The same is true for temporal limitations. For example, if the frequency of collisions is small, so that the mean free time is comparable to the time required to accelerate to energies where cross sections decrease with the electron energy, the runaway effects may be developed. Similar effects may be created due to temporal variations of the field that do not allow full equilibration. The pressure dependence of the results will develop under such conditions (and so would the dependence on the size of the vessel). The development of a non-hydrodynamic theory for solving the Boltzmann equation is difficult and the best solution is a Monte Carlo simulation technique. For that reason, rescaling procedures are essential in modeling of the non-hydrodynamic (non-local) development of charged particle ensembles.

Experiments in gases with a very large attachment (typically at low energies) may be difficult to carry out due to a large loss of electrons. The fact that experiments in diluted gas mixtures of such gases may be feasible, means that cross sections may be obtained. Yet, one should be aware of two main problems. Even in such mixtures and depending on the size of the experiment, attachment may be high enough to induce depletion of the distribution function thus making results pressure dependent or abundance dependent. If one wants to extend the calculations to pure attaching gas for smaller vessels and pressures, one needs to be aware that only techniques that take full non-hydrodynamic description of the swarm development, are required. Similar effects have been observed in gases always associated with strong attachment such as oxygen [76] and water vapor [83]. In any case, the critical effects that include NDC for bulk drift velocity as a result of excessive loss of electrons in attachment can be observed in gases like SF_6 and CF_3I based on hydrodynamic expansion and even based on the two term theory provided that theory takes into account the explicit and implicit non-conservative effects of the attachment.

4. Conclusion

In this paper, we have presented the development, implementation and benchmarking of the rescaling procedures for Monte Carlo simulations of electron transport in strongly attaching gases. The capabilities of the rescaling procedures have been described by systematic investigation of the influence of electron attachment on transport coefficients of electrons in SF_6 and CF_3I . Among many important points, the key results arising from this paper are:

- (1) We have presented two distinctively different methods for compensation of electrons in Monte Carlo simulations of electron transport in strongly attaching gases, e.g. the discrete and the continuous procedures. In order to avoid the

somewhat arbitrary choice of the fictitious ionization rate, we have extended the continuous rescaling procedure, initially developed by Li *et al* [61], by introducing a time-dependent collision frequency for the fictitious ionization process.

- (2) One of the initial motivating factors for this work was to provide accurate data for transport properties of electrons in SF₆ and CF₃I which are required as input in fluid models of plasma discharges. In this work, for the first time, we have calculated the mean energy, drift velocity and diffusion coefficients as well as rate coefficients for lower E/n_0 for electrons in SF₆ and CF₃I.
- (3) We have demonstrated the differences which can exist between the bulk and flux transport coefficients and the origin of these differences. Our study has shown that the flux and bulk transport properties can vary substantially from one another, particularly in the presence of intensive attachment heating. Thus, one of the key messages of this work is that theories which approximate the bulk transport coefficients by the flux are problematic and generally wrong.
- (4) We have demonstrated and interpreted physically the phenomenon of the anomalous behavior of the mean energy of electrons in SF₆, in which the mean energy is reduced for increasing E/n_0 . The phenomenon was associated with the interplay between attachment heating and inelastic cooling. The same phenomenon has not been observed for electrons in CF₃I indicating that the role of the cross sections is vital.
- (5) We have explained and identified a region of NDC in the bulk drift velocity, originating from the explicit influence of electron attachment. The phenomenon has been explained using the concept of spatially-resolved transport properties along the swarm.
- (6) The publicly available two term Boltzmann solver, BOLSIG+, has been shown to be accurate for calculations of mean energy, drift velocity and rate coefficients for electrons in SF₆ and CF₃I. On the other hand, significant differences between our Monte Carlo and BOLSIG+ results for diffusion coefficients have been observed, particularly for electrons in CF₃I in the limit of the lowest E/n_0 considered in this work.

Various rescaling procedures for Monte Carlo simulations described in this work have recently been applied to modeling of electron transport in strongly attaching gases under the influence of time-dependent electric and magnetic fields. It will be challenging to investigate the synergism of magnetic fields and electron attachment in radio-frequency plasmas. Likewise, the remaining step to be taken, is to apply the rescaling procedures presented in this work to investigate the influence of positronium formation on the positron transport properties. This remains the focus of our future investigation. Finally, we hope that this paper will stimulate further discussion on methods of correct representation of the effects induced by electron attachment on transport properties of electrons in strongly attaching gases.

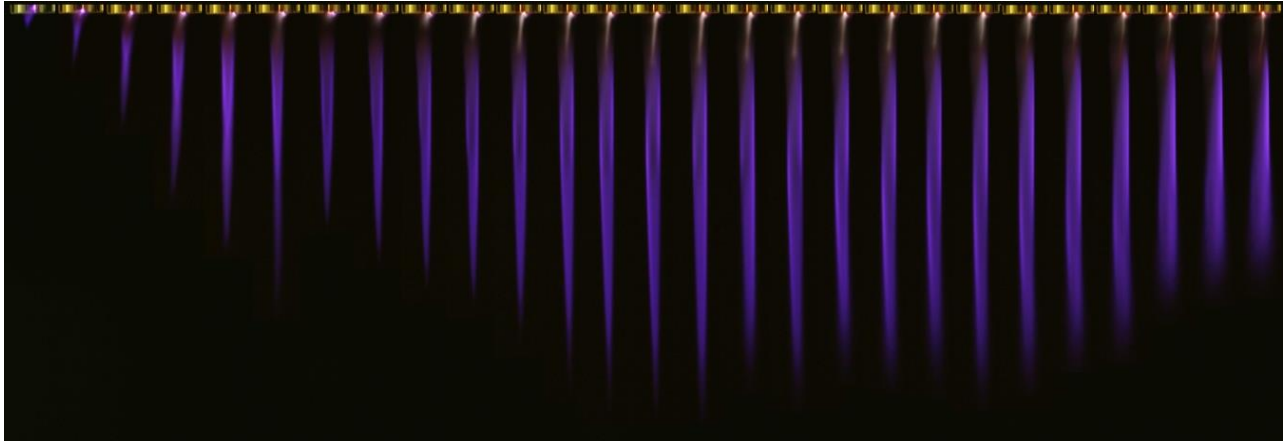
Acknowledgments

The authors acknowledge support from MPNTRRS Projects OI171037 and III41011.

References

- [1] Christophorou L G and Olthoff J K 2004 *Fundamental Electron Interactions with Plasma Processing Gases* (New York: Springer)
- [2] Makabe T and Petrović Z Lj 2014 *Plasma Electronics: Applications in Microelectronic Device Fabrication* (New York: CRC Press)
- [3] Christophorou L G and Pinnaduwege L A 1990 *IEEE Trans. Electr. Insul.* **25** 55
- [4] Rolandi L, Riegler W and Blum W 2008 *Particle Detection with Drift Chambers* (Berlin: Springer)
- [5] Sauli F 2014 *Gaseous Radiation Detectors* (Cambridge: Cambridge University Press)
- [6] Bošnjaković D, Petrović Z Lj, White R D and Dujko S 2014 *J. Phys. D: Appl. Phys.* **47** 435203
- [7] Petrović Z Lj, Dujko S, Marić D, Malović G, Nikitović Ž, Šašić O, Jovanović J, Stojanović V and Radmilović-Radjenović M 2009 *J. Phys. D: Appl. Phys.* **42** 194002
- [8] Petrović Z Lj, Šuvakov M, Nikitović Ž, Dujko S, Šašić O, Jovanović J, Malović G and Stojanović V 2007 *Plasma Sources Sci. Technol.* **16** S1
- [9] Huxley L G H and Crompton R W 1974 *The Drift and Diffusion of Electrons in Gases* (New York: Wiley)
- [10] Christophorou L G, McCorkle D L and Anderson V E 1971 *J. Phys. B: At. Mol. Phys.* **4** 1163
- [11] Phelps A V and van Brunt R J 1988 *J. Appl. Phys.* **64** 4269
- [12] Christophorou L G and Olthoff J K 2000 *J. Phys. Chem. Ref. Data* **29** 267
- [13] Jarvis G K, Kennedy R A and Mayhew C A 2001 *Int. J. Mass Spectrom.* **205** 253
- [14] Dahl D A and Franck C M 2013 *J. Phys. D: Appl. Phys.* **46** 445202
- [15] Rabie M, Haefliger P, Chachereau A and Franck C M 2015 *J. Phys. D: Appl. Phys.* **48** 075201
- [16] Hunter S R and Christophorou L G 1984 *J. Chem. Phys.* **80** 6150
- [17] Novak J P and Frechette M F 1988 *J. Appl. Phys.* **63** 2570
- [18] Hunter S R, Carter J G and Christophorou L G 1988 *Phys. Rev. A* **38** 58
- [19] Petrović Z Lj, Wang W C and Lee L C 1988 *J. Appl. Phys.* **64** 1625
- [20] Petrović Z Lj, Wang W C, Suto M, Han J C and Lee L C 1990 *J. Appl. Phys.* **67** 675
- [21] Raju G G 2006 *Gaseous Electronics: Theory and Practice* (New York: CRC Press)
- [22] Raju G G 2012 *Gaseous Electronics: Tables, Atoms, and Molecules* (New York: CRC Press)
- [23] Cavalleri G 1969 *Phys. Rev.* **179** 186
- [24] Petrović Z Lj and Crompton R W 1985 *J. Phys. B: At. Mol. Phys.* **17** 2777
- [25] Ness K F and Robson R E 1986 *Phys. Rev. A* **34** 2185
- [26] Nolan A M, Brennan M J, Ness K F and Wedding A B 1997 *J. Phys. D: Appl. Phys.* **30** 2865
- [27] Dujko S, Raspopović Z M, Petrović Z Lj and Makabe T 2003 *IEEE Trans. Plasma Sci.* **31** 711
- [28] White R D, Robson R E and Ness K F 1999 *Phys. Rev. E* **60** 7457
- [29] Dujko S, Ebert U, White R D and Petrović Z Lj 2011 *Japan J. Appl. Phys.* **50** 08JC01
- [30] Robson R E 1991 *Aust. J. Phys.* **44** 685

- [31] White R D, Robson R E, Dujko S, Nicoletopoulos P and Li B 2009 *J. Phys. D: Appl. Phys.* **42** 194001
- [32] Dujko S, White R D, Raspopović Z M and Petrović Z Lj 2012 *Nucl. Instrum. Methods Phys. Res. B* **279** 84
- [33] Robson R E, White R D and Petrović Z Lj 2005 *Rev. Mod. Phys.* **77** 1303
- [34] Dujko S, Markosyan A H, White R D and Ebert U 2013 *J. Phys. D: Appl. Phys.* **46** 475202
- [35] Markosyan A H, Dujko S and Ebert U 2013 *J. Phys. D: Appl. Phys.* **46** 475203
- [36] Bletzinger P 1990 *J. Appl. Phys.* **67** 130
- [37] Stoffels E, Stoffels W, Venderm D, Haverlaag M, Kroesen G M W and de Hoog F J 1995 *Contrib. Plasma Phys.* **35** 331
- [38] Chabert P and Sheridan T E 2000 *J. Phys. D: Appl. Phys.* **33** 1854
- [39] Kono A 2002 *Appl. Surf. Sci.* **192** 115
- [40] Zhao S X, Gao F, Wang Y N and Bogaerts A 2012 *Plasma Sources Sci. Technol.* **21** 025008
- [41] Chabert P, Lichtenberg A J, Lieberman M A and Marakhtanov A M 2003 *J. Appl. Phys.* **94** 831
- [42] Robson R E 1986 *J. Chem. Phys.* **85** 4486
- [43] Vrhovac S B and Petrović Z Lj 1996 *Phys. Rev. E* **53** 4012
- [44] Yousfi M, Segur P and Vassiliadis T 1985 *J. Phys. D: Appl. Phys.* **18** 359
- [45] Itoh H, Miurat Y, Ikuta N, Nakao Y and Tagashira H 1988 *J. Phys. D: Appl. Phys.* **21** 922
- [46] Itoh H, Kawaguchi M, Satoh K, Miura Y, Nakano Y and Tagashira H 1990 *J. Phys. D: Appl. Phys.* **23** 299
- [47] Itoh H, Matsumura T, Satoh K, Date H, Nakano Y and Tagashira H 1993 *J. Phys. D: Appl. Phys.* **26** 1975
- [48] Frechette M F and Novak J P 1987 *J. Phys. D: Appl. Phys.* **20** 438
- [49] Pinheiro M J and Loureiro J 2002 *J. Phys. D: Appl. Phys.* **35** 3077
- [50] Tezcan S S, Akcayol M A, Ozerdem O C and Dincer M S 2010 *IEEE Trans. Plasma Sci.* **38** 2332
- [51] Li X, Zhao H, Wu J and Jia S 2013 *J. Phys. D: Appl. Phys.* **46** 345203
- [52] Deng Y and Xiao D 2014 *Japan J. Appl. Phys.* **53** 096201
- [53] Dujko S, White R D, Petrović Z Lj and Robson R E 2010 *Phys. Rev. E* **81** 046403
- [54] Yousfi M, Hennad A and Alkaa A 1994 *Phys. Rev. E* **49** 3264
- [55] Dincer M S and Gaju G R 1983 *J. Appl. Phys.* **54** 6311
- [56] Dincer M S, Ozerdem O C and Bektas S 2007 *IEEE Trans. Plasma Sci.* **35** 1210
- [57] Satoh K, Itoh H, Nakano Y and Tagashira H 1988 *J. Phys. D: Appl. Phys.* **21** 931
- [58] Kawaguchi S, Satoh K and Itoh H 2014 *Eur. Phys. J. D* **68** 100
- [59] Rapopović Z M, Sakadžić S, Bzenić S and Petrović Z Lj 1999 *IEEE Trans. Plasma Sci.* **27** 1241
- [60] Dyatko N A and Napartovich A P 1999 *J. Phys. D: Appl. Phys.* **32** 3169
- [61] Li Y M, Pitchford L C and Moratz T J 1989 *Appl. Phys. Lett.* **54** 1403
- [62] Mirić J, Šašić O, Dujko S and Petrović Z Lj 2014 *Proc. 27th Summer School and Int. Symp. on the Physics of Ionized Gases (Belgrade)* (Belgrade: Institute of Physics) p 122
- [63] Kimura M and Nakamura Y 2010 *J. Phys. D: Appl. Phys.* **43** 145202
- [64] Mirić J, de Urquijo J, Bošnjaković D, Petrović Z Lj and Dujko S 2016 *Plasma Sources Sci. Technol.* submitted
- [65] Ristivojević Z and Petrović Z Lj 2012 *Plasma Sources Sci. Technol.* **21** 035001
- [66] Dujko S, White R D and Petrović Z Lj 2008 *J. Phys. D: Appl. Phys.* **41** 245205
- [67] Petrović Z Lj, Raspopović Z, Dujko S and Makabe T 2002 *Appl. Surf. Sci.* **192** 1
- [68] Hagelaar G J M and Pitchford L C 2005 *Plasma Sources Sci. Technol.* **14** 722
- [69] Kline L and Siambis J 1972 *Phys. Rev. A* **5** 794
- [70] Kunhardt E and Tzeng Y 1986 *J. Comput. Phys.* **67** 279
- [71] Gallagher J W, Beaty E C, Dutton J and Pitchford L C 1983 *J. Phys. Chem. Ref. Data* **12** 109
- [72] Morrow R 1986 *IEEE Trans. Plasma Sci.* **PS-14** 234
- [73] Ness K F and Makabe T 2000 *Phys. Rev. E* **62** 4083
- [74] White R D, Robson R E, Ness K F and Makabe T 2005 *J. Phys. D: Appl. Phys.* **38** 997
- [75] Skullerud H R 1983 *Aust. J. Phys.* **36** 845
- [76] McMahon D R A and Crompton R W 1983 *J. Chem. Phys.* **78** 603
- [77] Hegerberg R and Crompton R W 1983 *Aust. J. Phys.* **36** 831
- [78] Banković A, Dujko S, White R D, Marler J P, Buckman S J, Marjanović S, Malović G, Garcia G and Petrović Z Lj 2012 *New J. Phys.* **14** 035003
- [79] Banković A, Dujko S, White R D, Buckman S J and Petrović Z Lj 2012 *Nucl. Instrum. Methods B* **279** 92
- [80] Aschwanden Th 1984 *Gaseous Dielectrics IV* ed L G Christophorou and M O Pace (New York: Pergamon) p 24
- [81] Hasegawa H, Date H, Shimozuma M and Itoh H 2009 *Appl. Phys. Lett.* **95** 101504
- [82] de Urquijo J, Juarez A M, Basurto E and Hernandez-Avila J L 2007 *J. Phys. D: Appl. Phys.* **40** 2205
- [83] Robson R E, White R D and Ness K F 2011 *J. Chem. Phys.* **134** 064319



JSPP2014
COST MP1101 WS

9th EU-Japan Joint Symposium on Plasma Processing (JSPP2014) and EU COST MP1101 Workshop on Atmospheric Plasma Processes and Sources

PROCEEDINGS



January 19th — January 23th 2014 | Bohinj Bistrica, Slovenia (EU)

Programme and abstracts

Click on the title of a talk to see the abstract.

The 9th EU-Japan Joint Symposium on Plasma Processing (19.-23. January 2014, Slovenia)

Sun. 19. Jan			
15.00 - 17.00	Registration		
17.00 - 17.30	INV	S. Milošević (CRO); Tailoring plasma sources and their diagnostics in various applications	slobodan@ifs.hr
17.30 - 18.00	INV	M. Gorjanc (SLO); Advantages and limitations of using plasma technology for modification of textiles	marija.gorjanc@ntf.uni-lj.si
18.00 - 18.30	INV	K. Kutasi (HUN); Layer-by-layer assembly of thin organic films on PTFE activated by air diffuse coplanar surface barrier discharge	kutasi.kinga@wigner.mta.hu
19.00 - 20.00	Dinner		
20.00 - 23.00	Welcome reception		

Mon. 20. Jan			
8.50 - 9.00	Opening	S. Hamaguchi (JPN), U. Cvelbar (SLO)	
9.00 - 9.45	Plenary	T. Makabe (JPN); Local distribution of gas temperature in an atmospheric- pressure microcell plasma in Ar	makabe@mkbe.elec.keio.ac.jp
9.45 - 10.30	Plenary	M. M. Turner (IRE); Uncertainty and error in complex plasma chemistry models	miles.turner@dcu.ie
10.30 - 11.00	Break		
11.00 - 11.30	INV	S. Hamaguchi (JPN); Nano-scale damage formation during plasma etching analysed by multi-beam experiments and molecular dynamics (MD) simulations	hamaguch@ppl.eng.osaka-u.ac.jp
11.30 - 12.00	INV	S. Dujko (SRB); Recent results from studies of non-equilibrium electron transport in modelling of low-temperature plasmas and particle detectors	sasha@ipb.ac.rs
12.00 - 12.30	INV	T. Murakami (JPN); Reactive species in atmospheric pressure plasmas operated in ambient humid air	murakami@es.titech.ac.jp
12.30 - 13.00	INV	M. Sekine (JPN); Plasma nano-interface with organic materials for surface roughness formation	sekine@nagoya-u.jp
13.00 - 14.15	Lunch		
14.15 - 15.00	Plenary	M. Shiratani (JPN); Nanoparticle composite plasma CVD films - Fundamental and applications	siratani@ed.kyushi-u.ac.jp
15.00 - 15.30	INV	R. Hatakeyama (JPN); Plasma-processed control of graphene nanostructures and transport properties	hatake@ecei.tohoku.ac.jp
15.30 - 16.00	INV	J. Kim (JPN); Microwave plasma CVD technologies for the synthesis of nanocrystalline diamond and graphene films	jaeho.kim@aist.go.jp
16.00 - 16.30	Break		

Recent results from studies of non-equilibrium electron transport in modeling of low-temperature plasmas and particle detectors

S. Dujko¹, D. Bošnjaković¹, J. Mirić¹, I. Simonović¹, Z.M. Raspopović¹, R.D. White², A.H. Markosyan³, U. Ebert³ and Z.Lj. Petrović¹

¹Institute of Physics, University of Belgrade, Pregrevica 118, 11080 Belgrade, Serbia

²ARC Centre for Antimatter-Matter Studies, School of Engineering and Physical Sciences, James Cook University, Townsville 4810, Australia

³Centrum Wiskunde & Informatica (CWI), PO Box 94079, 1090 GB Amsterdam, The Netherlands

sasa.dujko@ipb.ac.rs

A quantitative understanding of charged particle transport processes in gases under highly non-equilibrium conditions is of interest from both fundamental and applied viewpoints, including modeling of non-equilibrium plasmas and particle detectors used in high energy physics. In this work we will highlight how the fundamental kinetic theory for solving the Boltzmann equation [1] and fluid equations [2,3] as well as Monte Carlo simulations [3], developed over many years for charged particle swarms are presently being adapted to study the various types of non-equilibrium plasma discharges and particle detectors.

Non-equilibrium plasma discharges sustained and controlled by electric and magnetic fields are widely used in materials processing [4]. Within these discharges the electric and magnetic fields can vary in space, time and orientation depending on the type of discharge. Moreover, the typical distances for electron energy and momentum relaxation are comparable to the plasma source dimensions. Consequently, the transport properties at a given point are usually no longer a function of instantaneous fields. This is the case for a variety of magnetized plasma discharges where, before the electrons become fully relaxed, it is likely that the electrons will be

reflected by the sheath or collide with the wall [5]. In this work we will illustrate various kinetic phenomena induced by the spatial and temporal non-locality of electron transport in gases. Two particular examples of most recent interest for the authors are the magnetron and ICP discharges. The magnetron discharge is used in the sputtering deposition of in films [6] where magnetic field confines energetic electrons near the cathode. These confined electrons ionize neutral gas and form high density plasma near the cathode surface while heavy ions and neutrals impinge on the solid surface ejecting material from that surface which is then deposited on the substrate. Within these discharges the angle between the electric and magnetic fields varies and thus for a detailed understanding and accurate modeling of this type of discharge, a knowledge of electron transport in gases under the influence of electric and magnetic fields at arbitrary angles is essential. In this work we will investigate the electron transport in N_2 - O_2 mixtures when electric and magnetic fields are crossed at arbitrary angles for a range of pressures having in mind applications for low-pressure magnetized discharges and discharges at atmospheric pressure. Special attention is placed upon the explicit effects of three-body attachment in oxygen on both the drift and diffusion in low energy range [7]. The duality of transport coefficients arising from the explicit effects of non-conservative collisions will be discussed not only for vectorial and low-order tensorial transport coefficients but also for the high-order tensorial transport properties. The errors associated with the two-term approximation and inadequacies of Legendre polynomial expansions for solving the Boltzmann equation will be illustrated and highlighted.

In addition to magnetron discharges, we focus on the time-dependent behavior of electron transport properties in ICP discharges where electric and magnetic fields are radiofrequency. We systematically investigate the explicit effects associated with the electric and magnetic fields including field to density ratios, field frequency to density ratio, field phases and field orientations. A multitude of kinetic phenomena were observed that are generally inexplicable through the use of steady-state dc transport theory. Phenomena of significant note include the existence of transient

reflected by the sheath or collide with the wall [5]. In this work we will illustrate various kinetic phenomena induced by the spatial and temporal non-locality of electron transport in gases. Two particular examples of most recent interest for the authors are the magnetron and ICP discharges. The magnetron discharge is used in the sputtering deposition of in films [6] where magnetic field confines energetic electrons near the cathode. These confined electrons ionize neutral gas and form high density plasma near the cathode surface while heavy ions and neutrals impinge on the solid surface ejecting material from that surface which is then deposited on the substrate. Within these discharges the angle between the electric and magnetic fields varies and thus for a detailed understanding and accurate modeling of this type of discharge, a knowledge of electron transport in gases under the influence of electric and magnetic fields at arbitrary angles is essential. In this work we will investigate the electron transport in N_2 - O_2 mixtures when electric and magnetic fields are crossed at arbitrary angles for a range of pressures having in mind applications for low-pressure magnetized discharges and discharges at atmospheric pressure. Special attention is placed upon the explicit effects of three-body attachment in oxygen on both the drift and diffusion in low energy range [7]. The duality of transport coefficients arising from the explicit effects of non-conservative collisions will be discussed not only for vectorial and low-order tensorial transport coefficients but also for the high-order tensorial transport properties. The errors associated with the two-term approximation and inadequacies of Legendre polynomial expansions for solving the Boltzmann equation will be illustrated and highlighted.

In addition to magnetron discharges, we focus on the time-dependent behavior of electron transport properties in ICP discharges where electric and magnetic fields are radiofrequency. We systematically investigate the explicit effects associated with the electric and magnetic fields including field to density ratios, field frequency to density ratio, field phases and field orientations. A multitude of kinetic phenomena were observed that are generally inexplicable through the use of steady-state dc transport theory. Phenomena of significant note include the existence of transient

negative diffusivity, time-resolved negative differential conductivity and anomalous anisotropic diffusion. Most notably, we propose a new mechanism for collisional heating in inductively coupled plasmas which results from the synergism of temporal non-locality and cyclotron resonance effect. This mechanism is illustrated for discharges in pure CF_4 and pure O_2 .

As an example of fluid modeling of plasmas, we will discuss the recently developed high order fluid model for streamer discharges [2,3]. Starting from the cross sections for electron scattering, it will be shown how the corresponding transport data required as input in fluid model should be calculated under conditions when the local field approximation is not applicable. The temporal and spatial evolution of electron number density and electric field in the classical first order and in the high order model are compared and the differences will be explained by physical arguments. We will illustrate the non-local effects in the profiles of the mean energy behind the streamer front and emphasize the significance of the energy flux balance equation in modeling. We consider the negative planar ionization fronts in molecular nitrogen and noble gases. Our results for various streamers properties are compared with those obtained by a PIC/Monte Carlo approach. The comparison confirms the theoretical basis and numerical integrity of our high order fluid model for streamers discharges.

In the last segment of this talk we will discuss the detector physics processes of resistive plate chambers and time-projection chambers that are often used in many high energy physics experiments [8]. For resistive plate chambers the critical elements of modeling include the primary ionization, avalanche statistics and signal development. The Monte Carlo simulation procedures that implement the described processes will be presented. Time resolution and detector efficiency are calculated and compared with experimental measurements and other theoretical calculations. Among many critical elements of modeling for time-projection chambers, we have investigated the sensitivity of electron transport properties to the pressure and temperature variations in the mixtures of Ne and CO_2 . In particular, we have investigated how to reduce

the transverse diffusion of electrons by calculating the electron trajectories under the influence of parallel electric and magnetic fields and for typical conditions found in these detectors.

References

- [1] S. Dujko, R.D. White, Z.Lj. Petrović and R.E. Robson "Benchmark calculations of nonconservative charged-particle swarms in dc electric and magnetic fields crossed at arbitrary angles", Phys. Rev. E 80, (2010) 046403.
- [2] S. Dujko, A.H. Markosyan, R.D. White and U. Ebert, "High-order fluid model for streamer discharges: I. Derivation of model and transport data" J. Phys. D: Appl. Phys. 46 (2013) 475202.
- [3] A.H. Markosyan, S. Dujko and U. Ebert "High-order fluid model for streamer discharges: II. Numerical solution and investigation of planar fronts" J. Phys. D: Appl. Phys. 46 (2013) 475202.
- [4] T. Makabe and Z.Lj. Petrović " Plasma Electronics: Applications in Microelectronic Device Fabrication" (New York: Taylor and Francis 2006).
- [5] H. Date, P. L. G. Ventzek, K. Kondo, H. Hasegawa, and M. Shimozuma "Spatial characteristics of electron swarm parameters in gases" J. Appl. Phys., Vol. 83. no. 8, (1988) 4024.
- [6] C.H. Shon and J.K. Lee "Modeling of magnetron sputtering plasma" Appl. Surf. Sci. 192 (2002) 258.
- [7] S. Dujko, U. Ebert, R.D. White and Z.Lj. Petrović, "Boltzmann equation analysis of electron transport in a N₂-O₂ streamer discharge" Jpn. J. Appl. Phys. 50 (2011) 08JC01.
- [8] G. Aad et al. "The ATLAS Experiment at the CERN Large Hadron Collider" J. Inst. Vol. 3 (2008) S08003.



27th Summer School and International Symposium on the Physics of Ionized Gases

August 26-29, 2014, Belgrade, Serbia

CONTRIBUTED PAPERS &

**ABSTRACTS OF INVITED LECTURES,
TOPICAL INVITED LECTURES, PROGRESS
REPORTS AND WORKSHOP LECTURES**

Editors:

Dragana Marić

Aleksandar R. Milosavljević

Zoran Mijatović



Institute of Physics, Belgrade
University of Belgrade



Serbian Academy
of Sciences and Arts

THIRD-ORDER TRANSPORT COEFFICIENTS FOR ELECTRONS I. STRUCTURE OF SKEWNESS TENSOR

I. Simonović, Z.Lj. Petrović and S. Dujko

*Institute of Physics, University of Belgrade,
Pregrevica 118, 11080 Belgrade, Serbia*

Abstract. Third-order transport properties are calculated through a Monte Carlo simulation for electrons moving in an infinite gas under the influence of spatially homogeneous electric and magnetic fields. The structure of the skewness tensor and symmetries along individual elements are studied by means of a group projector technique.

1. INTRODUCTION

Electron transport in gases under the influence of electric and magnetic fields has long been of interest, with many scientific and technological applications. These applications have been usually modeled assuming hydrodynamic conditions, in which the electron flux was analyzed in terms of drift and diffusion terms. The truncation of the electron flux to low order transport coefficients, e.g., to the drift velocity and diffusion tensor, may be invalid for a number of reasons, such as the presence of sources and sinks or physical boundaries. Before applying the strict non-hydrodynamic treatment, it is desirable to analyze the high-order transport coefficients and it is important to develop methods for their calculations. This issue has been addressed by several authors in the context of an electric field only case. The semi-quantitative momentum transfer theory developed by Vrhovac *et al.* [1] and Monte Carlo simulation performed by Penetrante and Bardsey [2] were used to analyze the skewness tensor for electrons in rare gases. A three-temperature treatment of the Boltzmann equation and molecular dynamics simulation were used by Koutselos to calculate the third order transport coefficients of ions in atomic gases [3].

In this work we apply the group projector method [4] to investigate the structure of the skewness tensor and symmetries along its individual

elements when both the electric and magnetic fields are present. Using a Monte Carlo simulation technique, the longitudinal and transverse skewness coefficients are calculated for the ionization model of Lucas and Saelee [5].

2. THEORETICAL METHODS

The starting point in our analysis is the flux gradient relation

$$\mathbf{\Gamma}(\mathbf{r}, t) = \sum_{k=0}^{\infty} \Gamma^{(k+1)}(t) \odot (-\nabla)^k n, \quad (1)$$

and diffusion equation

$$\frac{\partial n(\mathbf{r}, t)}{\partial t} = \sum_{k=0}^{\infty} \omega^{(k)}(t) \odot (-\nabla)^k n. \quad (2)$$

where $n(\mathbf{r}, t)$ is the electron density while $\mathbf{\Gamma}(\mathbf{r}, t)$ is the electron flux. $\Gamma^{(k+1)}(t)$ are time dependent tensors of rank k and \odot denotes a k -fold scalar product.

As pointed out in [1] one should make a difference between microscopic and macroscopic transport coefficients. Microscopic bulk transport coefficient of an order k , $\omega^{(k)}(t)$, is a tensor of rank k , which multiplies the k -th gradient of concentration, in (2). Microscopic flux can be obtained from microscopic bulk by subtracting the term associated with the explicit effects of non-conservative collisions. Macroscopic flux transport coefficient of order k , $\Gamma^{(k)}(t)$, is a tensor of rank k , which in the flux gradient relation (1), multiplies the $(k - 1)$ -th gradient of concentration. These tensors are, starting from rank 3, symmetric by every permutation of indices, that does not change position of the first index, because all indices, except the first, are contracted with partial derivatives of concentration.

In this work, we consider a co-ordinate system in which the z -axis is defined by the electric field \mathbf{E} while the magnetic field \mathbf{B} lies along the z -axis (parallel field configuration) or along the y -axis (an orthogonal field configuration) or makes an angle ψ with \mathbf{E} and lies in the $y - z$ plane (an arbitrary field configuration). Using the method based on group projectors and identifying the symmetries along the individual elements of the skewness tensor we have determined the following structures of the tensor depending on the field configuration:

1. Electric field only configuration ($\mathbf{E} = E e_z$):

$$\begin{aligned} Q_{x|ij} &= \begin{pmatrix} 0 & 0 & Q_{xxz} \\ 0 & 0 & 0 \\ Q_{xxz} & 0 & 0 \end{pmatrix}, & Q_{y|ij} &= \begin{pmatrix} 0 & 0 & 0 \\ 0 & 0 & Q_{xxz} \\ 0 & Q_{xxz} & 0 \end{pmatrix}, \\ Q_{z|ij} &= \begin{pmatrix} Q_{zxx} & 0 & 0 \\ 0 & Q_{zxx} & 0 \\ 0 & 0 & Q_{zzz} \end{pmatrix}. \end{aligned} \quad (3)$$

2. Parallel field configuration ($\mathbf{E} = E\mathbf{e}_z$, $\mathbf{B} = B\mathbf{e}_z$):

$$\begin{aligned} Q_{x|ij} &= \begin{pmatrix} 0 & 0 & Q_{xxz} \\ 0 & 0 & Q_{xyz} \\ Q_{xxz} & Q_{xyz} & 0 \end{pmatrix}, & Q_{y|ij} &= \begin{pmatrix} 0 & 0 & -Q_{xyz} \\ 0 & 0 & Q_{xxz} \\ -Q_{xyz} & Q_{xxz} & 0 \end{pmatrix}, \\ Q_{z|ij} &= \begin{pmatrix} Q_{zxx} & 0 & 0 \\ 0 & Q_{zxx} & 0 \\ 0 & 0 & Q_{zzz} \end{pmatrix}. \end{aligned} \quad (4)$$

3. Crossed field configuration ($\mathbf{E} = E\mathbf{e}_z$, $\mathbf{B} = B\mathbf{e}_y$):

$$\begin{aligned} Q_{x|ij} &= \begin{pmatrix} Q_{xxx} & 0 & Q_{xxz} \\ 0 & Q_{xyy} & 0 \\ Q_{xxz} & 0 & Q_{xzz} \end{pmatrix}, & Q_{y|ij} &= \begin{pmatrix} 0 & Q_{yxy} & 0 \\ Q_{yxy} & 0 & Q_{yyz} \\ 0 & Q_{yyz} & 0 \end{pmatrix}, \\ Q_{z|ij} &= \begin{pmatrix} Q_{zxx} & 0 & Q_{zxx} \\ 0 & Q_{zyy} & 0 \\ Q_{zxx} & 0 & Q_{zzz} \end{pmatrix}, \end{aligned} \quad (5)$$

where $i, j = x, y, z$. For an arbitrary field configuration, $Q_{ijk} = Q_{ikj}$ for any individual element of the skewness tensor.

3. RESULTS AND DISCUSSIONS

In the hydrodynamic regime the skewness tensor is given by

$$\mathbf{Q}_{abc} = \frac{1}{3!} \frac{d}{dt} \langle \mathbf{r}_a^* \mathbf{r}_b^* \mathbf{r}_c^* \rangle, \quad (6)$$

where (a, b, c) take values from the set $\{x, y, z\}$ while the angular brackets $\langle \rangle$ denote ensemble averages in configuration space and $\mathbf{r}^* = \mathbf{r} - \langle \mathbf{r} \rangle$. From (3) it is clear that \mathbf{Q} has seven non-vanishing elements, three of which are independent, Q_{zzz} , $Q_{zxx} = Q_{zyy}$ and $Q_{xzx} = Q_{xxz} = Q_{yzy} = Q_{yyz}$. Due to direct sampling of swarm dynamic properties in our Monte Carlo code only two independent components of the skewness tensor can be isolated, the longitudinal skewness coefficient $Q_L = Q_{zzz}$ and transverse skewness coefficient $Q_T = Q_{zxx} + Q_{xzx} + Q_{xxz} = Q_{zyy} + Q_{yzy} + Q_{yyz}$.

In Fig. 1 we show the variation of $n_0^2 Q_L$ with E/n_0 for the ionization model of Lucas Saelee. We see that $n_0^2 Q_L$ monotonically decreases with increasing E/n_0 and/or with increasing parameter F . For the conservative case ($F = 0$) gas model is reduced to elastic and excitation cross sections and no ionization occurs while for non-conservative case ($F = 1$) the gas model consists of elastic and ionization cross sections and no excitation occurs. In this model, for increasing E/n_0 the collision frequency for inelastic collisions is also increased while the collision frequency for the momentum transfer in elastic collisions remains unaltered. This suggests that for increasing E/n_0 inelastic collisions tend to reduce $n_0^2 Q_L$. A decrease

in $n_0^2 Q_L$ with increasing F is a clear sign that the skewness coefficients are more sensitive than the lower order transport coefficients with respect to small variation in the distribution function induced by the ionization cooling.

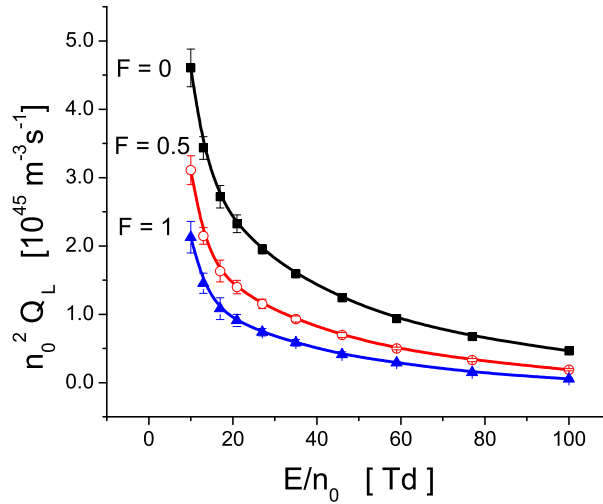


Figure 1. Variation of the longitudinal skewness coefficient with E/n_0 for three different ionization models as indicated on the graph.

Acknowledgments

This work was supported by MPNTRRS Projects OI171037 and III41011.

REFERENCES

- [1] S.B. Vrhovac, Z.Lj. Petrović, L.A. Viehland and T.S. Santhanam, *J. Chem. Phys.* 110, 2423 (1999).
- [2] B.M. Penetrante and J.N. Bardsley, in *Non-equilibrium Effects in Ion and Electron Transport*, edited by J.W. Gallagher, D.F. Hudson, E. E. Kunhardt, and R.J. Van Brunt, (Plenum, New York, 1990), p. 49.
- [3] A.D. Koutselos, *Chem. Phys.* 315, 193 (2005).
- [4] A.O. Barut and R. Raczka, *Theory of group representations and applications* (World Scientific, Singapore, 1986).
- [5] J. Lucas and H. Saelee, *J. Phys. D: Appl. Phys.* 8, 640 (1975).

THIRD-ORDER TRANSPORT COEFFICIENTS FOR ELECTRONS II. MOLECULAR GASES

I. Simonović, Z.Lj. Petrović and S. Dujko

*Institute of Physics, University of Belgrade,
Pregrevica 118, 11080 Belgrade, Serbia*

Abstract. A Monte Carlo simulation technique is used to calculate the third-order transport coefficients for electrons and positrons in molecular gases. Values and general trends of the longitudinal and transverse skewness coefficients as a function of the reduced electric field in N_2 , CH_4 and CF_4 are reported here. We investigate the way in which the skewness transport coefficients are influenced by the energy dependence of cross sections for electron/positron scattering. Correlations between the skewness and diffusion coefficients have been found and studied.

1. INTRODUCTION

Studies of third-order transport coefficients for charged particles in gases are very useful under conditions when transport is greatly affected by non-conservative collisions and/or under conditions when the truncation of the charged particle flux to low order transport coefficients is not sufficient for accurate description of transport phenomena. There is a huge body of data for electrons (and ions), and since recently even for positrons, when it comes to low order transport coefficients, including the drift velocity and diffusion tensor, and rate coefficients. In contrast, little is known about high-order transport coefficients, particularly for electrons and positrons. This is understandable having in mind that the traditional swarm experiments have been interpreted without the consideration of high order transport [1], though it has been suspected to influence the motion of the electrons [2] and ions [3]. Third-order transport coefficients are most likely to be measured in the near future and hence it is of great importance to develop methods for their theoretical calculations. Such information can help in the design of future experiments as well as in the interpretation of their results.

The aims of this work are (1) to provide Monte Carlo calculations of the skewness transport coefficients for electrons and positrons in molecular gases, (2) to investigate the correlations between skewness and low order transport coefficients (e.g., the drift velocity and diffusion tensor), and (3) to study the explicit and implicit effects of non-conservative collisions on the skewness transport properties. In section 2 we give a brief discussion of our Monte Carlo method while in section 3 we present a few examples of our results for electrons in N_2 .

2. THEORETICAL METHODS

The Monte Carlo code applied in this work follows a large number of particles (usually 10^7 and sometimes even more) moving in an infinite gas under the influence of spatially homogeneous electric field. Particles (positrons or electrons) gain energy from the electric field and dissipate this energy through binary collisions with background neutral particles. The charged particle interactions are neglected since the transport is considered in the limit of low charged-particle density. All calculations are performed at zero gas temperature. For more details about our Monte Carlo simulation code see recent reviews [4, 5].

Skewness transport coefficients are determined after relaxation to steady state. The bulk values are calculated using the following formulas:

$$Q_L^{(B)} = \frac{1}{3!} \frac{d}{dt} (\langle z^3 \rangle - 3\langle z \rangle \langle z^2 \rangle + 2\langle z \rangle^3), \quad (1)$$

$$Q_T^{(B)} = \frac{1}{3!} \frac{d}{dt} (\langle zy^2 \rangle - \langle z \rangle \langle y^2 \rangle), \quad (2)$$

while the corresponding flux components are determined as follows:

$$Q_L^{(F)} = \frac{1}{3!} (3\langle z^2 V_z \rangle - 3\langle V_z \rangle \langle z^2 \rangle - 6\langle z \rangle \langle z V_z \rangle + 6\langle V_z \rangle \langle z \rangle^2), \quad (3)$$

$$Q_T^{(F)} = \frac{1}{3!} (\langle y^2 V_z \rangle + 2\langle zy V_y \rangle - \langle y^2 \rangle \langle V_z \rangle - 2\langle z \rangle \langle y V_y \rangle), \quad (4)$$

where indices B and F refer to *bulk* and *flux*. We consider a coordinate system in which the electric field lies along the z -axis.

3. RESULTS AND DISCUSSIONS

In figure 1 we show the variation of the longitudinal and transverse skewness coefficients, $n_0^2 Q_L$ and $n_0^2 Q_T$, respectively, with E/n_0 for electrons in N_2 . In order to understand the correlation between skewness and diffusion coefficients, on the same figure we show the variation of the longitudinal and transverse, $n_0 D_L$ and $n_0 D_T$, diffusion coefficients with E/n_0 . For lower E/n_0 , less than 40 Td, we observe that $n_0 D_L$ is a decreasing function

of E/n_0 . For the same E/n_0 , $n_0^2 Q_L$ decreases markedly. For $E/n_0 \geq 40$ Td, $n_0 D_L$ is a monotonically increasing function of E/n_0 while $n_0^2 Q_L$ increases with increasing E/n_0 , reaching a peak, and then it starts first to decrease and then again to increase. If we take a careful look, we see that after reaching the peak, $n_0^2 Q_L$ is decreased when the profile of $n_0^2 Q_L$ is changed from a typical convex to a more concave profile. This illustrates high sensitivity of $n_0^2 Q_L$ with respect to the collisional process that control the behavior of diffusion along the field direction. For $E/n_0 \geq 400$ Td both $n_0 D_L$ and $n_0^2 Q_L$ are monotonically increasing functions of E/n_0 . From the profile of $n_0^2 Q_T$, we see that the transverse skewness coefficient is correlated very well with both $n_0 D_L$ and $n_0 D_T$. This applies for electrons in N_2 ; for electrons in CF_4 we have identified the regions of E/n_0 where $n_0^2 Q_T$ exhibits better correlation with $n_0 D_T$ than with respect to $n_0 D_L$.

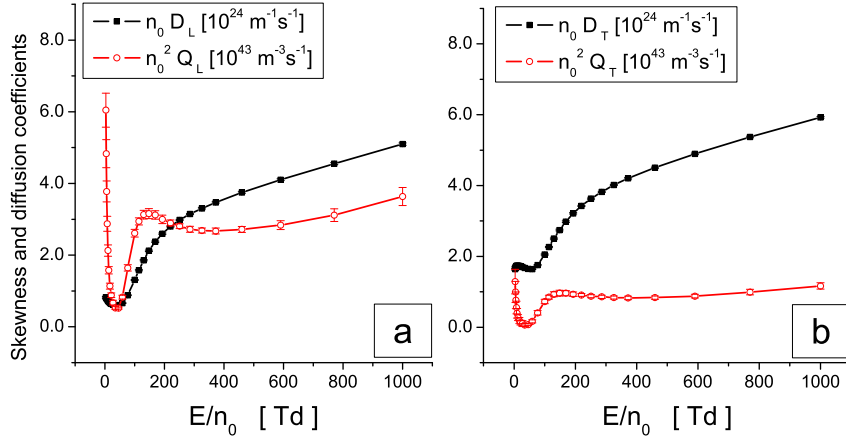


Figure 1. Variation of the longitudinal skewness and longitudinal diffusion coefficients with E/n_0 (a) and variation of the transverse skewness and transverse diffusion coefficients with E/n_0 (b) for electrons in N_2 .

Figure 2 displays the variation of the bulk and flux values of $n_0^2 Q_L$ (a) and $n_0^2 Q_T$ (b) with E/n_0 for electrons in N_2 . Increasing E/n_0 results in a more pronounced distinction between bulk and flux values. The explicit effects of ionization on the skewness properties become clearly evident for $E/n_0 \geq 150$ Td. For both $n_0^2 Q_L$ and $n_0^2 Q_T$ the bulk values overestimate the corresponding flux values and this is exactly what has been previously observed for the drift and diffusion in N_2 [6]. The differences between bulk and flux values do not exceed 60% for both $n_0^2 Q_L$ and $n_0^2 Q_T$ for E/n_0 considered in this work. Better understanding of the explicit effects of ionization on the skewness transport properties requires knowledge of the spatially resolved data along the swarm, particularly those associated with the high-order variations of the average energy.

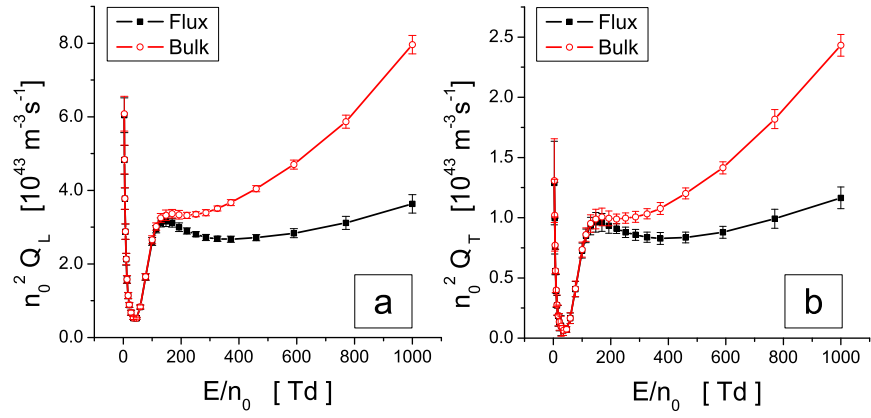


Figure 2. Variation of the bulk and flux longitudinal (a) and transverse (b) skewness coefficients with E/n_0 for electrons in N_2 .

Acknowledgments

This work was supported by MPNTRRS Projects OI171037 and III41011.

REFERENCES

- [1] L.G.H. Huxley and R.W. Crompton, *The Drift and Diffusion of Electrons in Gases* (New York: Wiley Interscience, 1973).
- [2] B.M. Penetrante and J.N. Bardsley, in *Non-equilibrium Effects in Ion and Electron Transport*, edited by J.W. Gallagher, D.F. Hudson, E. E. Kunhardt, and R.J. Van Brunt, (Plenum, New York, 1990), p. 49.
- [3] A.D. Koutselos, *Chem. Phys.* 270, 165 (2001).
- [4] S. Dujko, Z.M. Raspopović and Z.Lj. Petrović, *J.Phys.D: Appl. Phys.* 38, 2952 (2005).
- [5] S. Dujko, R.D. White and Z.Lj. Petrović, *J.Phys.D: Appl. Phys.* 41, 245205 (2008).
- [6] S. Dujko, U. Ebert, R.D. White and Z.Lj. Petrović, *Jpn. J. Appl. Phys.* 50, 08JC01 (2011).



28th Summer School and International Symposium on the Physics of Ionized Gases

Aug. 29 - Sep. 2, 2016, Belgrade, Serbia

CONTRIBUTED PAPERS

&

ABSTRACTS OF INVITED LECTURES,
TOPICAL INVITED LECTURES, PROGRESS REPORTS
AND WORKSHOP LECTURES

Editors:

Dragana Marić, Aleksandar Milosavljević,
Bratislav Obradović and Goran Poparić



University of Belgrade,
Faculty of Physics



Serbian Academy
of Sciences and Arts

MONTE CARLO SIMULATIONS OF ELECTRON TRANSPORT IN CF₃I AND SF₆ GASES

J. Mirić, D. Bošnjaković, I. Simonović, Z. Lj. Petrović and S. Dujko

*Institute of Physics, University of Belgrade,
Pregevica 118, 11080 Belgrade, Serbia*

Abstract. Electron transport coefficients in CF₃I and SF₆ gases are calculated using Monte Carlo simulations for a wide range of reduced electric field strengths. In order to compensate for the loss of electrons in simulation due to strong attachment, three different rescaling techniques are considered and applied. Among many observed phenomena, in case of SF₆ we highlight the reduction of mean electron energy with increasing electric field. In addition, we observe that for both gases bulk drift velocities exhibit negative differential conductivity which is not present in the flux drift velocity.

1. INTRODUCTION

Electron attachment in strongly electronegative gases, such as CF₃I and SF₆, has many industrial applications. For example, in high-voltage circuit breakers, it is the most significant process for the prevention of electric breakdown [1]. Electronegative gases are also used for plasma etching and cleaning in semiconductor fabrication [2].

On the other hand, electron attachment imposes practical difficulties in experiments for measurement of transport coefficients [1,3]. Considerable difficulties also appear in Monte Carlo simulations of electron transport in strongly electronegative gases at low electric fields where electron attachment is the dominant process. Due to this process, the number of electrons in a simulation can reach extremely low values leading to poor statistics or complete loss of electrons in the simulation [4,5]. In order to compensate for this loss of electrons, some sort of rescaling techniques must be used.

In this work, we discuss the existing rescaling techniques for Monte Carlo simulations of electron transport in strongly electronegative gases. Furthermore, we introduce our modified rescaling procedure and demonstrate how these techniques affect the calculated transport data for CF₃I and SF₆ gases.

2. RESCALING TECHNIQUES

The following rescaling techniques, applicable for Monte Carlo simulations, can be found in the literature:

1. Duplication of electrons randomly chosen from the remaining swarm at certain discrete time steps [6];
2. Duplication of the entire electron swarm (one or more times) at certain time steps [5] or at certain distance steps [7];
3. Introduction of an additional fictitious ionization [4] or attachment process [8] with a constant collision frequency.

An unaltered electron distribution function and its evolution are a common objective for all these techniques. In this work, the first technique will be referred to as discrete rescaling, the second as swarm duplication and the third as continuous rescaling. However, we introduce a modification to the third procedure where the fictitious ionization process is dynamically adjusted during the simulation in such way that the fictitious ionization rate is chosen to be equal to the attachment rate. Therefore, it is not necessary to define a fictitious ionization rate in advance and as a benefit, the number of electrons is kept nearly constant during the simulation.

3. RESULTS

In this section, we present the transport data for CF_3I and SF_6 gases, calculated using our Monte Carlo code [6,9] with three different rescaling techniques. The cross section set for electron scattering in SF_6 is taken from Itoh *et al.* [10]. In case of CF_3I , we use our modified cross section set [11] which is based on cross sections of Kimura and Nakamura [12]. This modification of the CF_3I set was necessary in order to provide a better agreement between the calculated data and the reference data measured in a pulsed Townsend experiment for pure CF_3I and its mixtures with Ar and CO_2 .

Figure 1(a) shows the variation of mean electron energy with E/n_0 in CF_3I . Calculations are performed assuming the three rescaling techniques. Excellent agreement between the cases of discrete rescaling and swarm duplication can be understood, having in mind that these two techniques are essentially the same. The only difference between the two is the fact that in case of discrete rescaling, the probability for duplication of an electron is determined by the ratio of current number and desired number of electrons, while in case of swarm duplication technique, this probability is set to unity i.e. the duplication is performed for all electrons. Continuous rescaling is also in a good agreement with the other two techniques.

In case of mean electron energy for the SF_6 gas, Figure 1(b) shows excellent agreement between the three rescaling techniques. Furthermore, one anomalous behavior is observed — a decrease of mean energy with increasing electric field. This phenomenon is associated with mutual influence of attachment heating and inelastic cooling. Since it is observed only in case of SF_6 ,

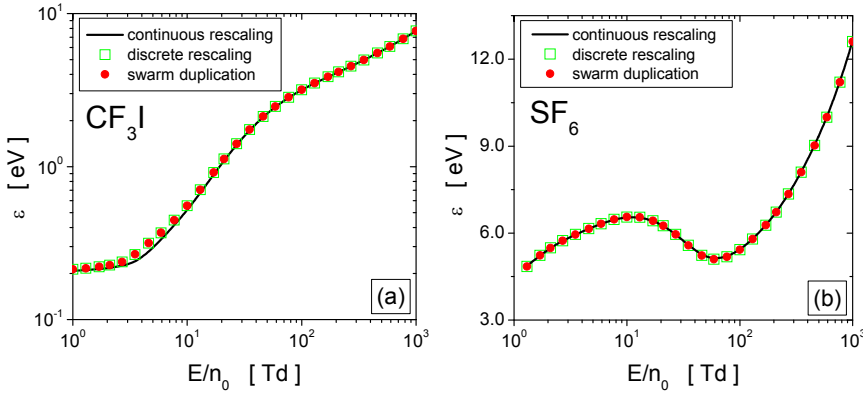


Figure 1. Mean electron energy in (a) CF_3I and (b) SF_6 gases as a function of reduced electric field. The profiles are calculated using three different rescaling techniques.

it is evident that the specific cross sections for electron scattering are essentially responsible for the occurrence of this phenomenon.

Figure 2 shows flux and bulk drift velocities in (a) CF_3I and (b) SF_6 gases, obtained with three rescaling techniques. For electrons in CF_3I , the drift velocities calculated using discrete rescaling and swarm duplication are again in excellent agreement while continuous rescaling at low electric fields gives slightly lower values than the other two techniques. For drift velocities in the SF_6 gas, all three rescaling techniques are in good agreement over the entire range of reduced electric fields considered in this work. We can conclude that the nature of the cross sections for electron scattering in CF_3I and SF_6 and their energy dependence are responsible for the differences between the results obtained using different rescaling techniques.

Two interesting phenomena are also observed in Figure 2. First, for

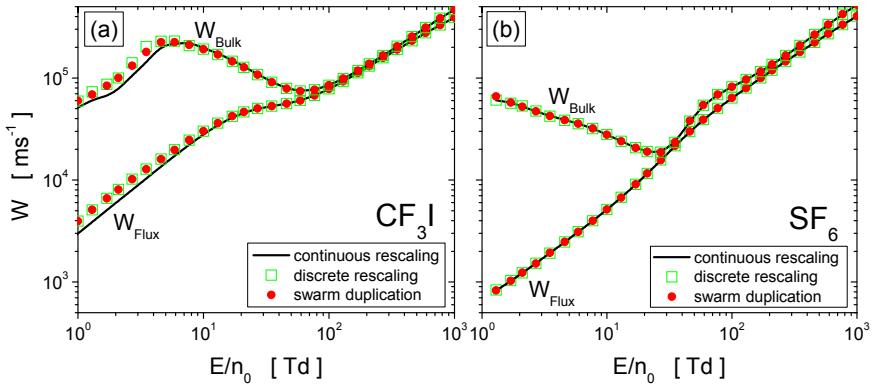


Figure 2. Variation of the drift velocity with E/n_0 for electrons in (a) CF_3I and (b) SF_6 gases. The profiles are calculated using three different rescaling techniques.

both gases the bulk drift velocity is higher than the flux drift velocity. In low energy range, this is a consequence of strong attachment heating (the consumption of slow electrons due to attachment) while in higher energy range the explicit effect of ionization is responsible. As a result, new electrons are preferentially created at the front of the swarm and/or slow electrons are consumed at the back of the swarm resulting in a forward shift of centre of mass of the swarm which is observed as an increase of bulk drift velocity over the flux drift velocity. The other phenomenon is a very strong NDC effect (negative differential conductivity) which is noticed for both gases, but only in case of bulk component drift velocity. This behavior appears to be common for all strongly electronegative gases since it is induced by explicit effects of electron attachment.

Acknowledgements

This work is supported by MPNTRRS Projects OI171037 and III41011.

REFERENCES

- [1] L. G. Christophorou and J. K. Olthoff, *Fundamental electron interactions with plasma processing gases*, (Springer, New York, 2004).
- [2] T. Makabe and Z. Lj. Petrović, *Plasma Electronics: Applications in Microelectronic Device Fabrication*, (CRC Press, New York, 2014).
- [3] Z. Lj. Petrović *et al.*, J. Phys. D: Appl. Phys. 42, 194002 (2009).
- [4] M. Yousfi, A. Hennad and A. Alkaa, Phys. Rev. E 49, 3264 (1994).
- [5] A. M. Nolan, M. J. Brennan, K. F. Ness and A. B. Wedding, J. Phys. D 30, 2865 (1997).
- [6] Z. M. Raspopović, S. Sakadžić, S. Bzenić and Z. Lj. Petrović, IEEE Trans. Plasma Sci. 27, 1241 (1999).
- [7] N. A. Dyatko and A. P. Napartovich, J. Phys. D 32, 3169 (1999).
- [8] Y. M. Li, L. C. Pitchford and T. J. Moratz, Appl. Phys. Lett. 54, 1403 (1989).
- [9] S. Dujko, R. D. White and Z. Lj. Petrović, J. Phys. D: Appl. Phys. 41, 245205 (2008).
- [10] H. Itoh, T. Matsumura, K. Satoh, H. Dane, Y. Nakano and H. Tagashira, J. Phys. D 26, 1975 (1993).
- [11] J. Mirić, O. Šašić, S. Dujko and Z. Lj. Petrović, Proc. 27th Summer School and International Symposium on the Physics of Ionized Gases (Belgrade) 2014, p. 122.
- [12] M. Kimura and Y. Nakamura, J. Phys. D 43, 145202 (2010).

ELECTRON TRANSPORT IN MERCURY VAPOR: DIMER INDUCED NDC AND ANALYSIS OF TRANSPORT PHENOMENA IN ELECTRIC AND MAGNETIC FIELDS

J. Mirić, I. Simonović, D. Bošnjaković, Z. Lj. Petrović and S. Dujko

*Institute of Physics, University of Belgrade,
Pregevica 118, 11080 Belgrade, Serbia*

Abstract. Transport coefficients for electron swarms in mercury vapor in the presence of electric and magnetic fields are calculated and analyzed using a multi term theory for solving the Boltzmann equation and Monte Carlo simulation technique. Particular attention is paid to the occurrence of negative differential conductivity (NDC) at higher gas pressures and temperatures. It is shown that the correct representation of the presence of mercury dimers and superelastic collisions plays a key role in the analysis of NDC. When both the electric and magnetic fields are present, another phenomenon arises: for certain values of electric and magnetic field, we find regions where swarm mean energy increases with increasing magnetic field for a fixed electric field. Spatially-resolved electron transport properties are calculated using a Monte Carlo simulation technique in order to understand these phenomena.

1. INTRODUCTION

In this work we discuss the transport of electrons in mercury vapor and its mixtures with argon under conditions relevant for metal vapor lamps. Current models of such lamps require knowledge of transport coefficients as a function of electric field strengths, gas pressures and temperatures. Recently developed inductively coupled plasma light sources require the knowledge of transport coefficients when both the electric and magnetic fields are present and crossed at arbitrary angles [1]. These transport coefficients can be either measured in swarm experiments or calculated from transport theory. To date, no experiments exist that can measure all the required transport coefficients, including rate coefficients, drift velocities, and diffusion coefficients for electrons in gases in the presence of electric and magnetic fields.

In the present work we solve the Boltzmann equation for electron swarms undergoing ionization in mercury vapor and its mixtures with argon in the presence of electric and magnetic fields crossed at arbitrary angles. For the E -only case we discuss the occurrence of negative differential conductivity (NDC) for

higher gas pressures and temperatures in the limit of lower electric fields. NDC is a phenomenon where the drift velocity decreases with increasing electric field. For electrons in mercury vapor this behavior of the drift velocity is attributed to the presence of mercury dimers.

In the second part of this work we investigate the electron transport in varying configurations of electric and magnetic fields. In particular, we discuss the following phenomenon: for certain values of electric and magnetic fields, we find regions where swarm mean energy increases with increasing magnetic field for a fixed electric field. The phenomenon is discussed using spatially-resolved transport data calculated in Monte Carlo simulations.

2. CROSS SECTIONS AND SIMULATION TECHNIQUES

The cross section for momentum transfer in elastic collisions is made as follows. For lower electron energies, we use a cross section from [2] while for higher energies, we use a cross section tabulated in MAGBOLTZ code [3]. Cross sections for electronic excitations for levels 3P_0 , 3P_1 and 3P_2 are retrieved from [4] while electronic excitations to 1S_0 and 1P_1 states as well as a cross section for higher states are also taken from MAGBOLTZ code. For electron-impact ionization, we have used a cross section from [5]. The effective cross section which describes vibration and electronic excitations of mercury dimers is derived using the experimental measurements of Elford [6]. Cross sections were slightly modified during the calculations to improve agreement between the calculated swarm parameters and the experimental values [6].

Electron transport coefficients are calculated from the multi term solution of Boltzmann's equation. A Monte Carlo simulation technique is used to verify the Boltzmann equation results and also for the calculations of spatially-resolved transport data.

3. RESULTS AND DISCUSSIONS

In Figure 1 (a) we show the variation of the drift velocity with E/n_0 for a range of gas pressures, as indicated on the graph. Calculations are performed in a wide range of pressures, from 20.2 to 108.4 Torr. The temperature of the background gas is 573K. The same range of pressures and temperatures was considered by Elford in his experiments [6]. We extend his measurements by considering the drift of electrons for six additional gas pressures. For E/n_0 less than approximately 2.5 Td the pressure dependence of the drift velocity is clearly evident. For higher E/n_0 , however, the drift velocity does not depend on the pressure. For pressures higher than approximately 200 Torr, we see that the drift velocity exhibits a region of NDC, i.e. over a range of E/n_0 values the drift velocity decreases as the driving field is increased. The conditions for the occurrence of NDC have been investigated previously [7]. For electrons in mercury vapor, NDC arises for certain combinations of elastic cross sections of dimer-free mercury vapor and inelastic cross sections of mercury dimers in

which, on increasing the electric field, there is a rapid transition in the dominant energy loss mechanism from inelastic to elastic. For pressures lower than 200 Torr the elastic cross section of dimer-free mercury vapor dominates the effective inelastic cross section of mercury dimers. Thus, the conditions for the occurrence of NDC are not set. For higher pressures, the phenomenon is promoted by either or both of (i) a rapidly increasing cross section for elastic collisions and (ii) a rapidly decreasing inelastic cross section. It is clear that the presence of dimers plays a key role in the development of NDC in mercury vapor.

In Figure 1 (b) we show a comparison between our calculations and experimental measurements of the drift velocity for a range of pressures. Our Monte Carlo results (figure 1 (b)) agree very well with those measured in the Bradbury-Nielsen time-of-flight experiment [6]. The agreement is achieved only after careful implementation of superelastic collisions in our calculations. Cross sections for superelastic collisions are calculated directly in our code from the principle of detailed balance.

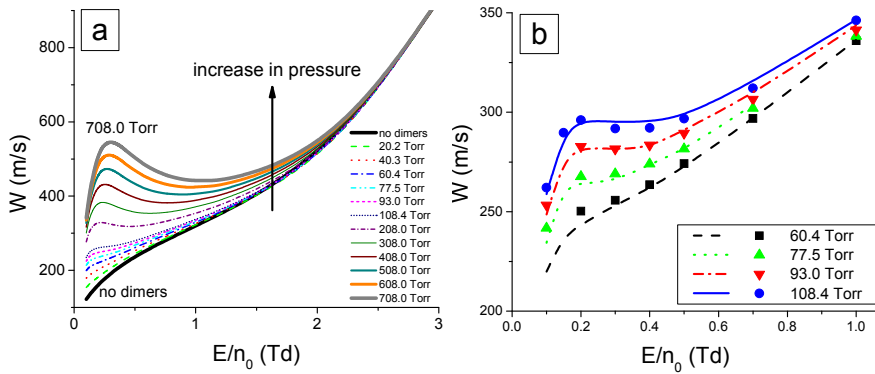


Figure 1. Variation of the drift velocity with E/n_0 for a range of pressures (a) and comparison between our Monte Carlo results and experimental measurements. Calculations are performed for electrons in mercury vapor. The temperature of the background gas is 573K.

In the last segment of this work we discuss the impact of a magnetic field on the electron transport in mercury vapor. The pressure and temperature of the mercury vapor are set to 1 Torr and 293K, respectively. As an example of our study, in figure 2 we show the variation of the mean energy with E/n_0 for a range of the reduced magnetic fields B/n_0 , in a crossed field configuration. In the limit of the lowest E/n_0 the electrons are essentially in the quasi-thermal equilibrium with the mercury vapor, independent of the strength of the applied magnetic field. In this regime, the longitudinal and transverse drift velocity components are dependent on both E/n_0 and B/n_0 while the diagonal diffusion tensor elements along the \mathbf{E} and $\mathbf{E} \times \mathbf{B}$ directions are dependent on B/n_0 only. The diffusion coefficient along the magnetic field direction is reduced to its thermal value as magnetic field only affects the diffusion in this direction indirectly, through the magnetic field's action to cool the swarm. Certainly one of the most striking

properties observed in the profiles of transport coefficients is an increase in the swarm mean energy with increasing magnetic field for a fixed electric field. The phenomenon is evident in the range $E/n_0=5-200$ Td for B/n_0 considered in this work. This behavior is contrary to previous experiences in swarm physics as one would expect the mean swarm energy to decrease with increasing B/n_0 for a fixed E/n_0 . The phenomenon could be associated with the interplay between magnetic field cooling and inelastic/ionization cooling, although the role of the cross sections in both phenomena is of course vital. The electron energy distribution function and spatially-resolved mean energy, rate coefficients and other properties are calculated using a Monte Carlo simulation technique in order to explain this phenomenon.

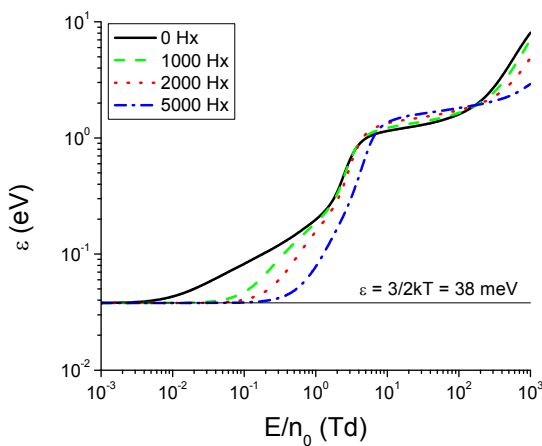


Figure 2. Variation of the mean energy with E/n_0 for a range of B/n_0 . Calculations are performed for electrons in mercury vapor.

Acknowledgements

This work is supported by MPNTRRS Projects OI171037 and III41011.

REFERENCES

- [1] G.G. Lister, J.E. Lawler, W.P. Lapatovich and V.A. Godyak, *Rev. Mod. Phys.* 76, 541 (2004)
- [2] J. P. England and M. T. Elford, *Aust. J. Phys.* 44, 647 (1991)
- [3] <http://magboltz.web.cern.ch/magboltz>
- [4] K. Bartschat, 3rd Int. Conf. on Atomic and Molecular Data and their Applications (New York: American Institute of Physics), 2003
- [5] L. J. Kieffer and G. H. Dunn, *Rev. Mod. Phys.* 38, 1 (1966)
- [6] M. T. Elford, *Aust. J. Phys.* 33, 231 (1980)
- [7] S.B. Vrhovac and Z.Lj. Petrovič, *Phys. Rev. E* 53, 4012 (1996)

TRANSPORT COEFFICIENTS FOR ELECTRON SWARMS IN LIQUID ARGON AND LIQUID XENON

I. Simonović¹, Z. L.J. Petrović¹, R.D. White² and S. Dujko¹

¹*Institute of Physics, University of Belgrade,
Pregrevica 118, 11080 Belgrade, Serbia*

²*College of Science & Engineering, James Cook University, Townsville 4810,
Australia*

Abstract. We have developed a Monte Carlo code for the calculation of transport coefficients for electron swarms in non-polar liquids. Transport coefficients for electron swarms in liquid argon and liquid xenon are calculated for $10^{-3} \leq E/n_0 \leq 10^3$ Td. Effects caused by fluctuations of density are neglected. Calculated transport coefficients in liquid phase are compared with those in the gas phase and differences are addressed using physical arguments.

1. INTRODUCTION

Transport of charged particles in liquids is a growing field of research, which addresses some fundamental questions and has many important applications. One of the most attractive applications is the interdisciplinary field of plasma medicine, which requires a detailed description of the behavior of electrons in liquid water and structures found in the living tissue. Additional applications are found in the technology behind the liquid argon and liquid xenon time projection chambers which are designed for detection of cosmic radiation, and search for dark matter particles.

Knowledge of transport coefficients in the liquid phase is also necessary for modeling of electrical discharges in liquids. There were many attempts to calculate transport coefficients of electron swarms in liquids. Cohen and Lekner calculated cross sections for electrons in the liquid phase argon which include coherent scattering effects [1,2]. In addition, they solved the Boltzmann equation using the two term approximation. Atrazhev and Iakubov [3] developed effective cross sections for electrons in liquid argon, krypton and xenon, which, for small energies, depend on density only. Numerical values of these cross sections, at low energies, must be found empirically. They subsequently had performed calculations in the framework of Cohen-Lekner theory and they obtained good agreement with experiment. Boyle et al [4,5] have recently determined *ab initio* differential cross sections for the gas phase argon and xenon by solving Dirac-

Fock scattering equations. Their cross sections are in a good agreement with experiment. They have derived liquid phase cross sections from those for the gas phase. In their work, the Cohen-Lekner procedure was extended to consider multipole polarizabilities and a non-local treatment of exchange. The calculation of transport coefficients in their work was performed using a multi term solution of Boltzmann's equation.

2. THEORETICAL EVALUATION

We have developed a Monte Carlo code for the calculation of transport coefficients of swarms of electrons and positrons in the liquid phase. Elastic scattering is treated in a way which is similar to the method described in the paper by Tattersall et al [6]. This method uses the fact that in the liquid phase mean free paths for the transfer of energy and momentum are different, due to structure effects. This allows the correct representation of the net transfer of momentum and energy, by including additional collisional processes in which only momentum/energy are exchanged. The mean free paths for the transfer of energy and momentum are given by the following equations,

$$\Lambda_0 = \left(n_0 2\pi \int_0^\pi d\chi \sin \chi (1 - \cos \chi) \sigma_{sp}(\varepsilon, \chi) \right)^{-1}, \quad (1)$$

$$\Lambda_1 = \left(n_0 2\pi \int_0^\pi d\chi \sin \chi (1 - \cos \chi) \sigma_{sp}(\varepsilon, \chi) S(\Delta\vec{k}) \right)^{-1}, \quad (2)$$

where $\sigma_{sp}(\varepsilon, \chi)$ is the differential cross section for electron scattering on a single molecule, and $S(\Delta\vec{k})$ is the static structure factor. The validity of our code is verified by comparison with benchmark calculations for the Percus Yevick model liquid [6]. Due to the lack of an adequate theory for the treatment of inelastic collisions in liquids, we have implemented the following strategy. For electron-impact ionization, we applied the gas phase cross sections, with thresholds which are reduced to the values suggested in the literature. For excitations, however, we apply two different scenarios. In the first scenario, the excitations are completely neglected. This is the so-called two-level model in which only ground state and conduction band are present [7]. In the second scenario, the gas phase excitations, with thresholds which are lower than the reduced threshold for ionization, are included in our set of cross sections. The remaining excitations are neglected. Fluctuations of density, and effects which are produced by interaction of swarm particles with polar background molecules are not included. Therefore, the applicability of our code is limited to non-polar liquids in which bubble/cluster formation is not appreciable.

3. RESULTS AND DISCUSSIONS

In figure 1 we show the variation of ionization rate coefficient with E/n_0 for electrons in liquid and gas xenon. We see that the ionization rate coefficients for electrons in both liquid scenarios are significantly greater than the corresponding rate coefficient for electrons in the gas phase. This is in part due to the cooling action associated with the inelastic collisions in the gas system, and also due to the modifications of the scattering potential between the gas and liquid phases. Comparing the two liquid scenarios, the ionization rate is greater without excitations. The reason is obvious: the competitive processes that lead to electronic excitation in which electrons lose energy are removed. It should be noted that the difference between ionization rate coefficients for different liquid scenarios is more pronounced for electrons in liquid argon than for electrons in liquid xenon.

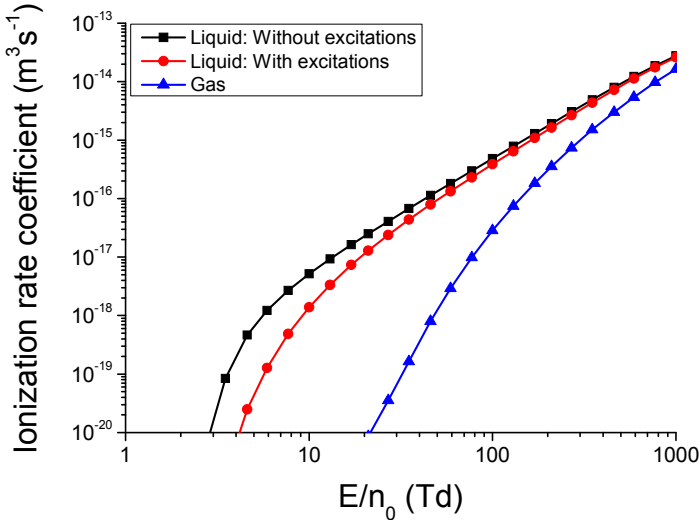


Figure 1. Variation of the ionization rate coefficient with E/n_0 for electrons in liquid and gas xenon.

In figure 2 we show the variation of the bulk drift velocity with E/n_0 for electrons in liquid and gas xenon. In the profile of the bulk drift velocity for electrons in the liquid phase, we observe negative differential conductivity (NDC). NDC is characterized by a decrease in the drift velocity despite an increase in the magnitude of applied electric field. While NDC has been demonstrated in the past to be a consequence of inelastic or non-conservative processes [8], its occurrence here is purely a result of including structure effects. The same effect has been already reported in the literature [3,4], and an analytic prescription for its occurrence has been presented [9,10]. For electrons in liquid Xe, NDC occurs for $0.01 \leq E/n_0 \leq 1$ Td. The corresponding range of mean energies is between 0.5 eV and 1.9 eV. In these field (energy) regions an

increase in the field leads to a sharp increase in the momentum-transfer cross section and hence a decrease in drift velocity. Structure induced NDC will be further investigated in our work, by simulating the spatially-resolved transport properties for electron swarms in liquid argon and liquid xenon.

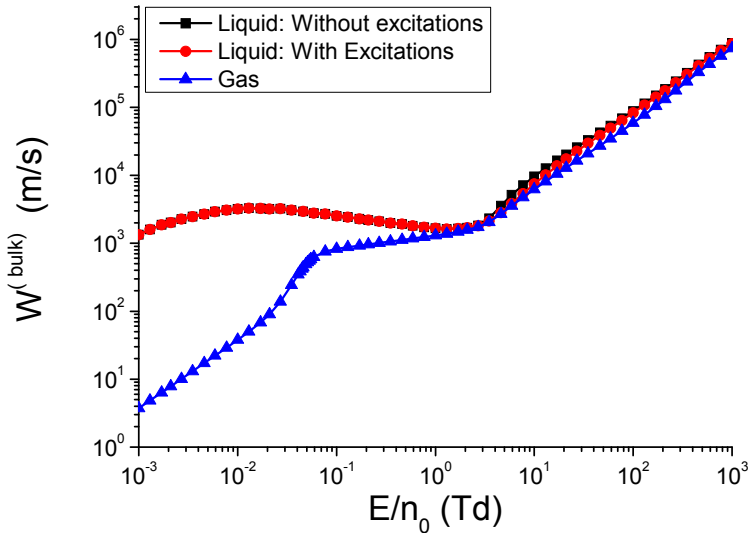


Figure 2. Variation of the bulk drift speed with E/n_0 for electrons in liquid and gas xenon.

Acknowledgements

This work was supported by MPNTRRS Projects OI171037 and III41011. RDW would like to thank the Australian Research Council.

REFERENCES

- [1] M. H. Cohen and J. Lekner, Phys. Rev. 158, 305 (1967)
- [2] J. Lekner Phys. Rev. 158, 130 (1967)
- [3] V.M. Atrazhev and I.T. Iakubov J. Phys. C 14, 5139 (1981)
- [4] G.J. Boyle et al. J. Chem. Phys. 142, 154507 (2015)
- [5] G.J. Boyle et al. arXiv:1603.04157v1 [physics.atom-ph]
- [6] W. J. Tattersall et al. Phys. Rev. E 91, 043304 (2015)
- [7] V M Atrazhev and E G Dmitriev J. Phys. C 18 (1985) 1205-1215.
- [8] S.B. Vrhovac and Z.Lj. Petrovič, Phys. Rev. E 53, 4012 (1996)
- [9] R.D. White et al, Phys. Rev. Lett. 102, 230602 (2009)
- [10] G.J. Boyle et al. New J. Phys. 14, 045011 (2012)

TRANSITION OF AN ELECTRON AVALANCHE INTO A STREAMER IN LIQUID ARGON AND LIQUID XENON

I. Simonović¹, Z. L.J. Petrović¹, R.D. White² and S. Dujko¹

*¹Institute of Physics, University of Belgrade,
Pregrevica 118, 11080 Belgrade, Serbia*

*²College of Science & Engineering, James Cook University, Townsville 4810,
Australia*

Abstract. In this work we investigate transition of an electron avalanche into a streamer, in liquid argon and liquid xenon, using 1.5 dimensional first-order fluid model. Electron transport coefficients used as input in fluid equations are calculated by our Monte Carlo simulation code. Streamer results in the liquid phase are compared to those in the gas phase.

1. INTRODUCTION

Electrical discharges in liquids have many important applications ranging from plasma medicine and water purification to transformer oils and miniaturized chemical analysis of liquid composition. However, detailed understanding of these discharges, which is necessary for their better stabilization and control, remains elusive, due to their complexity and diversity. Bubble formation and evolution, presence of impurities and solvation of electrons in polar liquids can all have significant impact on discharge dynamics in the liquid phase. Moreover, it is not possible to set up some experiments in liquids, the equivalent of which have been very useful for the study of gas discharges. Experiments which investigate electron avalanches in plane parallel geometry, in order to determine electron impact ionization coefficient, are one such example. In the case of liquids, high electric fields necessary for electron impact ionization, would lead immediately to breakdown [1]. This hinders the possibility to experimentally observe the gradual transition of an electron avalanche into a discharge, in a uniform external field. The presence of such experimental difficulties increases the importance of theoretical studies, both for the purpose of developing insight into the relevant physical phenomena, and for designing the future experiments. However, theoretical investigation of the behavior of charged particles in liquids also faces many problems. Many of those problems are related to accurate description of interaction between charged particles and the background molecules. The most recent advancement in the theoretical description of

transport of electrons in the liquid phase is presented in the papers by Boyle et al [2,3].

In this work we study the transition of an electron avalanche into a streamer in liquid argon and liquid xenon, in the presence of a constant external electric field, by employing 1.5 dimensional first-order fluid model. A similar study has been recently performed by Naidis [4] for electrons in liquid cyclohexane, although his simulations were done in point to plane geometry.

2. THEORETICAL EVALUATION

In this work we apply the first-order fluid model which is based on the drift-diffusion equation for electrons (1) and number balance equations for ions (2)

$$\frac{\partial n_e}{\partial t} = \frac{\partial}{\partial x} \left(D \frac{\partial n_e}{\partial x} - w n_e \right) + n_e (v_i - v_a), \quad (1)$$

$$\frac{\partial n_p}{\partial t} = n_e v_i, \quad \frac{\partial n_n}{\partial t} = n_e v_a, \quad (2)$$

where n_e , n_p and n_n are number densities of electrons, positive and negative ions, respectively, while w , D , v_i and v_a are drift velocity, longitudinal diffusion coefficient, and rate coefficients for ionization and attachment. The electric field produced by the space charge effects is given as follows

$$E(x, t) = \frac{e}{2\epsilon_0} \int_0^d \left(\text{sgn}(x - x') - \frac{x - x'}{\sqrt{(x - x')^2 + R_0^2}} \right) n_e(x', t) dx'. \quad (3)$$

Here we assume the cylindrically symmetric 2D charge distribution, where R_0 is a parameter of the model. The equations are solved numerically using 4th order Runge-Kutta method for the integration in time and 2nd order central differences for the spatial derivatives in 1 dimension. This corresponds to the so-called 1.5D dimensional model. Ions are considered stationary, since their velocity is negligible compared to the velocity of electrons for the time scale considered in this work.

Our fluid model is based on the local field approximation and requires the tabulation of electron transport coefficients as a function of the reduced electric field. We have used our Monte Carlo simulation code to calculate electron transport coefficients in both the gaseous and liquid systems. The code we use is similar to the Monte Carlo code developed by Tattersall et al [5]. We apply two scenarios regarding cross sections. In the first scenario excitations are completely neglected (No Excitation scenario) while in the second scenario, they are

approximated by the gas phase excitations (Excitation scenario). A more detailed introduction to our Monte Carlo code, and calculations of transport coefficients is given in our accompanying paper in the Proceedings of this conference. Comparison of the results, obtained by using these two scenarios, gives a rough estimate of the importance of accurate representation of excitations for modeling of streamer dynamics.

3. RESULTS AND DISCUSSION

In figures 1 and 2 we show the temporal evolution of the electron density in gas argon and liquid argon, respectively, for the several instants. The initially Gaussian electron density grows due to the ionization processes; then charge separation occurs in the electric field due to the drift of oppositely charged particles in opposite directions, and the initially homogeneous electric field is distorted; and finally, when the field in the ionized region becomes more and more screened, the ionization is reduced and the typical ionization front profiles of electron and ion densities and of the electric field are established. The initial ionization avalanche is then said to have developed into a streamer.

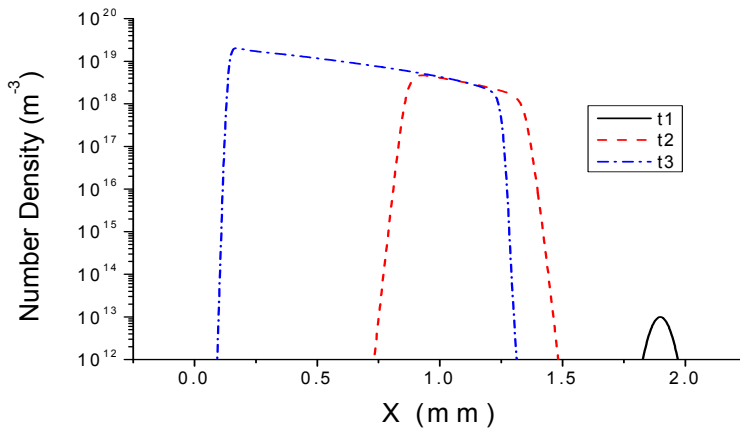


Figure 1. Transition of an electron avalanche into a streamer in the gas phase argon. Time moments t_1 , t_2 and t_3 correspond to 0ns, 9.2ns and 12ns respectively. The electric field vector is oriented to the right.

We observe that the transition of an electron avalanche into a streamer occurs much faster, and in a much smaller spatial range, in the liquid than in a gas system. It can also be seen that streamer dynamics is significantly different in the two scenarios regarding the treatment of excitations in the liquid phase. The

transition of an electron avalanche into a streamer is much faster in scenario without excitations, due to the absence of inelastic losses, which would decrease the rate for ionization. Thus, different estimations of the inelastic cross sections could yield great differences in the streamer properties. This suggests that accurate representation of the cross sections for excitations, in the liquid phase, is essential for modeling of discharges in liquids. The same holds for accurate description of cross sections for ionization.

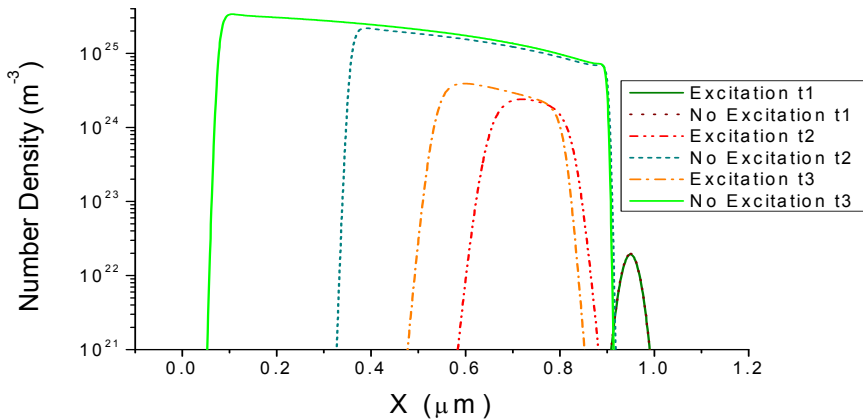


Figure 2. Transition of an electron avalanche into a streamer in the liquid argon. Time moments t1, t2 and t3 correspond to 0ps, 2.3ps and 2.9ps respectively. The electric field vector is oriented to the right.

Acknowledgements

This work was supported by MPNTRRS Projects OI171037 and III41011. RDW acknowledges the support from the Australian Research Council.

REFERENCES

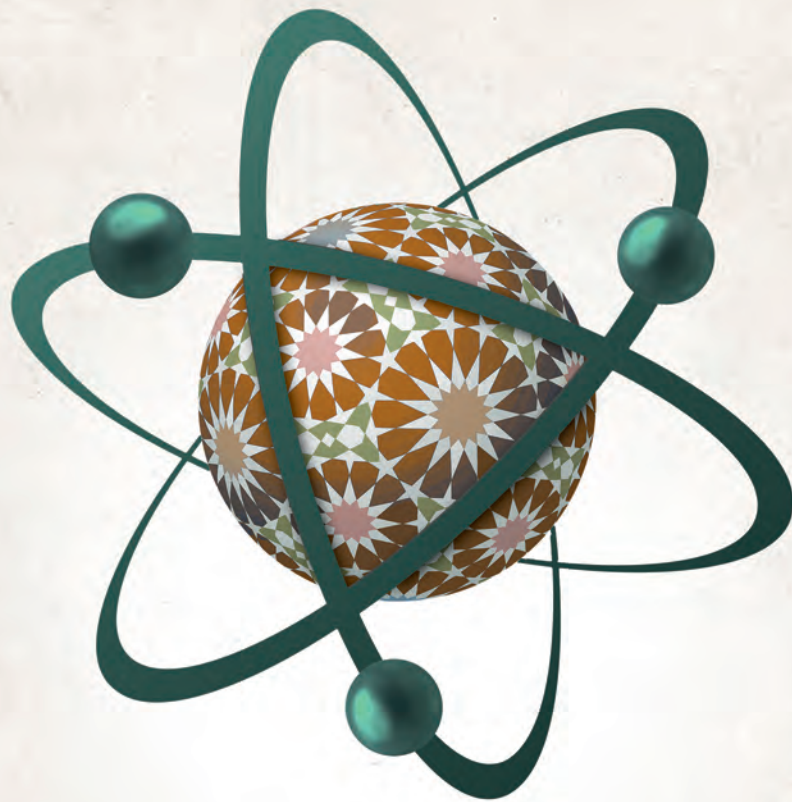
- [1] N. Bonifaci et al. *J. Phys. D: Appl. Phys.* **30** (1997) 2717–2725
- [2] G.J. Boyle et al. *J. Chem. Phys.* **142**, 154507 (2015)
- [3] G.J. Boyle et al. arXiv:1603.04157v1 [physics.atom-ph]
- [4] G.V. Naidis *J. Phys. D: Appl. Phys.* **48** (2015) 195203
- [5] W. J. Tattersall et al. *Phys. Rev. E* **91**, 043304 (2015)

CONFERENCE PROGRAM

ICPEAC 2015

XXIX INTERNATIONAL CONFERENCE
on Photonic, Electronic
and Atomic Collisions

22-28 JULY 2015 TOLEDO · SPAIN



Transport processes for electrons and positrons in gases and soft-condensed matter: Basic phenomenology and applications

S. Dujko*¹, Z.Lj. Petrović*, R.D. White†, G. Boyle†, A. Banković*, I. Simonović*, D. Bošnjaković*, J. Mirić*, A.H. Markosyan♥ and S. Marjanović*

* Institute of Physics, University of Belgrade, Pregrevica 118, 11080 Belgrade, Serbia

† College of Science, Technology & Engineering, James Cook University, Townsville 4810, Australia

♥ Electrical Engineering and Computer Science Department, University of Michigan, Ann Arbor, MI 48109, USA

Synopsis An understanding of electron and positron transport in gases and soft-condensed matter under non-equilibrium conditions finds applications in many areas, from low-temperature plasmas, to positron emission tomography, radiation damage and particle detectors in high-energy physics. In this work we will highlight how the fundamental kinetic theory for solving the Boltzmann equation and fluid equation models are presently being adapted to study the various types of non-equilibrium plasma discharges and positron-based technologies.

The transport theory of electrons and positrons in gases and soft-condensed matter is of interest both as a problem in basic physics and for its potential for application to modern technology. For electrons, these applications range from low-temperature plasmas to particle detectors in high energy physics and to understanding radiation damage in biological matter. For positron based systems, the emission of back-to-back gamma rays resulting from annihilation of a positron and an electron is a fundamental process used as a tool in many areas, ranging from fundamental atomic and molecular physics, particle and astrophysics, to diagnostics in biological and material sciences.

In this work we explore analytical framework and numerical techniques for a multi term solution of Boltzmann's equation [1], for both electrons and positrons in gases and soft-condensed matter, and associated fluid equation models [2,3]. Together with the basic elements of our Monte Carlo method, the particular attention will be placed upon the rescaling procedures for compensation of electrons for losses under conditions when transport is greatly affected by electron attachment in strong electro-negative gases.

For electrons, we will highlight recent advancements in the determination of the high-order transport coefficients in both atomic and molecular gases. Then we will discuss the elementary physical processes of electrons in the mixtures of gases used to model planetary atmospheric discharges. In particular, we will present the results of our theoretical calculations for expected heights of occurrence of sprites above lightning discharges in atmospheres of planets in our Solar system.

As an example of fluid equation models, we will discuss the recently developed high order fluid model for streamer discharges [3]. The balance equations for electron density, average electron velocity, average electron energy and average electron energy flux have been obtained as velocity moments of Boltzmann's equation and are coupled to the Poisson equation for the space charge electric field. Starting from the cross sections for electron scattering, it will be shown how the corresponding transport data required as input in fluid model should be calculated under conditions when the local field approximation is not applicable. We will illustrate the non-local effects in the profiles of the mean energy behind the streamer front and emphasize the significance of the energy flux balance equation in modeling. Numerical examples include the streamers in N₂ and noble gases.

In the last segment of this talk we will discuss the interaction of primary positrons, and their secondary electrons, with water vapor and its mixture with methane using complete sets of cross sections having bio-medical applications in mind [4]. We will also highlight recent advancements in the testing/validation of complete cross section sets for electrons in biologically relevant molecules, including water vapor and tetrahydrofuran [5].

References

- [1] S. Dujko *et al* 2010 *Phys. Rev. E* **81** 056403
- [2] R.D. White *et al* 2009 *J. Phys.D: Appl. Phys.* **42** 194001
- [3] S. Dujko *et al* 2013 *J. Phys.D: Appl. Phys.* **46** 475202
- [4] S. Marjanović *et al* 2015 *Plasma Sources Sci. Technol.* **24** 025016
- [5] White *et al* 2014 *Eur. Phys. J. D* **68** 125

¹ E-mail: sasa.dujko@ipb.ac.rs

- TH-086 **Mutual neutralization in He⁺ and H⁻ collisions**
Sifiso Musa Nkambule, Nils Elander, Ann E. Orel, Åsa Larson
- TH-087 **Ionization and ionic fragmentation for the components of a sample by electron collisions**
Ramaz Lomsadze, Malkhaz Gochitashvili, David Kuparashvili, Giorgi Takadze
- TH-088 **X-ray spectroscopy of multicharged xenon ions at the EBIT plasma**
Dariusz Banaś, Łukasz Jabłoński, Paweł Jagodziński, Aldona Kubala-Kukuś, Daniel Sobota, Martyna Puchala, Marek Pajek
- TH-089 **Third order transport coefficients for electrons and positrons in gases**
Ilija Simonović, Zoran Lj. Petrović, Sasa Dujko
- TH-090 **Laser trapped ⁶He as a probe of the weak interaction and a test of the sudden approximation**
Arnaud Leredde, Y. Bagdasarova, K. Bailey, X. Fléchar, A. Knecht, A. García, R. Hong, E. Liénard P. Müller, O. Naviliat-Cuncic, T. P. O'Connor, M. Sternberg, D. Storm, E. Swanson, F. Wauters, D. Zumwalt
- TH-091 **Positronium beam production and scattering at low energies**
Samuel Edward Fayer, Simon J. Brawley, Michael Shipman, Laszlo Sarkadi, Gaetana Laricchia
- TH-092 **Atomic wavelength in a kappa-distribution plasma**
Sabyasachi Kar, Zishi Jiang, Yongjun Cheng, Y. K. Ho
- TH-093 **Uncertainty Quantification of theoretical atomic and molecular collisional data**
Hyun-Kyung Chung, Bastiaan Johan Braams
- TH-094 **Preliminary measurements of the Bremsstrahlung doubly differential cross section for electrons between 20 and 100 keV in Au**
Juan Alejandro García-Alvarez, Nora Lia Maidana, Tiago Fiorini Silva, José María Fernández-Varea, Marcos Nogueira Martins, Vito Roberto Vanin
- TH-095 **Strong effect of the electron spin on bremsstrahlung observed in the relativistic regime**
Oleksiy Kovtun, Valery Tioukine, Andrey Surzhykov, Vladimir A. Yerokhin, Bo Cederwall, Stanislav Tashenov
- TH-096 **Recombination of H₂D⁺ and HD₂⁺ ions with electrons at 80 K**
Petr Dohnal, Abel Kalosi, Artem Kovalenko, Radek Plašil, Juraj Glosík
- TH-097 **Linear polarization of x rays due to dielectronic recombination into highly charged ions**
Chintan Shah, Holger Jörg, Zhimin Hu, Sven Bernitt, Hendrik Bekker, Michael A. Bleszenohl, Daniel Hollain, Sebastian Weber, Stepan Dobrodey, Stephan Fritzsche, Andrey Surzhykov, José R. Crespo López-Urrutia, Stanislav Tashenov
- TH-098 **Complete measurements of anisotropic x-ray emission following recombination of highly charged ions**
Chintan Shah, Pedro Amaro, René Steinbrügge, Christian Beilmann, Sven Bernitt, Stephan Fritzsche, Andrey Surzhykov, José R. Crespo López-Urrutia, Stanislav Tashenov
- TH-099 **Atomic Zero Energy Resonance in Plasmas**
Cesar Clauser, Raul Barrachina
- TH-100 **Simultaneous measurement of photorecombination and electron-impact ionization of Fe¹⁴⁺ ions**
Dietrich Bernhardt, Arno Becker, Manfred Grieser, Michael Hahn, Claude Krantz, Michael Lestinsky, Oldrich Novotny, Roland Repnow, Kaija Spruck, Daniel Savin, Andreas Wolf, Alfred Müller, Stefan Schippers
- TH-101 **Electron-ion recombination of the open-4f-shell ion W¹⁹⁺**
N. Badnell, K. Spruck, C. Krantz, O. Novotny, A. Becker, D. Bernhardt, M. Grieser, M. Hahn, R. Repnow, D. Savin, A. Wolf, A. Mueller, S. Schippers

THURSDAY

6. Lepton - Molecule / Small Cluster

- TH-102 **Positron scattering from biomolecules**
Joshua R Machacek, Wade Tattersall, Roisin Boadle, Ron White, Michael Brunger, Stephen Buckman, James Sullivan

Third order transport coefficients for electrons and positrons in gases

I. Simonović, Z.Lj. Petrović, and S. Dujko

Institute of Physics, University of Belgrade, Pregrevica 118, 11080 Belgrade, Serbia

Synopsis Structure and symmetries along individual elements of the skewness tensor (transport coefficient of the third order) are determined by the group projector technique. Skewness components are calculated using a Monte Carlo simulation technique and multi term solutions of Boltzmann's equation for electrons and positrons in model and real gases. A strong correlation between longitudinal skewness and longitudinal diffusion coefficients is observed.

Third order transport coefficients have been systematically ignored in the interpretations of traditional swarm experiments. However, recent Monte Carlo studies [1,2] have revealed that the spatial distributions of electrons are not well described by a perfect Gaussian. It was also shown that the third order transport coefficients are much more sensitive with respect to the energy variations of cross sections for elementary processes than those of lower order, including drift velocity and/or diffusion tensor [3,4].

Third order transport coefficients have been addressed by several authors for magnetic field free case. The semi-quantitative momentum transfer theory developed by Vrhovac et al. [3], and Monte Carlo simulation and solutions of Boltzmann's equation by Penetrante and Bardsley [4] were used to analyze the behavior of skewness tensor for electrons in rare gases. A three-temperature treatment of the Boltzmann equation and molecular dynamic simulation were used by Koutselos to calculate the third order transport coefficients for ions in atomic gases [5,6].

In this work we extend previous studies by considering the explicit and implicit effects of non-conservative collisions (e.g. electron attachment and ionization for electrons and Positronium formation for positrons) on various skewness components when both the electric and magnetic fields are present. In addition, the sensitivity of the skewness components to post-ionization energy partitioning is studied by comparison of three ionization energy partitioning regimes for a range of electric fields. Calculations are performed by a Monte Carlo simulation technique [1,2] and multi term theory for solving Boltzmann's equation [7].

Among many important points, we found a strong correlation between longitudinal skewness $n_0^2 Q_L$ and longitudinal diffusion $n_0 D_L$ coef-

ficients for both model and real gasses. If $n_0 D_L$ decreases, or increases as a concave function, with increasing electric field E/n_0 , then $n_0^2 Q_L$ decreases. On the other hand, when $n_0 D_L$ increases as a convex function with increasing E/n_0 , $n_0^2 Q_L$ also increases. This is illustrated in figure 1 for positrons in N_2 . It is generally observed that skewness coefficients vary more markedly than diffusion coefficients with E/n_0 .

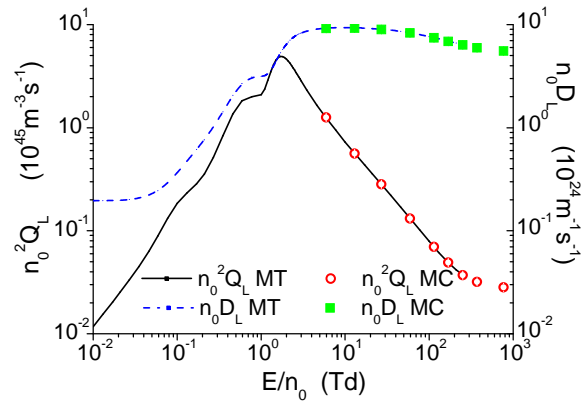


Figure 1. Correlation between flux longitudinal skewness and flux longitudinal diffusion for positrons in N_2 . MT and MC refer to Multi Term and Monte Carlo results, respectively.

References

- [1] Dujko et al. Eur. Phys. J. D 2014 68 166
- [2] Bošnjaković et al 2014 *J. Phys. D: Appl. Phys.* 47 435203
- [3] Vrhovac et al 1999 *J. Chem. Phys.* 110 2423
- [4] B.M. Penetrante and J.N. Bardsley, in *Non-equilibrium Effects in Ion and Electron Transport* (Plenum, New York, 1990) p. 49
- [5] A.D. Koutselos 1996 *J. Chem. Phys.* 104 8442
- [6] A.D. Koutselos 2005 *Chem. Phys.* 315 193
- [7] Dujko et al. Phys. Rev. E 2010 81 046403

EMS

XIX International Symposium on Electron-Molecule Collisions and Swarms

Book of Abstracts

POSMOL 2015

17-20 July 2015, LISBOA, PORTUGAL



XVIII International Workshop on Low-Energy Positron and Positronium Physics &
XIX International Symposium on Electron-Molecule Collisions and Swarms
17 - 20 July 2015, Lisboa, Portugal

POSMOL 2015

Swarms as an exact representation of weakly ionized gases

Zoran Lj. Petrović¹, Saša Dujko¹, Dragana Marić¹, Danko Bošnjaković¹, Srđan Marjanović¹, Jasmina Mirić¹, Olivera Šašić¹, Snježana Dupljanin¹, Ilija Simonović¹, Ronald D. White²

¹Institute of Physics University of Belgrade POB 68 11080 Zemun Serbia

²James Cook University of Northern Queensland, Townsville QL Australia

Zoran@ipb.ac.rs

Often swarms are regarded as idealized ensembles of charged particles that may be realized in specialized experiments to provide accurate transport coefficients, which after some analysis, yield "complete" sets of cross sections and accurate representations of non-equilibrium electron energy distribution function (EEDF) for a given E/N . Generally it is believed nowadays that swarms are just a tool for modeling non-equilibrium (low temperature) plasmas, as some kind of an interface through which atomic physics enters plasmas. In this review we shall show some new results that extend that picture into several directions:

- New results for the cross sections in systems where information from beam experiments and binary collision theories are insufficient such as $C_2H_2F_4$ that is commonly used as a cooling gas in modern refrigerators and air conditioners, but also it is used in particle detectors and has a potential for plasma processing applications.
- Ionized gases where swarms are exact representation of the system. Those include weakly ionized gases such as atmosphere, gas breakdown, afterglow (after the breakup of the ambipolar field), steady state Townsend regime of discharges, conduction of electricity through gases, interaction of secondary electrons produced by high energy particles with the gas or liquid background and many more. A special example will be modeling of Resistive Plate Chambers, the most frequently used gas phase detectors of elementary particles in high energy experiments.
- Swarm studies provide best insight into non-hydrodynamic (or as plasma specialists call it non-local) development of the ionized gas. It is not only that simulations are simple but also some of the accurate experiments operate in such conditions and thus allow testing of such theories. One such example are the Franck Hertz oscillations. Temporal and spatial relaxation of properties of ensembles to the final distribution belong to this group as well and are of interest for a number of positron applications and trapping in general.
- Fluid models when applied to swarms provide a good way to test the fluid models as used in more general plasmas. This has yielded the need to generalize fluid equations and extend them to a one step further while using a higher order transport coefficients.
- Finally we shall address the open issues for transport theorists and atomic and molecular collision population in the attempt to represent transport of electrons, positrons and other particles in liquids, especially in water that has a strong dipole moment. Hydrated electrons and positrons are the actually particles of interest for modeling these particles in the human tissue.

As an interface between atomic and molecular collision physics on a lower phenomenological (but deeper) level and plasmas on a higher (but less fundamental) level swarm physics has the responsibility of providing plasma physics with its intellectual basis and fundamental importance. It is how we combine the building blocks of atomic and molecular physics, transport theory and other relevant elementary processes that will define generality of the conclusions about non-equilibrium plasmas that are all different and require a special approach.

The models that we provide here are simple, yet realistic and real systems that may be described by swarm models and that may be regarded as low ionization limits of some more complex non-equilibrium plasmas.

Higher order transport coefficients for electrons and positrons in gases

I. Simonović¹, Z. Lj. Petrović¹, R.D. White² and S. Dujko¹

¹ Institute of Physics, University of Belgrade, Pregrevica 118, 11080 Belgrade, Serbia

² College of Science, Technology & Engineering, James Cook University, Townsville 4810, Australia

Higher order transport coefficients usually have not been included in the interpretations of traditional swarm experiments where it is assumed that electrons have a Gaussian profile in space. However, recent application of a Monte Carlo simulation technique has revealed that the spatial distribution of electrons is not well described by a perfect Gaussian [1,2]. It has also been demonstrated that third order transport coefficients are generally required for conversion of hydrodynamic transport coefficients to those measured under steady-state Townsend (SST) conditions [3]. Finally, it has been shown in [4,5] that third order transport coefficients are much more sensitive with respect to the energy dependence of cross sections for elementary processes than transport coefficients of lower order, including drift velocity and diffusion coefficients.

The behavior of third order transport coefficients for electrons under the influence of electric field only was analyzed by several authors. Solutions of the Boltzmann equation and Monte Carlo simulation by Penetrante and Bardsley [4] and momentum transfer theory developed by Vrhovac et al [5] were used to study the behavior of skewness tensor for electrons in atomic gases. A molecular dynamic simulation and a three-temperature treatment of Boltzmann's equation were used by Koutselos to evaluate the third order transport coefficients for ions in rare gases [6,7].

In this work we extend these previous studies by addressing the structure of skewness tensor when both electric and magnetic fields are present and by considering the effects of inelastic and non-conservative processes (e.g. ionization and electron attachment for electrons and Positronium formation for positrons) for electrons and positrons in model and real gases. A group projector technique is employed to determine the structure and symmetries along individual elements of the skewness tensor. Calculations are performed by a multi term theory for solving the Boltzmann equation [8] and Monte Carlo simulation technique [1,2]. Various aspects in the behavior of skewness tensor elements are investigated, including the existence of correlation with low-order transport coefficients, sensitivity to post-ionization energy partitioning and errors of two-term approximation for solving Boltzmann's equation. Special attention is paid to the comparison between skewness tensor elements for electrons and positrons in H₂, N₂ and CF₄.

References

- [1] Dujko *et al*, *Eur. Phys. J. D*, **68**, (2014), 166
- [2] Bošnjaković *et al*, *J. Phys. D: Appl. Phys.*, **47**, (2014), 435203
- [3] Dujko *et al*, *J. Phys. D: Appl. Phys.*, **41**, (2008), 245205
- [4] Vrhovac *et al*, *J. Chem. Phys.*, **110**, (1999), 2423
- [5] B. M. Penetrante and J. N. Bardsley, in *Non-equilibrium Effects in Ion and Electron Transport* (Plenum, New York, (1990) p. 49
- [6] A.D. Koutselos, *J. Chem. Phys.*, **104**, (1996), 8442
- [7] A.D. Koutselos, *Chem. Phys.*, **315**, (2005), 193
- [8] Dujko *et al*, *Phys. Rev. E*, **81**, (2010), 046403



GASEOUS ELECTRONICS MEETING

PRELIMINARY PROGRAMME

Sunday 14th February to Wednesday 17th February 2016.
Deakin University, Geelong, Victoria, Australia.



Third-order transport properties of electrons and positrons in electric and magnetic fields

I. Simonović, Z.Lj. Petrović, S. Dujko

¹ Institute of Physics, University of Belgrade, Serbia

Email contact: ilija.simonovic@ipb.ac.rs

Transport of a swarm of light charged particles, including electrons or positrons, in neutral gases under the influence of spatially homogeneous electric and magnetic fields has been studied thoroughly in the past, primarily through the investigation of the drift and diffusion. Third-order transport properties have not been measured systematically so far, and consequently have been ignored in the interpretations of the traditional swarm experiments. However, recent Monte Carlo studies [1] have revealed that the spatial distributions of electrons are not well described by a perfect Gaussian, particularly under conditions when charged particle transport is greatly affected by non-conservative collisions. Moreover, it has been demonstrated that the knowledge of third-order transport properties is required for the conversion of hydrodynamic transport properties to those found in the steady-state Townsend (SST) experiment [2].

In this work we investigate the structure and symmetries along individual elements of the skewness tensor (transport coefficient of the third order) by applying the group projector technique. Skewness components are calculated using a Monte Carlo simulation technique and multi term solutions of Boltzmann's equation for electrons and positrons in model and real gases. We extend previous studies [3] by considering explicit and implicit effects of non-conservative collisions (e.g. electron attachment and ionization for electrons and Positronium formation for positrons) on various skewness components when both electric and magnetic fields are present. In addition, sensitivity of the skewness components to positronization energy partitioning is studied by comparison of three ionization energy partitioning regimes for a range of electric fields.

[1] S. Dujko, Z.M. Raspopović, R.D. White, T. Makabe and Z.Lj. Petrović, *Eur. Phys. J. D* 2014, **68** 166.

[2] S. Dujko, R.D. White and Z.Lj. Petrović, *J.Phys. D: Appl. Phys.* 2008, **41** 245205.

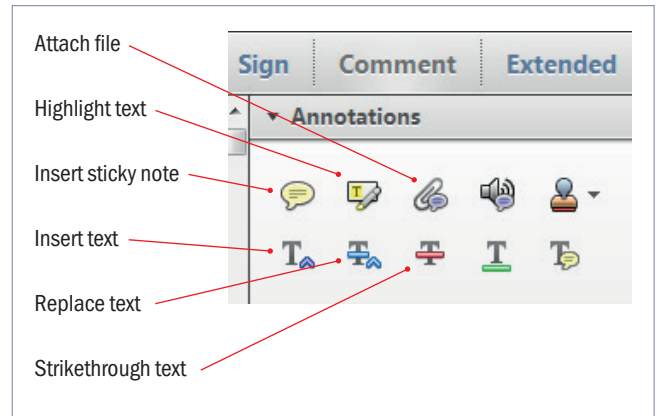
[3] S.B. Vrhovac, Z.Lj. Petrović, L.A. Viehland and T.S. Santhanam, *J. Chem. Phys.* 1999, **110** 242.

Making corrections to your proof

Please follow these instructions to mark changes or add notes to your proof. Ensure that you have downloaded the most recent version of Acrobat Reader from <https://get.adobe.com> so you have access to the widest range of annotation tools.

The tools you need to use are contained in **Annotations** in the **Comment** toolbar. You can also right-click on the text for several options. The most useful tools have been highlighted here. If you cannot make the desired change with the tools, please insert a sticky note describing the correction.

Please ensure all changes are visible via the 'Comments List' in the annotated PDF so that your corrections are not missed.

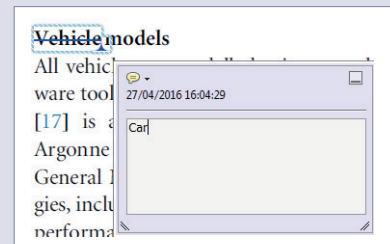


Do not attempt to directly edit the PDF file as changes will not be visible.



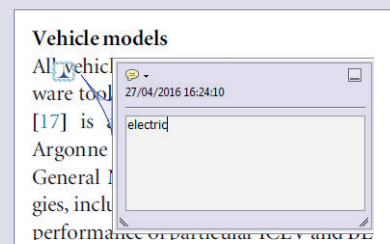
Replacing text

To replace text, highlight what you want to change then press the replace text icon, or right-click and press 'Add Note to Replace Text', then insert your text in the pop up box. Highlight the text and right click to style in bold, italic, superscript or subscript.



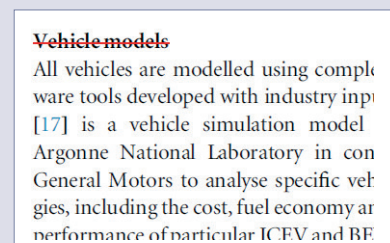
Inserting text

Place your cursor where you want to insert text, then press the insert text icon, or right-click and press 'Insert Text at Cursor', then insert your text in the pop up box. Highlight the text and right click to style in bold, italic, superscript or subscript.



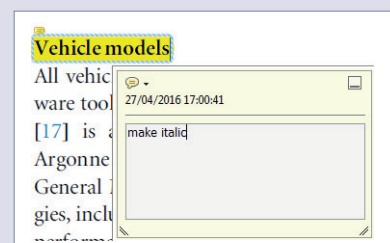
Deleting text

To delete text, highlight what you want to remove then press the strikethrough icon, or right-click and press 'Strikethrough Text'.



Highlighting text

To highlight text, with the cursor highlight the selected text then press the highlight text icon, or right-click and press 'Highlight text'. If you double click on this highlighted text you can add a comment.



QUERIES

Page 1

AQ1

Please check that the names of all authors as displayed in the proof are correct, and that all authors are linked correctly to the appropriate affiliations. Please also confirm that the correct corresponding author has been indicated.

AQ2

Please specify the corresponding author and provide his/her email address.

AQ3

Please be aware that the colour figures in this article will only appear in colour in the online version. If you require colour in the printed journal and have not previously arranged it, please contact the Production Editor now.

Page 2

AQ4

'developed in' OK; 'dedicated' is not the right word.

AQ5

Vrhovac *et al* (1999) and Marjanović and Petrović (2016) are cited in text but not provided in the list. Please provide complete publication details to insert in the list, else delete the citation from the text.

Page 4

AQ6

Figures 4–6 are provided but has not been cited in the text. Please remove the details or provide citation.

AQ7

Please define; 'Boltzmann equation'? If so, it will need to be defined earlier.

Page 5

AQ8

Note that the reference citations Santonico *et al* (2012) and Nietsin *et al* (2015) have been changed to Santonico (2012) and Natisin *et al* (2015) with respect to the reference list provided. Please check.

Page 6

AQ9

Please check the edits made to the sentence "Explanation and quantitative...".

Page 7

AQ10

Please check the edits made to the sentence "It may also be...".

Page 8

AQ11

Please check that the funding information below is correct for inclusion in the article metadata. Serbian Academy of sciences and arts: 155; Ministry of Education Science and technological research: OI171037 and III41011.

AQ12

If an explicit acknowledgment of funding is required, please ensure that it is indicated in your article. If you already have an Acknowledgments section, please check that the information there is complete and correct.

AQ13

Please check the details for any journal references that do not have a link as they may contain some incorrect information. If any journal references do not have a link, please update with correct details and supply a Crossref DOI if available.

AQ14

Please provide the volume and page/article number in Bošnjaković *et al* (2016) and Marjanović *et al* (2016).

AQ15

Dujko *et al* (2005) and Marjanovic *et al* (2011) listed in the reference list but not cited in the text. Please cite in the text, else delete from the list.

Page 9

AQ16

Please update the the publication details if appropriate in Simonović *et al* (2016).

AQ17

Please provide the city name of the publisher in Tung (1984).

Non-equilibrium of charged particles in swarms and plasmas—from binary collisions to plasma effects



Z L Petrović^{1,2}, I Simonović, S Marjanović¹, D Bošnjaković¹, D Marić¹, G Malović¹ and S Dujko¹

¹ Institute of Physics, University of Belgrade, POB 68, 11080 Zemun, Belgrade, Serbia

AQ1 ² Serbian Academy of Sciences and Arts, 11001 Belgrade, Serbia

AQ2 E-mail: xxxx



Received 23 July 2016, revised 12 September 2016

Accepted for publication 22 September 2016

Published



CrossMark

Abstract

In this article we show three quite different examples of low-temperature plasmas, where one can follow the connection of the elementary binary processes (occurring at the nanoscopic scale) to the macroscopic discharge behavior and to its application. The first example is on the nature of the higher-order transport coefficient (second-order diffusion or skewness); how it may be used to improve the modelling of plasmas and also on how it may be used to discern details of the relevant cross sections. A prerequisite for such modeling and use of transport data is that the hydrodynamic approximation is applicable. In the second example, we show the actual development of avalanches in a resistive plate chamber particle detector by conducting kinetic modelling (although it may also be achieved by using swarm data). The current and deposited charge waveforms may be predicted accurately showing temporal resolution, which allows us to optimize detectors by adjusting the gas mixture composition and external fields. Here kinetic modeling is necessary to establish high accuracy and the details of the physics that supports fluid models that allows us to follow the transition to streamers. Finally, we show an example of positron traps filled with gas that, for all practical purposes, are a weakly ionized gas akin to swarms, and may be modelled in that fashion. However, low pressures dictate the need to apply full kinetic modelling and use the energy distribution function to explain the kinetics of the system. In this way, it is possible to confirm a well established phenomenology, but in a manner that allows precise quantitative comparisons and description, and thus open doors to a possible optimization.

Keywords: charged particle swarms, non-equilibrium plasma, skewness, resistive plate chambers, positron traps, Monte Carlo simulations, Boltzmann equation

AQ3 (Some figures may appear in colour only in the online journal)

1. Introduction

The idea of thermodynamic equilibrium (TE) is one of the most widely used ideas in the foundations of plasma physics. Not only is TE used as a background gas, but it is also used as the plasma itself, and, further, TE is implicitly incorporated in most theories through application of the Maxwell Boltzmann distribution function. On the other hand, the idea of local thermodynamic equilibrium (LTE) in

principle means that TE is not maintained, and that energy converted into the effective temperature is being used as a fitting parameter, but also that all the principles of TE still apply for the adjusted (local) temperature. It is often overlooked that TE implies that each process is balanced by its inverse process. It is difficult to envisage just exactly how this condition could be met under circumstances where most of the energy that is fed into the non-equilibrium, low-temperature discharges comes from an external electric field.

The notion of non-equilibrium is implemented very well in a wide range of plasma models, starting from fluid models and hybrid models, all the way to fully kinetic codes such as particle-in-cell (PIC) modelling.

At end of a field of ionized gases, opposite to the fully developed plasma, at the lowest space charge densities, electrons are accelerated (gain energy) from the external electric field and dissipate in collisions with the background gas. This realm is known as a swarm (swarm physics), and is often described by simple swarm models. We shall try to illustrate how and where one may employ concepts developed in low-temperature plasmas for problems that are not traditional non-equilibrium plasmas such as positrons in gases and gas-filled traps, gas breakdown and particle detectors.

The three selected examples are: the use and properties of higher-order transport coefficients (skewness) and how they may be implemented to close the system of equations for modeling of atmospheric plasmas; modeling of resistive plate chamber (RPC) particle detectors with a focus on the development of avalanches, and prediction of the current and deposited charge; and, finally, modeling of a generic representation of the three stage gas-filled positron trap, where the same models as for electrons may be employed in a full kinetic description to calculate the temporal development of the energy distribution function, and, through that, to describe how and when individual elementary processes affect the performance of the trap.



AQ4

This is a review article as it covers three different topics that will (or have been) be presented in detail elsewhere. Yet the majority of the results will be developed in this paper. Necessarily, as it is a broad review, some finer points will be omitted in pursuit of the bigger picture, however, all will be covered elsewhere and the relevant literature is cited.

2. Higher-order transport and plasma modeling

The fluid equations often employed in plasma modeling are a part of an infinite chain, and whenever the chain is broken one needs a higher-order equation and related quantities to close the system of equations (Dujko *et al* 2013). That is why a closing of the equations is forced, sometimes labeled as ansatz, although the closure is not quite arbitrary. It is often based on some principles or simplifying arguments (Robson *et al* 2005) involving higher-order equations and related transport coefficients. Robson *et al* (2005) claimed that some serious errors have been incorporated into fluid equations that are commonly used in plasma modeling, and suggested benchmarks to test plasma models.

Equations (1) and (2) shown below, are the flux gradient equation and generalized diffusion equation, respectively, truncated at the contribution of the third order transport coefficients (also known as skewness). The terms, including $\widehat{Q}^{(F)}$ and $\widehat{Q}^{(B)}$ are terms that represent the contribution of the skewness tensor:

$$\vec{\Gamma}(\vec{r}, t) = \vec{W}^{(F)} n(\vec{r}, t) - \widehat{D}^{(F)} \cdot \nabla n(\vec{r}, t) + \widehat{Q}^{(F)} : (\nabla \otimes \nabla) n(\vec{r}, t) + \dots \quad (1)$$

$$\begin{aligned} \frac{\partial n(\vec{r}, t)}{\partial t} + \vec{W}^{(B)} \cdot \nabla n(\vec{r}, t) - \widehat{D}^{(B)} \\ : (\nabla \otimes \nabla) n(\vec{r}, t) + \widehat{Q}^{(B)} : (\nabla \otimes \nabla \otimes \nabla) n(\vec{r}, t) + \dots \\ = Rn(\vec{r}, t) \end{aligned} \quad (2)$$

where $\vec{\Gamma}(\vec{r}, t)$, $n(\vec{r}, t)$, $\vec{W}^{(F)}$, $\widehat{D}^{(F)}$, $\widehat{Q}^{(F)}$, $\vec{W}^{(B)}$, $\widehat{D}^{(B)}$, $\widehat{Q}^{(B)}$, R are the flux of charged particles, charged particle number density, flux drift velocity, flux diffusion tensor, flux skewness tensor, bulk drift velocity, bulk diffusion tensor, bulk skewness tensor and rate for reactions, respectively. If equations (1) and/or (2) are coupled to the Poisson equation for an electric field then the system of corresponding differential equations might be closed in the so-called local field approximation. This means that all transport properties are functions of the local electric field. The skewness tensor has been systematically ignored in previous fluid models of plasma discharges, although its contribution may be significant for discharges operating at high electric fields, and in particular for discharges in which the ion dynamics play an important role.

As for experimental determination of the higher-order diffusion of electrons, there have been some attempts, but those were mostly regarded as unsuccessful due to the end effects (Denman and Schlie 1990). In other words, those experiments may have failed to comply with both the requirements for negligible non-hydrodynamic regions and for lower pressures. An estimate was made that reliable skewness experiments would have to be up to 10 m long with pressures that are at least ten times smaller than those in standard swarm experiments. It seems that the only reliable yet very weak result was observed for H₂ in time of flight (TOF) emission experiments of Blevin *et al* (1976, 1978), as described in the PhD thesis by Hunter (1977). This is because the measurement was made away from the electrodes, thus providing a hydrodynamic environment.

At the same time some calculations were performed based on the available cross sections either by using a Monte Carlo simulation (MCS) and two term solutions of the Boltzmann equation (Penetrante and Bardsley 1990) or by using the momentum transfer theory (Vrhovac *et al* 1999). Whealton and Mason (1974) were the first to determine the correct structure of the skewness tensor in the magnetic field free case. For ions there have been more general studies and in particular theoretical studies. Koutselos gave a different prediction of the structure and symmetry of the tensor (Koutselos 1997) but those results were challenged (corrected) by Vrhovac *et al* (1999), who confirmed the structure of the skewness tensor previously determined by Whealton and Mason. Subsequently Koutselos confirmed the structure of the skewness tensor obtained by previous authors (Koutselos 2001).

Finally, having in mind the need for data in fluid modeling and the poor likelihood of experimental studies in the near future, a systematic study has been completed by Simonović *et al* (2016) dealing with the symmetry by using the group projector method (Barut and Raczka 1980, Tung 1984), multi-term Boltzmann equation solutions and MCS results in general terms. It should be noted that the third-order transport coefficients are often called skewness, but in principle it is the term that was to be applied only for the longitudinal diagonal

AQ5

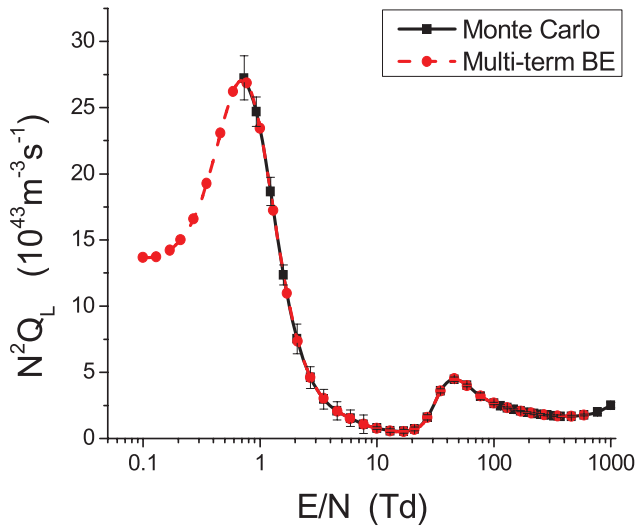


Figure 1. The longitudinal component of the skewness tensor calculated for electrons in methane.

term, which defines most directly the (departure from the) shape of the moving Gaussian. We will, however, use the term skewness for the entire tensor and all its terms.

The structure of the skewness tensor is the following (Wheaton and Mason 1974, Vrhovac *et al* 1999, Koutselos 2001, Simonović *et al* 2016):

$$Q_{xab} = \begin{pmatrix} 0 & 0 & Q_{xxz} \\ 0 & 0 & 0 \\ Q_{xxz} & 0 & 0 \end{pmatrix}, \quad Q_{yab} = \begin{pmatrix} 0 & 0 & 0 \\ 0 & 0 & Q_{xxz} \\ 0 & Q_{xxz} & 0 \end{pmatrix}$$

$$Q_{zab} = \begin{pmatrix} Q_{zxx} & 0 & 0 \\ 0 & Q_{zxx} & 0 \\ 0 & 0 & Q_{zzz} \end{pmatrix},$$

where $a, b \in \{x, y, z\}$ and Q_{abc} are the independent, non-zero terms in the tensor (although some of them may be identical if they are established for different permutations of the same derivatives). The components of the tensor may be grouped as longitudinal $Q_L = Q_{zzz}$ and transverse $Q_T = \frac{1}{3}(Q_{zxx} + Q_{xxz} + Q_{xxz})$.

In this paper, we present results for skewness of electron swarms in methane. Methane is known for producing negative differential conductivity (NDC) and in this work we will demonstrate the unusual variation of the longitudinal and transverse components of the skewness tensor for E/N (electric field over the gas number density) regions in which NDC occurs. NDC is characterized by a decrease in the drift velocity despite an increase in the magnitude of the applied reduced electric field. Cross sections for electron scattering in methane are taken from Šašić *et al* (2004). For the purpose of this calculation we assumed a cold gas approximation: $T = 0\text{K}$, which is justified as we covered mostly the E/N range where mean energies are considerably higher than the thermal energy. The initial number of electrons in the simulations was 10^7 and those were followed for sufficient time to achieve full equilibration with the applied field before sampling was applied. Sampling in an MCS is performed either

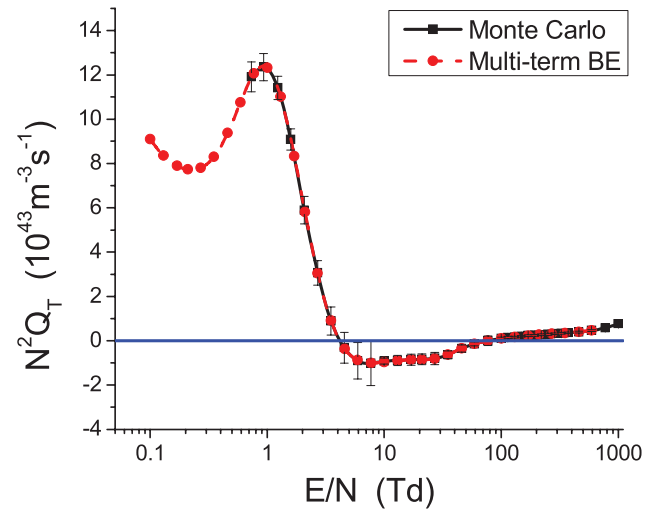


Figure 2. The transverse component of the skewness tensor calculated for electrons in methane.

for the flux (velocity space) $Q_{abc}^{(f)} = \frac{1}{3!} \left\langle \frac{d}{dt} (r_a^* r_b^* r_c^*) \right\rangle$ or for the bulk (real space) $Q_{abc}^{(b)} = \frac{1}{3!} \frac{d}{dt} \langle r_a^* r_b^* r_c^* \rangle$ components (Simonović *et al* 2016) where $r_a^* = r_a - \langle r_a \rangle$.

Uncertainties are established as the root mean square deviations. Statistical fluctuations in MCSs are more pronounced for skewness than for the lower-order transport coefficients. Thus, it is very important to present statistical uncertainties (errors) associated with the results. In addition to Monte Carlo results, the skewness tensor is calculated from the multi-term Boltzmann equation solution. The explicit formulas for skewness tensor elements in terms of moments of the distribution function will be given in a forthcoming paper (Simonović *et al* 2016).

In figures 1 and 2 we show the variation of the longitudinal and transverse skewness tensor components with E/N for electrons in CH_4 , respectively. In figure 3 we show the variation of independent components of the skewness tensor with E/N . The independent components of the skewness tensor have been calculated from a multi-term solution of the Boltzmann equation.

The first observation that is very important is that the multi-term Boltzmann equation results agree very well with those obtained in MCSs. This is an important cross check and it means that the techniques to calculate the skewness are internally consistent, although two very different approaches are implemented (having said that we assume that the solution to the Boltzmann equation and the MC are both well established and tested (Dujko *et al* 2010)).

We see that Q_T becomes negative in the same range of E/N where NDC occurs. At the same time Q_L remains positive. Q_{zxx} and the sum of Q_{xxz} and Q_{xxz} are negative in different regions of E/N .

Comparing the second- and third-order longitudinal transport coefficients we noticed that if diffusion decreases with increasing E/N then the skewness also decreases, but even faster. When it comes to the effect of the cross sections (or inversely to the ability to determine the cross sections from the transport data) it seems that skewness has a

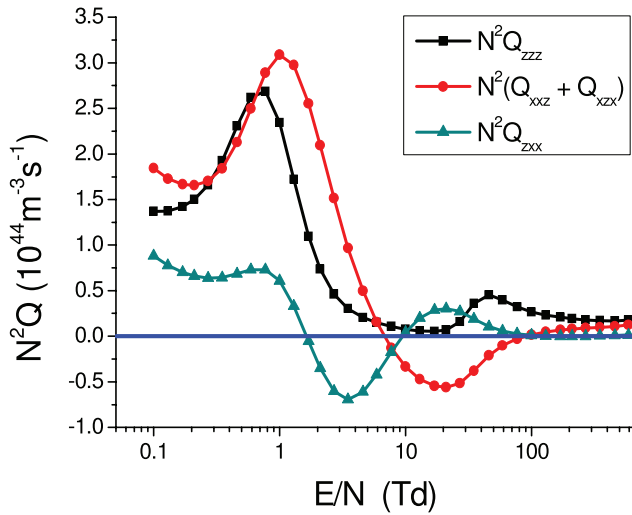


Figure 3. All independent components of the skewness tensor calculated for electrons in methane.

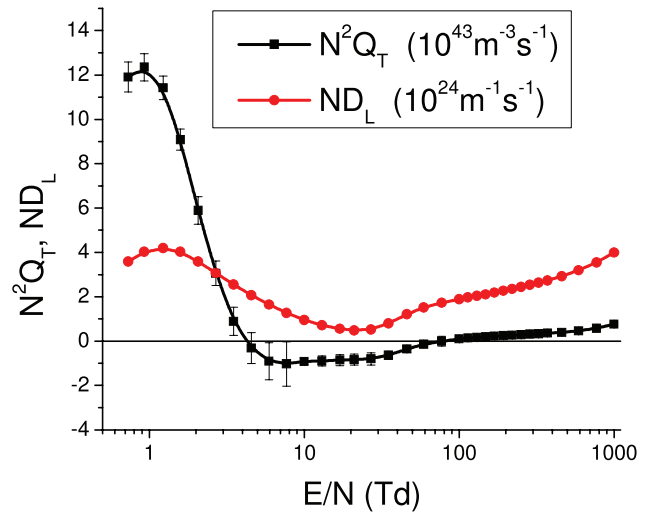


Figure 5. Comparison between longitudinal diffusion and transverse skewness for electrons in methane (the scale for the two different transport coefficients are provided in the legend).

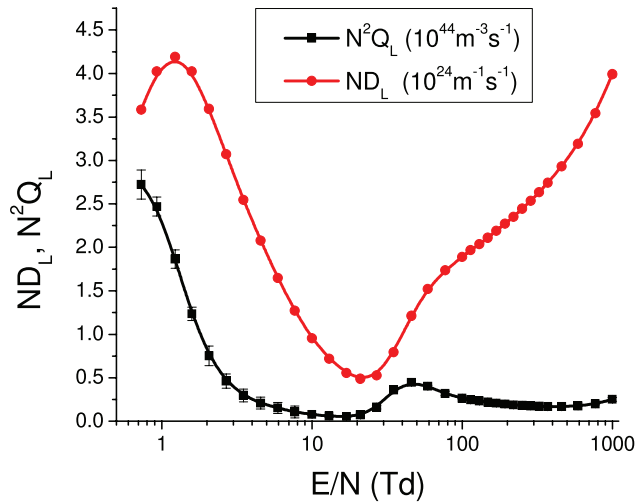


Figure 4. Comparison between longitudinal diffusion and skewness for electrons in methane (the scale for the two different transport coefficients are provided in the legend).

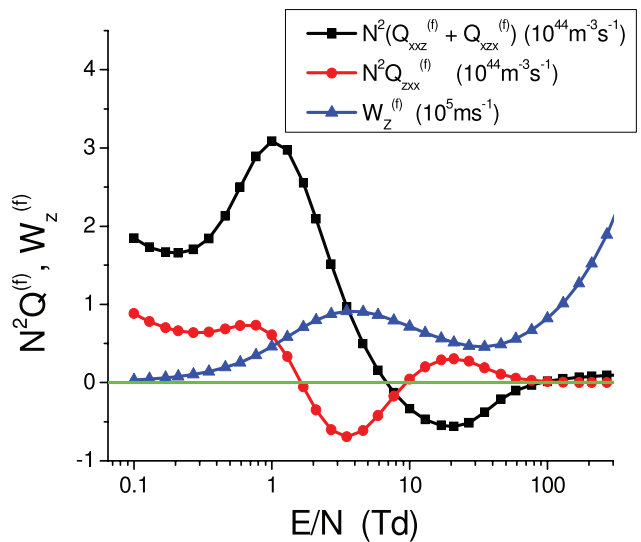


Figure 6. Off-diagonal components of skewness compared to the drift velocity for electrons in methane (the scale for the two different transport coefficients are provided in the legend).

more pronounced structure, and thus is more useful in fixing the shape and absolute values of the cross sections. If the diffusion increases, then we are able to distinguish between the two scenarios: if diffusion increases as a concave function, then the skewness decreases, while if the diffusion increases as a convex (or linear) function then the skewness increases.

We have observed that the transverse skewness is also in a good, if not better, correlation with the longitudinal diffusion. This is a good example that illustrates that the skewness tensor represents directional motion.

Different transverse components have different E/N profiles. Q_{zxx} follows the behavior of the drift velocity while the remaining components change their trends of behavior near the end of the NDC region. For different gases we have seen different trends and a clear correlation was not found (Simonović *et al* 2016).

Furthermore, but without illustrating it with special figures, the explicit effect of non-conservative collisions (ionization in this case) has been observed. However, in many cases the

agreement between multi-term BE results and those obtained in MCSs is better than what would be expected based on the estimated errors. At the same time it turned out that discrepancies between a two-term and multi-term (MCS) results may be quite large, ranging up to a factor of 10.

Possible measurements of higher-order transport coefficients seem possible and also profitable for the sake of determining the cross sections. Nevertheless the difficulties and possible uncertainties may outweigh the benefits. Thus, calculation of the data seems like an optimum choice for application in higher-order plasma models. The behavior of higher-order transport coefficients provides an insight into the effect of individual cross sections (their shape and magnitude), and their features such as the Ramsauer Townsend effect or resonances on the overall plasma behavior. The transport coefficients as an intermediate step give a guidance, especially when they develop special features (kinetic effects

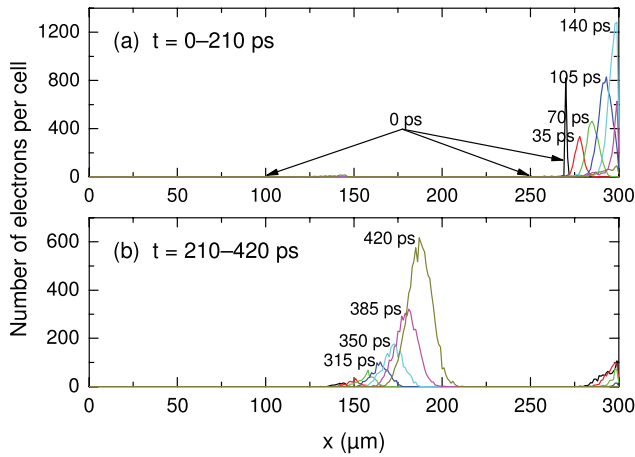


Figure 7. The spatio-temporal development of electron avalanches ((a) and (b)) in an RPC device. The number of electrons per cell (1D integration of a 3D simulation) is shown where the cells (1 cell = 1 μm) are along the discharge axis x . The cathode corresponds to $x = 0$ while the anode corresponds to $x = 300 \mu\text{m}$.

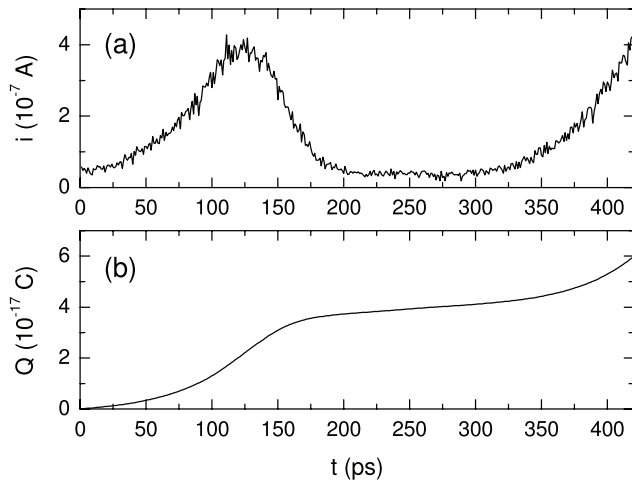


Figure 8. The time development of (a) electron induced current and (b) induced charge in the RPC device.

(Petrović *et al* 2009)) that may also be easily implemented in the determination of the cross sections.

3. Avalanches in resistive plate chambers

The next example of the connection of the elementary processes to plasma behavior through intermediate swarm-like phenomenology modeling will be modeling of RPC detectors. These devices are used for timing and triggering purposes in many high-energy physics experiments at CERN and elsewhere (The ATLAS Collaboration 2008, Santonico 2012). RPCs may be both used for spatial and temporal detection while providing large signal amplifications. They are usually operated in avalanche (swarm) or plasma (streamer) regimes depending on the required amplification and performance characteristics. Numerous models have been developed to predict RPC performance and modes of operation (Lippmann *et al* 2004, Moshaii *et al* 2012). We have studied systematically the swarm data (Bošnjaković *et al* 2014a) and

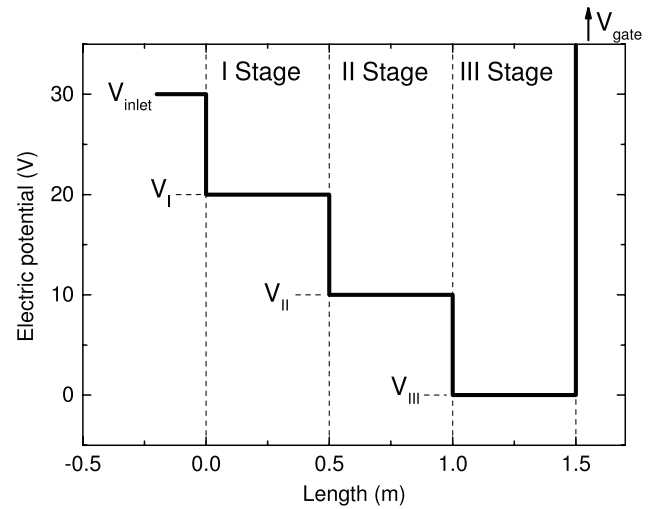


Figure 9. Schematic drawing of a generic Surko trap consisting of three equal potential drops. The composition of the background gas, its pressure and geometry are given in table 1.

Table 1. Parameters for simulation of a generic positron Surko trap.

Parameters	Stage I	Stage II	Stage III
Radius (mm)	5	20	20
Length (m)	0.5	0.5	0.5
Pressure (Torr)	10^{-3}	10^{-4}	10^{-5}
Background gas	N_2	N_2	$\text{N}_2^{0.5} + \text{CF}_4^{0.5}$
Magnetic field (G)	530	530	530
Voltage (V)	20	10	0
The initial parameters			
Potential of the entrance electrode (V)	30		
Potential of the source (V)	0.1		
Width (FWHM) of the initial energy distribution (eV)	1.5		

then the model of RPCs (Bošnjaković *et al* 2014b) where RPC efficiency and timing resolution have been predicted by MCS without any adjustable parameters, and were found to agree with experiment very well. Here we show some of the data not presented in Bošnjaković *et al* (2014b), which focuses on avalanche development and furthermore the induced current and charge.

Calculations of the development of the Townsend avalanche have been performed for a timing RPC gas mixture of $\text{C}_2\text{H}_2\text{F}_4:i\text{-C}_4\text{H}_{10}:\text{SF}_6 = 85:5:10$ with realistic chamber geometry (gas gap = 0.3 mm) at $E/N = 421 \text{ Td}$. We show in figure 7 the development of an avalanche in the gap with three initial clusters of charges (first generation secondary electrons indicated by arrows at 0 ps) formed by an incoming high-energy particle. The first cluster (from the left) has one electron, the second has nine and the third has 983 initial electrons. The distribution over a small group of cells has been randomly selected according to well-established distributions. At the beginning, the initial condition shapes the profile of the ensemble, but eventually a Gaussian is formed that drifts under the influence of an electric field and diffuses due to numerous collisions.

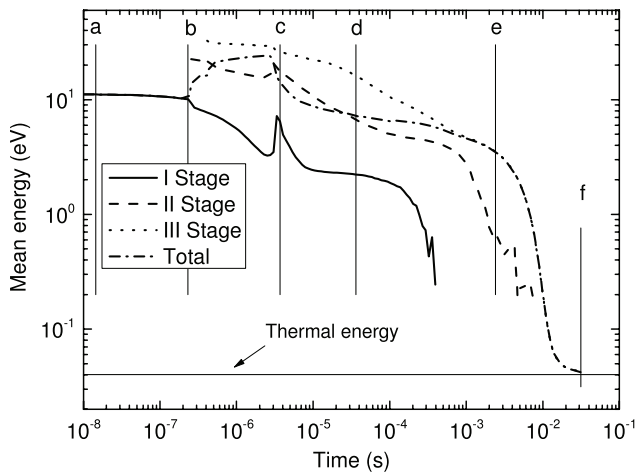


Figure 10. The mean energy of the positron ensemble (swarm) as a function of time. Averages for each stage and for the entire volume (total) are provided. The energy distribution function is plotted in figure 11 for the times marked by the points (a)–(f) in this figure.

We will first follow the development of the cluster closest to the anode (at $270 \mu\text{m}$), as indicated by spatial electron profiles at different times in figure 7(a). The largest initial group, which is also the closest to the anode, develops the fastest: from the initial very sharp profile it quickly establishes a Gaussian shape that also very quickly gets absorbed by the anode. The second peak (from the right) is quick to follow but it is very small and cannot be observed clearly due to interference from the first pulse. In figure 7(b), we show the development of the first cluster (at $100 \mu\text{m}$) for longer times. This cluster is the furthest from the anode and it takes the most time to reach the anode, again as a well developed moving Gaussian. It develops, however, a well-separated and defined current pulse (unlike the second cluster of charged particles). The induced current and the corresponding induced charge are shown in figure 8.

The predictions in figure 8, extended to provide important information on the temporal resolution, may be used to optimize the device by changing gas composition, field and geometry, and also may be extended to allow for the formation of the plasma in later stages when a streamer discharge may be generated at atmospheric pressure (Bošnjaković *et al* 2016). Trial and error development of such devices is simply too costly to allow for an empirical learning curve. Nevertheless, one could argue that it could be possible to develop a model based on a standard swarm description of a moving Gaussian with drift and diffusion plus the benefit of multiplication through ionization. All of these processes have their swarm coefficients. However, the very short times of the formation of the initial cluster, it being inhomogeneous and a very nonlinear growth with a possible separation of faster and slower electrons, dictate the need to perform an MCS in order to achieve the required accuracy. Thus, this example allows for the use of transport coefficients, but is better accomplished by full kinetic modeling. Transport coefficients are better taken advantage of in fluid modeling of the possibly developing streamer (Bošnjaković *et al* 2016). In any case, the ionized gas and the developing plasma channel are both represented very

accurately (qualitatively and quantitatively). Here we have used kinetic swarm modeling, although using transport coefficients may also be an option, albeit a less accurate option.

4. Gas-filled positron (and electron) traps

While it is often assumed that keeping the antimatter away from the matter is a way of preserving it longer, the introduction of background gas to the vacuum magnetic field trap led to the birth of the so-called Penning Malmberg Surko traps (often known simply as Surko traps). These devices take advantage of the very narrow region of energies, where in nitrogen electronic excitation can compete and even overpower the otherwise dominant (for almost all other gases and inelastic processes) positronium (Ps) formation (Murphy and Surko 1992, Cassidy *et al* 2006, Clarke *et al* 2006, Sullivan *et al* 2008, Marjanović *et al* 2011, Danielson *et al* 2015). To be fair, the principles of the trap have been worked out in great detail, but mostly based on beam-like considerations (Murphy and Surko 1992, Charlton and Humberston 2000). However the device consists of a charge being released in a gas in the presence of electric and magnetic fields, and thus it is an ionized gas that is exactly described by a swarm model until the space charge effects begin to play a significant role, and then it is best described by a plasma model (again with a significant reference to collisions and transport). Thus, for quantitative representation and accurate modeling of traps, a swarm-like model is required and recently two such models were used to explain the salient features of Surko traps (Marjanović *et al* 2011, Petrović *et al* 2014, Natisin *et al* 2015). An explanation and quantitative comparisons will be the subject of a specialized publication (Marjanović and Petrović 2016). Here we only focus on the development of the energy distribution function, which is the primary medium connecting the large-scale behavior of the trap with microscopic binary collisions.

As pressures used in the gas-filled traps are very low, and the mean free paths become comparable to the dimensions of the trap, one may be assured that the description at the level of transport coefficients and fluid models would fail. This example thus requires a full kinetic level of description.

The generic (model) trap consists of three stages, each with a 10 V potential drop and each of the same length (figure 9). The properties, the pressures and other features are listed in table 1. A standard, well-tested (for electron benchmarks—Lucas and Saelee 1975, Reid 1979, Ness and Robson 1986, Raspopović *et al* 1999) Monte Carlo code has been used here. Realistic geometry was included along with the boundary conditions (potentials, energy distributions and losses). Special care was given to the testing of the modeling trajectories in magnetic fields (Raspopović *et al* 1999).

First results are shown in figure 10 where we plot mean energies as a function of time in three separate stages (chambers) and also averaged for the entire volume. The energy steps provided by the potential drops are observable for the mean energies in stages II and III. The overall increase in energy is also observed in the total volume average. The initial plateau of the mean energy is extended mainly due to



AQ9

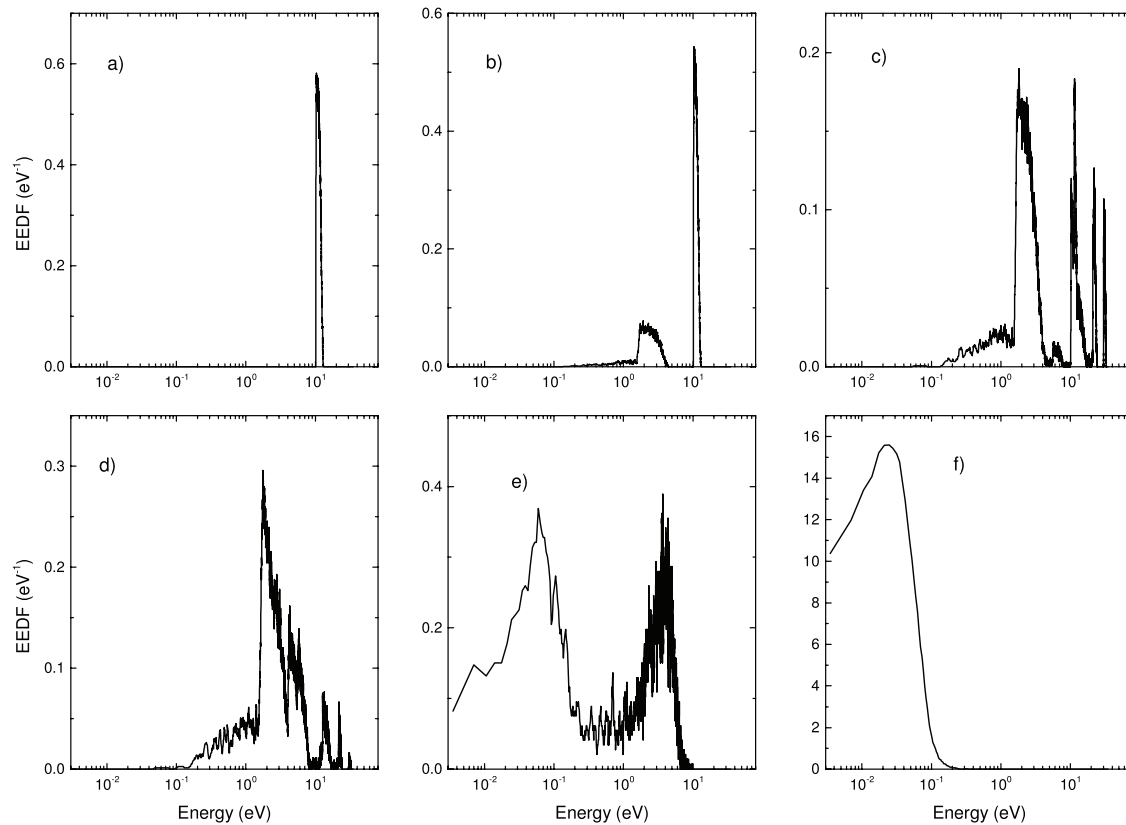


Figure 11. Positron kinetic energy distribution of the entire swarm sampled at different times (indicated in figure 10). Calculations were performed for the Surko trap as shown in figure 9 with the conditions listed in table 1.

the logarithmic nature of the plot. Following another plateau due to inelastic energy losses, the mean energy falls to the thermal value for the final thermalization.

The voltage drop in the initial stage is used to accelerate the positrons coming from the moderator into the energy range where electronic excitation of nitrogen is as efficient as Ps formation. Thus the initial distribution in figure 11 is a mono-energetic beam at 10 eV. Upon development of the group of positrons that have lost energy in excitation (figure 11(b)), positrons leave the stage I and pass into stages II and III so the two new peaks develop at 20 eV and 30 eV (figure 11(c)). The positrons that have collided form a group peaking at around 2 eV. During the next period two processes are obvious. The first is the quenching of the initial beams into the group, peaking at around 2 eV but extending up to 7 eV, where Ps formation removes the particles. The second is the process that uses vibrational excitation of CF_4 and thermalizes the 2 eV group into a low-energy group peaking at around 0.07 eV (figures 11(d) and (e)). It is interesting to see that the peak at around 2 eV is the first to disappear, leaving a group at around 5 eV to thermalize more slowly. At this point the low-energy positrons are also mainly localized in the third stage.

The final stage is characterized by two processes, the disappearance of the higher-energy group at around 5 eV and the gradual thermalization of the low-energy group at around 70 meV towards the thermal energy (f) of around 40 meV. At that point a quasi-thermal Maxwellian is developed. The transition appears to be rapid but, by the virtue of a logarithmic plot, it is the longest transition in the process of thermalization and

involves bouncing between the potential boundaries of the third stage many times. At the same time one should see that the properties of the trap are adjusted so that in the first bounce across the three stages most particles suffer electronic excitation/Ps formation collisions and either disappear or are trapped.

The simulation provides many different properties of the positron ensemble (swarm) but the point of this paper is to show a direct connection between binary collision processes and the macroscopic behavior. Using the energy distribution one can easily see the dominant processes and predict which aspects of the processes are promoted by the clever design of the Surko trap. It may also be used to optimize its characteristics (Marjanović *et al* 2016). Nevertheless, the principles of the trap were properly understood from the initial concepts but in this case we have detailed representation of the energy distribution, allowing accurate quantitative comparisons. For example, one may now adjust the details of the cross section in order to fit the measured properties (such as sampled mean energy that may be somewhat skewed by the sampling process). In that respect the measured observables from the trap may play a role in the swarm data that need to be fitted in order to tune the cross sections so that the number, momentum and energy balances may be preserved. As analysis of the positron swarm data led to a number of complex kinetic effects (Banković *et al* 2009, 2012) it would be interesting to see whether similar effects may be observed or even affect the operation of the traps.

These results are akin to the well-established initial equilibration for electrons in gases (Dujko *et al* 2014) with



temporal and spatial Holst Oosterhuis luminous layers (Hayashi 1982, Fletcher 1985) that are strongly related to the well-known Frank Hertz experiment (White *et al* 2012, Robson 2014). In addition, it must be noted that even if we were to start simulation with a Maxwellian distribution and try to follow the thermalization, due to the sharp energy dependence of the processes non-Maxwellian distribution function, it would develop immediately making it necessary to employ a full kinetic treatment. While fluid equations will not work well under the circumstances, and while transport coefficients may be difficult to define and even more difficult to implement in modeling, kinetic (Monte Carlo) modeling is still a typical swarm-like model that needs to be employed. Once we fill the trap with sufficient charge to allow for plasma effects, then we may need to add-in true plasma modeling based on fluid equations and on the calculation of the effective fields.

5. Conclusion

In this review we address three recent examples on how swarm based modeling may connect the microscopic binary processes to the macroscopic behavior of ionized gases, even plasmas. The necessary prerequisite for this approach to be effective is that the systems belong to the so-called collisional plasmas (also known as the non-equilibrium or low-temperature plasmas). The examples are chosen to reveal three different aspects of swarm modeling: (a) that based on transport coefficients and fluid models and how they may be improved, (b) a system that may be described by both fluid models and simulations where simulations are used here to verify the more basic modeling, while the fluid modeling is allowing us to extend predictions further to plasma conditions, and, finally, (c) for the situation where full kinetic modeling is required. Thus, these examples should be viewed as confirmation of the validity and usefulness of the swarm models that are often overlooked by plasma modelers. Swarm models are sometimes regarded as a limit that is unrealistic and useful only to describe well-designed experiments that provide swarm data. One subscribing to that view would then need to reply to why the use of swarm data and also swarm data based fluid equations is so successful. In fact, we believe that often an ‘overkill’ is performed by using plasma models to describe inherently swarm-like conditions. One such example is the popular modeling of breakdown by PIC of hybrid codes. If done properly, it is all fine, although less transparent due to a more complex nature of the codes. However, at the same time such complexity does not allow us to add special tests or sampling that may reveal more insight into the pertinent physical processes. Examples may include details of the energy distribution function, adjusting boundary conditions to include detailed representation of surface processes and observation and inclusion of the kinetic phenomena.

In doing modeling of low-temperature plasmas that may need to go both more towards the swarm-like and plasma conditions we would strongly recommend that all the plasma codes need to be verified against swarm benchmarks and include sampling of relevant data. It all may become more

and more difficult as one develops codes for inhomogeneous systems with complex geometry, but in the limit of a simple geometry and simple swarm conditions all swarm benchmarks should be satisfied to the highest of accuracy.

This article may be viewed as an extension of an article that has been recently submitted for a special issue on plasma modeling covering physical situations where swarm type models are valid and useful and accurate. There is no overlap of the two papers, although a common idea of the need to present the usefulness of the swarm model is obvious. The focus here is more on how elementary processes are producing an intermediate realm of phenomenology (swarm models and properties) that then clearly point at the macroscopic behavior. Be it sprite propagation or positron traps these connections not only reveal relevant physics, but also provide a means to tailor applications based on elementary processes and low-temperature plasmas.



References

- Banković A, Dujko S, White R D, Marler J P, Buckman S J, Marjanović S, Malović G, Garcia G and Petrović Z L 2012 *New J. Phys.* **14** 035003
- Banković A, Petrović Z L, Robson R E, Marler J P, Dujko S and Malović G 2009 *Nucl. Instrum. Methods Phys. Res. B* **267** 350–3
- Barut A O and Raczka R 1980 *Theory of Group Representations and Applications* (Warszawa, PWN: Polish Scientific Publishers)
- Blevin H A, Fletcher J and Hunter S R 1976 *J. Phys. D: Appl. Phys.* **9** 471
- Blevin H A, Fletcher J and Hunter S R 1978 *Aust. J. Phys.* **31** 299
- Bošnjaković D, Petrović Z L and Dujko S 2014b *J. Instrum.* **9** P09012
- Bošnjaković D, Petrović Z L and Dujko S 2016 *J. Phys. D: Appl. Phys.* accepted
- Bošnjaković D, Petrović Z L, White R D and Dujko S 2014a *J. Phys. D: Appl. Phys.* **47** 435203
- Cassidy D B, Deng S H M, Greaves R G and Mills A P 2006 *Rev. Sci. Instrum.* **77** 073106
- Charlton M and Humberston J 2000 *Positron Physics* (New York: Cambridge University)
- Clarke J, van der Werf D P, Griffiths B, Beddows D C S, Charlton M, Telle H H and Watkeys P R 2006 *Rev. Sci. Instrum.* **77** 063302
- Danielson J R, Dubin D H E, Greaves R G and Surko C M 2015 *Rev. Mod. Phys.* **87** 247–306
- Denman C A and Schlie L A 1990 Nonequilibrium effects in ion and electron transport *Proc. of the 6th Int. Swarm Seminar (Glen Cove, NY, 1989)* ed J W Gallagher *et al* (New York: Springer)
- Dujko S, Markosyan A H, White R D and Ebert U 2013 *J. Phys. D: Appl. Phys.* **46** 475202
- Dujko S, Raspopović Z M and Petrović Z Lj 2005 *J. Phys. D: Appl. Phys.* **38** 2952–66
- Dujko S, Raspopović Z M, White R D, Makabe T and Petrović Z L 2014 *Eur. Phys. J. D* **68** 166
- Dujko S, White R D, Petrović Z L and Robson R E 2010 *Phys. Rev. E* **81** 046403
- Fletcher J 1985 *J. Phys. D: Appl. Phys.* **18** 221–8
- Hayashi M 1982 *J. Phys. D: Appl. Phys.* **15** 1411–8
- Hunter S R 1977 *PhD Thesis* Flinders University, Adelaide, Australia unpublished
- Koutselos A D 1997 *J. Chem. Phys.* **106** 7117–23
- Koutselos A D 2001 *Chem. Phys.* **270** 165–175

AQ11

AQ12
AQ13

AQ14

AQ15

Lippmann C and Riegler W 2004 *Nucl. Instrum. Methods Phys. Res. A* **533** 11–5

Lucas J and Saelee H T 1975 *J. Phys. D: Appl. Phys.* **8** 640–50

Marjanović S, Banković A, Cassidy D, Cooper B, Deller A, Dujko S and Petrović Z L 2016 *J. Phys. B: At. Mol. Opt. Phys.* submitted

Marjanovic S, Šuvakov M, Bankovic A, Savic M, Malovic G, Buckman S J and Petrovic Z L 2011 *IEEE Trans. Plasma Sci.* **39** 2614–5

Moshaii A, Khosravi Khorashad L, Eskandari M and Hosseini S 2012 *Nucl. Instrum. Methods Phys. Res. A* **661** S168–71

Murphy T J and Surko C M 1992 *Phys. Rev. A* **46** 5696–705

Natisin M R, Danielson J R and Surko C M 2015 *Phys. Plasmas* **22** 033501

Ness K F, Robson R E 1986 *Transp. Theor. Stat. Phys.* **14** 257–90

Penetrante B M and Bardsley J N 1990 *Nonequilibrium Effects in Ion and Electron Transport* ed J W Gallagher *et al* pp 49–66 (New York: Plenum)

Petrović Z L, Dujko S, Marić D, Malović G, Nikitović Ž, Šašić O, Jovanović J, Stojanović V and Radmilović-Radenović M 2009 *J. Phys. D: Appl. Phys.* **42** 194002

Petrović Z L *et al* 2014 *J. Phys.: Conf. Ser.* **488** 012047

Raspopović Z M, Sakadžić S, Bzenić S and Petrović Z L 1999 *IEEE Trans. Plasma Sci.* **27** 1241–8

Reid I D 1979 *Aust. J. Phys.* **32** 231–54

Robson R E, White R D and Hildebrandt M 2014 *Euro. Phys. J. D* **68** 188

Robson R E, White R D and Petrović Z L 2005 *Rev. Mod. Phys.* **77** 1303

Santonico R 2012 *Nucl. Instrum. Methods Phys. Res. A* **661** S2–5

Simonović I *et al* 2016 unpublished

Šašić O, Malović G, Strinić A, Nikitović Ž and Petrović Z L 2004 *New J. Phys.* **6** 74–85

Sullivan J P, Jones A, Caradonna P, Makochekanwa C and Buckman S J 2008 *Rev. Sci. Instrum.* **79** 113105

Wheaton J H and Mason E A 1974 *Ann. Phys.* **84** 8–38

White R D, Robson R E, Nicoletopoulos P and Dujko S 2012 *Eur. Phys. J. D* **66** 117

The ATLAS Collaboration 2008 *J. Instrum.* **3** S08003

Tung W-K 1984 *Group Theory in Physics* (USA: Michigan State University)

AQ16

AQ17